

Impact of Aviation Tax and Policies on Amsterdam Airport Schiphol: an Airline Network Design Analysis

W.A. Mathoera

Flight departures | Vertrekken

Monday, 22 April

Time	Destination	Flight	Check-in	Remarks	Dep.
09:25:18					
09:55	Manchester	EZY 8673	28	Gate gaat dicht	3
09:55	Vienna	EZY 3442	28	Gate gesloten	3
09:55	Riga	KQ 1687	6-8	Gate gaat dicht	1
09:55	Tallinn	EI 841	19	Naar de gate a.u.b.	3
09:55	London City	DL 8479	6-8	Please go to gate	1
09:55	Cape Town	KQ 1253	6-8	Delayed 09:44	1
09:55	Houston	KQ 1705	6-8	Nu instappen	1
09:55	Lima	EI 603	19	Naar de gate a.u.b.	3
10:00	Belgrade	KL 1443	12-16	Nu instappen	2
10:00	Frankfurt	KL 1373	6-8	Nu instappen	1
10:00	Stavanger	AF 8324	6-8	Gate gesloten	1
10:05	Dar Es Salaam	MF 9397	6-8	Gate gaat dicht	1
10:05	Manchester	KQ 1209	6-8	Gate gaat dicht	1
10:05	Manchester	KQ 1179	6-8	Vertraagd 09:56	1
10:05	Manchester	KE 6417	6-8	Gate gesloten	1
10:15	London Heathrow	KQ 1957	6-8	Gate gaat dicht	1
10:15	Sofia	EZY 2514	28	Gate gaat dicht	3
10:15	Sofia	GA 9470	6-8	Gate gaat dicht	1
10:15	Sofia	MU 1855	12-16	Nu instappen	2
10:15	Sofia	KL 1419	6-8	Gate closing	1
10:15	Sofia	KQ 1417	6-8	Now boarding	1
10:15	Sofia	LX 725	2,3	Priority on row 4	1
10:15	Sofia	VS 6841	12-16	Nu instappen	2
10:15	Sofia	AF 3169	12-16	Gate gaat dicht	2
10:15	Sofia	VS 6851	12-16	Gate gesloten	2
10:15	Sofia	MH 5647	6-8	Naar de gate a.u.b.	1
10:15	Sofia	GA 9768	6-8	Naar de gate a.u.b.	1
10:15	Sofia	KQ 1363	6-8	Naar de gate a.u.b.	1
10:15	Sofia	GA 9082	6-8	First/Business 10-11	1
10:15	Sofia	KL 1971	6-8	Naar de gate a.u.b.	1

Have a nice trip

Flight departures | Vertrekken

Monday, 22 April

Time	Destination	Flight	Check-in	Remarks	Dep.
09:25:18					
09:55	Manchester	EZY 2162	28	Nu instappen	3
09:55	Vienna	OS 372	2,3	Priority on row 4	1
09:55	Riga	BT 618	18	Nu instappen	3
09:55	Tallinn	BT 858	18	Nu instappen	3
09:55	London City	BA 8496	19	Naar de gate a.u.b.	3
09:55	Cape Town	KL 0597	12-16	Vertraagd 10:20	2
09:55	Houston	VS 6836	12-16	Gate gaat dicht	2
09:55	Lima	AF 8243	12-16	Nu instappen	2
10:00	Belgrade	KL 2824	21		3
10:00	Frankfurt	LH 987	2,3	Priority on row 4	1
10:00	Stavanger	MH 5653	6-8	Naar de gate a.u.b.	1
10:05	Dar Es Salaam	KL 0569	12-16	Nu instappen	2
10:05	Manchester	CZ 7608	12-16	Naar de gate a.u.b.	2
10:15	London Heathrow	BA 429		Geannuleerd	
10:15	Sofia	FB 462	21	Naar de gate a.u.b.	3
10:15	Minneapolis	VS 3947	12-16	Nu instappen	2
10:15	London Heathrow	DL 9346	12-16	Geannuleerd	2
10:15	Berlin Brandenburg	DL 9190	6-8	Naar de gate a.u.b.	1
10:15	Billund	KQ 1343	6-8	First/Business 10-11	1
10:20	Dublin	FR 421	25	Naar de gate a.u.b.	3
10:20	Vilnius	BT 962	18		3
10:20	Paramaribo	KL 0713	12-16	Naar de gate a.u.b.	2
10:20	Milan Malpensa	G3 5543	6-8	First/Business 10-11	1
10:25	Copenhagen	SK 552	2,3	Priority on row 1	1
10:25	Barcelona	DL 9186	6-8	First/Business 10-11	1
10:30	Warsaw	LO 266	1	Priority on row 1	1
10:30	Barcelona	VY 8301	1A		1
10:30	Edinburgh	DL 9237	12-16	First/Business 10-11	2
10:35	Paris de Gaulle	DL 8405	6-8	First/Business 10-11	1
10:35	Portland	VS 3940	12-16	Naar de gate a.u.b.	2
10:35	Atlanta	VS 3943	12-16	Naar de gate a.u.b.	2

Have a nice trip

Flight departures | Vertrekken

Monday, 22 April

Time	Destination	Flight	Check-in	Remarks	Dep.
09:25:18					
10:35	Johannesburg	KL 0591	12-16	Naar de gate	
10:40	Oslo	SK 822	2,3	Priority on row	
10:40	Tbilisi	A9 0652	22	Naar de gate	
10:40	Salt L. City	VS 3942	12-16	First/Business	
10:40	Detroit	VS 3946	12-16	Naar de gate	
10:45	London Luton	EZY 2518	28		
10:45	Hamburg	KE 6435	6-8	First/Business	
10:50	London Gatwick	BA 2541	19		
10:50	New York JFK	VS 3941	12-16	First/Business	
10:55	Philadelphia	AY 5712	27	Naar de gate a.	
10:55	Bonaire	OR 377	22,23	Bag. drop-off	
10:55	London Gatwick	EJU 8675	28		
10:55	Stockholm	GA 9482	6-8	First/Business	
11:00	Chicago	UA 908	26	Vertraagd 16:30	
11:00	Cancun	OR 511	22,23	Bag. drop-off	
11:00	Madrid	DL 6766	5		
11:00	Stockholm	SK 556	2,3	Priority on row	
11:00	Taipei	CI 0074	24		
11:00	Entebbe	KL 0537	12-16	First/Business	
11:00	Dusseldorf	GA 9244	6-8	First/Business	
11:10	London Stansted	EJU 7839	28		
11:15	Singapore	SQ 323	31		
11:15	Houston	UA 021	26	Vertraagd 12:20	
11:15	Munich	LH 2303	2,3	Priority on row	
11:20	Istanbul Airport	TK 1952	17		
11:20	Boston	B6 0032	20		
11:20	Zagreb	OU 451	1A		
11:20	Toronto	VS 6864	12-16	First/Business	
11:25	London City	BA 8452	19		
11:25	Budapest	KL 1365	6-8	First/Business	
11:25	Bologna	MF 9345	6-8	First/Business	

Have a nice trip

This page is intentionally left blank.

Impact of Aviation Tax and Policies on Amsterdam Airport Schiphol: an Airline Network Design Analysis

by

W.A. Mathoera

to obtain the degree of Master of Science
at the Delft University of Technology,
to be defended publicly on Thursday, May 23rd, 2024.

Student number:	4775848	
Project duration:	February 2023 – May 2024	
Thesis committee:	Ir. P.C. Roling	TU Delft, Daily Supervisor
	M. Brouwer	Schiphol, Daily Supervisor
	Dr. A. Bombelli	TU Delft, Chair
	Dr. R. Merino Martinez	TU Delft, Examiner

Cover image by W.A. Mathoera

An electronic version of this thesis is available at <http://repository.tudelft.nl/>.

This page is intentionally left blank.

Acknowledgements

This master thesis marks the end of my academic career at the Delft University of Technology. After reaching each milestone, I was actually quite surprised by how far I have come. Even though I have always been very enthusiastic about aviation, I was not sure on following this path after highschool. I certainly would not have guessed I would eventually obtain a masters degree in aerospace engineering. I look back with great fondness to the past six years of my career, during which I have met many inspiring people who made this journey enjoyable.

I am extremely grateful towards Mark Brouwer and Paul Roling for supervising me during my research for the past year. I could always clear my mind on certain topics and I have gained many insights from the various meetings, but also from the spontaneous messages, which were able to help me in times when I was stuck. In addition, I would like to thank them, as well as the other members of the graduation committee, for dedicating their time to assess this thesis.

I would like to express my gratitude towards the members of the KDC and Schiphol that made it possible for me to perform this research in an exciting and fun environment. I would also like to thank all the colleagues at Schiphol that provided me with their time and expertise, which helped me advance my work.

Thank you to all the friends I made during my time in Delft. You made the journey even more enjoyable. The many group projects, skribbl sessions, and cup-a-soup trips are something I am definitely going to miss.

Lastly, I would like to thank all my family and friends that supported me during my work. I have always been able to clear up my mind and chat about the problems I encountered during my research. You kept me motivated and I will always be grateful for that.

Winand Austin Mathoera
Capelle aan den IJssel, May 2024

This page is intentionally left blank.

Contents

List of Figures	vii
List of Tables	ix
Introduction	xi
I Scientific Paper	1
II Appendix	19
A Determining Operational Costs	21
A.1 Aircraft Operational Costs	21
A.1.1 Fixed Costs	21
A.1.2 Variable Costs	22
A.2 Airport Fees	23
A.3 Fuel Calculations	24
B Verification and Validation	25
B.1 Verification	25
B.1.1 Aircraft Capacities	25
B.1.2 Aircraft Range	26
B.1.3 Implementing Non-Direct Routes	27
B.1.4 Airport Capacity	27
B.1.5 Airport Fees	27
B.1.6 Passenger Classes	28
B.2 Validation	28
B.2.1 Fuel Calculation	28
B.2.2 Direct Operational Costs	30
C Sensitivity Analysis	31
C.1 Value of Time	31
C.2 Fare Ratio	32
C.3 Ticket Tax	33
C.4 Passenger Demand Ratio	34
D Airport List	37
III Literature Study	
previously graded under AE4020	41
Bibliography	97

This page is intentionally left blank.

List of Figures

A.1	Landing and take-off fees for different periods of the day and 2 aircraft noise categories. There are in total 7 categories.	23
A.2	NOx charges, passenger charges, and parking charges at Amsterdam Airport Schiphol.	23
B.1	Map with distances between dummy airports. Airport 0 is indicated as hub.	25

This page is intentionally left blank.

List of Tables

A.1	Input data for the DOC method of the aircraft used in the model.	22
A.2	Fixed costs per hour, allocated to depreciation and crew, for the aircraft used in the model. . . .	23
A.3	Landing/take-off charges specified per aircraft type and passenger charges specified for inter/intra Europe travel and local/transfer passengers.	24
A.4	Generated fuel equations from Piano-X for the five aircraft in the model.	24
B.1	Fuel burn data for different block ranges compared to calculated fuel burn for the Boeing 777-300ER.	29
B.2	Fuel burn data for different block ranges compared to calculated fuel burn for the Airbus A350-900.	29
B.3	Fuel burn data for different block ranges compared to calculated fuel burn for the Airbus A321neoLR.	29
B.4	Fuel burn data for different block ranges compared to calculated fuel burn for the Airbus A320neo.	29
B.5	Fuel burn data for different block ranges compared to calculated fuel burn for the Embraer E195-E2.	29
B.6	Operational cost per hour from data compared to the calculated costs for the Boeing 777-300ER.	30
B.7	Operational cost per hour from data compared to the calculated costs for the Airbus A320neo. .	30
B.8	Operational cost per hour from data compared to the calculated costs for the Embraer E195-E2.	30
C.1	Changed Value of Time values in the air and during a lay-over in the sensitivity scenarios compared to the baseline inputs.	31
C.2	Key figures of the sensitivity analysis on the Value of Time.	32
C.3	Changed fare ratio variables in the sensitivity scenarios compared to the baseline inputs.	32
C.4	Key figures of the sensitivity analysis on the ratio between the fares.	33
C.5	Changed tax rate variables in the sensitivity scenarios compared to the baseline inputs.	33
C.6	Key figures of the sensitivity analysis on the ticket tax.	34
C.7	Changed demand ratio variables in the sensitivity scenarios compared to the baseline inputs. .	34
C.8	Key figures of the sensitivity analysis on the ratio between the demand classes.	35
D.1	Selection of 20 hub airports indicated by IATA code and latitude and longitude.	37
D.2	Selection of 200 non-hub airports indicated by IATA code and latitude and longitude.	37
D.2	Selection of 200 non-hub airports indicated by IATA code and latitude and longitude.	38
D.2	Selection of 200 non-hub airports indicated by IATA code and latitude and longitude.	39

This page is intentionally left blank.

Introduction

Of the total 61.7 million passengers that passed through [Amsterdam Airport Schiphol \(AAS\)](#) in 2023, 22.6 million passengers did not enter the country [4]. This large share of transfer passengers allows the airport to maintain a vast network of destinations. In line with the desire to counteract the climate impacts of the airports, there have been several proposals to curb its the growth. As early as in 2008, there have been experiments with implementing new air passenger taxes to reduce the demand for air travel [6]. Another more direct approaches that has been proposed is a limit on the number of yearly flight movements [8].

There are many of these future scenarios that could impact the position of [AAS](#) in the transfer market. The airport currently owns a cost-based optimisation model that is used to gain insights into the effects of changing fuel costs on the traffic flows through a network of 60 airports. However, this model is not yet capable to test the tax regimes and policies that [AAS](#) may face in the future. The model lacks certain aspects of realism, for example there are no airport capacities, but the most notable deficiency is found in the modelling of demand; the passengers are treated as commodities without any preference in routing.

The aim of this research is to improve the original model in order to investigate the effects of possible future policy changes and tax regimes might have on the network quality of the hub. A focus point of the research is the nature of demand, an area that has not seen much coverage in the literature regarding the modelling of airline networks. A new model is proposed that considers multiple passenger classes to differentiate between route preferences based on a time sensitivity factor. In addition, the model is switched to profit-based optimisation, allowing it to make strategic decisions regarding which passengers to fly and which routes to offer.

This thesis report summarises the work done during this research. The report is organised as follows: Part I presents the scientific paper. Part II shows the appendices of the paper. Finally, in Part III, the literature study that supports this research is presented.

This page is intentionally left blank.

I

Scientific Paper

This page is intentionally left blank.

Impact of Aviation Tax and Policies on Amsterdam Airport Schiphol: an Airline Network Design Analysis

W.A. Mathoera¹

Delft University of Technology, Delft, The Netherlands

Abstract

Amsterdam Airport Schiphol characterises itself as a major hub in Europe. Its network is not sustainable with only the Dutch catchment area. Instead, it relies on transfer passengers. When new tax regimes and policies are implemented to combat the environmental impacts of the airport, a change in passenger flows could affect Schiphol's network quality. This paper presents a MILP model to analyse the effects of new policies by simulating passenger flows between airports. A profit-based optimisation model with a greenfield airline network is formulated, which incorporates passenger classes with different time sensitivities to account for passenger preferences in the network design. This approach predicts that hubs at the edges of Europe are better gateways to the continent based on the higher share of transfers. A case study on the implementation of a transfer tax at Schiphol shows that the share of transfers declines, but the network will only see reduced frequencies of destinations.

1 Introduction

Amsterdam Airport Schiphol (AAS) characterises itself as a large hub airport in the European market. The airport sits among the top five global airports regarding hub connectivity [1]. The large network of routes that is created at AAS is however not viable with only the Dutch catchment area [2]. Transfer passengers are needed to support the network. This dependency on transfers originated from the increased competition in the aviation market due to deregulations. In order to gain a prominent place in the market, the concept of mainport was introduced. The aim of this process is to act as a gateway between primary and secondary inter-continental destinations [2]. The effects of this policy can clearly be seen in the annual figures: transfer passengers accounted for 36% of the total of 61.7 million passengers passing through Schiphol in 2023 [3].

This dependency could however post a threat to the position of Schiphol in the aviation market. Any disruptions in the flow of transfer passengers could result in degrading the network quality of AAS. Several tax regimes, such as implementing a transfer tax, have been proposed in order to increase the tax collected by the Dutch government and to have a positive impact on the environment. Besides this proposal, there are many other scenarios in the future that could affect the position of the airport. Other examples might include: a restriction on the number of yearly aircraft movements or a flight-distance based tax for all EU airports.

There have been several studies into the effects of such policies. The Dutch government has instructed studies related to the introduction of various tax regimes of air passenger taxes and the European Commission has instructed for a study regarding a harmonised European tax system. These studies utilised forecasting models to predict the effect on traffic flows of passengers and aircraft through the Netherlands and the European Free Trade Association (EFTA) respectively. These models are not however not public as they

rely on private datasets to describe the competitive environment of the network.

The aim of this research is to investigate the effects that the proposed policy changes and tax regimes, aiming to reduce the climate impacts of AAS, might have on the network quality of the hub.

For this purpose, a Mixed Integer Linear Program (MILP) is proposed that is capable of simulating the passenger and aircraft flows through a network of hub and non-hub airports. A greenfield approach, without an existing competitive market, is used in the modelling of the network. This allows for possible better performing hubs to emerge in the simulations. A profit-based optimisation is performed by taking into account the operational costs and the passenger fares, which results in a route network of direct and connecting itineraries. Different preferences of direct and connecting itineraries are taken into account by implementing multiple passenger classes, each with a different time sensitivity. One of the possible policy changes is investigated with this model during this research; this paper presents a case study on the introduction of a transfer tax.

The paper is structured as follows: section 2 presents the background literature that is used in this research. Section 3 outlines the methodology followed to create the model. Section 4 presents the transfer tax case study and its results. Section 5 presents a discussion on the obtained results. Section 6 gives the conclusion of the research. At last, section 7 offers recommendations for further research.

2 Background

This section reviews relevant contributions that investigate the effects of several tax regimes and policies that may be applicable to Amsterdam Airport Schiphol (AAS). Different types of modelling methods are examined, as well as the methods of acquiring the required inputs of an analysis.

¹Msc Student, Sustainable Air Transport, Faculty of Aerospace Engineering, Delft University of Technology

2.1 Tax Regimes and Policies

In the Netherlands, there have been several proposals of policies to reduce the impact of the aviation industry on the climate. The Dutch government announced in 2017 it would be in favour of introducing an aviation tax. A harmonised European tax and a tax on noisy and polluting aircraft were favoured. The current policy is to levy a flat-rate air passenger tax on departing Origin and Destination (OD) passengers and was implemented in 2021. The decision to implement this tax was based on an analysis of several tax regimes, such as a tax based on an aircraft's noise certificate, a tax based on flight distance, or a flat-rate tax for all OD passengers, with the aim of raising €200 million in tax revenue. The aviation impacts of these tax regimes were analysed by CE Delft using the AEOLUS forecasting model developed by Significance [4]. The chosen variant of a flat-rate tax of €7.50 was expected to have little physical impact: the total number of passengers would change between -0.6% and 0% depending on future welfare scenarios [5]. This model has been used again in studies on raising the tax rate for increased revenues [6] and on removing the exemption of transfer passengers on the aviation tax [7]. The AEOLUS model used is a global strategic model that makes decisions in a competitive environment. The model is focused on the Netherlands and other destinations are defined as zones. These zones reduce in precision with distance from the Netherlands. The output of the model specifies the number of yearly passengers, cargo, and aircraft to and from a given zone. It does not give detailed route structures or timetables of the flights in the network [8]. A similar model is the AERO-MS model, which is used in a study by the European Commission on an European harmonised aviation tax [9]. The model gives similar outputs specified per country in the European Free Trade Association (EFTA). This study analysed the aviation and climate impacts of an European-wide fuel tax and distance-based tax. However, compared to the policies of the Dutch Government, the aim of these tax regimes is not mainly based on a desired revenue, but a reduction in emissions of 90% in 2025.

Both models are used in studies on the effects of policies to reduce the climate impacts of aviation. However, the models are not available to the public and both rely on non-publicly available datasets. The paper proposes a different approach that will simulate the passenger flows in a network of airport nodes, which gives insights in the effects of the larger network, instead of one focus region.

2.2 World-Wide Airport Network

The design of a world-wide airport network entails the strategic decision of which routes to offer. There are two types of itineraries that can be considered when designing a network: Point-to-Point (P2P), where passengers are flown using a direct flights, and Hub-and-Spoke (HS), where passengers are connected through hub airports. The problem of finding the location of a hub for optimal flows in a network has been given much attention in literature. O'Kelly (1986) has presented the one- and two-hub location problem, where the flow of commodities which minimise the operational costs are de-

termined [10]. This model has been extended in O'Kelly (1987) to the p-hub median problem, with an unlimited number of hubs [11]. This model has been implemented in studies such as Bernardes Real et al. (2018), where they model a global network of airports, distinguishing between gateway and domestic hubs [12]. Several advances have been presented in the literature, such as the use of multiple-allocation systems in Campbell (1990), where airports can be connected to multiple hubs [13], and the rewriting of the problem as a multi-commodity flow problem in Ernst and Krishnamoorthy (1996) allowing for higher computational efficiency [14]. A more advanced approach is presented in Jaillet et al. (1996), where a focus is placed on itineraries of the airline network [15]. Instead of following an implicit HS structure, hubs emerge based on optimal flows of multiple types of aircraft.

A review on hub location problems by Alumur et al. (2021) highlights the nature of demand in airport networks as one area that has not seen much coverage in the literature [16]. Most studies omit the use of elastic demands, however an empirical analysis presented in Hsiao and Hansen (2011) shows that demand is heavily influenced by parameters, such as fares, frequencies and flight time. These influences were incorporated to result in estimates of price sensitivity and value of time of the demand [17]. There have been several attempts to incorporate these effects in hub location problems: in Han and Zhang (2013) an adapted p-hub median problem is presented which optimises for profit includes demand elasticities based on ticket prices and perceived travel time cost [18]. The model is linearised per route by selecting the ticket price for the highest profit. Another method of price-sensitive demands is presented in O'Kelly et al. (2015), which linearises the problem by finding an economic equilibrium between each submarket [19].

The literature of this section presents the background of this research and is built upon by proposing a new approach to analyse the discussed tax regimes and policies. The next section will elaborate on the methodology used in this research.

3 Methodology

The aim of this research is to evaluate the effects that various policy changes might have on the traffic flows through Amsterdam Airport Schiphol (AAS). The influence of these policy changes, such as introducing transfer fees or levying distance-based taxes, are not limited to the targeted flights, but have an effect on all of the flights in the network. For example, introducing transfer fees at one airport may lead to a shift in traffic at nearby hubs. In order to capture all these dependent effects, the traffic flows in a world-wide airport network will be modelled. The following sections will describe the method followed during the research. First, the choice of model is established in subsection 3.1. In section subsection 3.2 - 3.5, the methods of determining the different inputs of the model are discussed. In subsection 3.6, the model formulation and notation are presented. The solution method of the model is described in subsection 3.7. At last, in subsection 3.8 the verification & validation method is discussed.

Table 1: Example dataset of AirportIS from IATA showing direct and connecting itineraries starting from Amsterdam Airport Schiphol, in addition of the passenger count and average fare on the given itinerary.

Month	Airline	Origin	Destination	Stop 1	Stop 2	Origin Region	Dest. Region	Pax. Count	Fare
Jul 2023	BA	AMS	LHR			Europe	Europe	18,294	128.25
Jul 2023	KL	AMS	SFO			Europe	North America	4,142	683.01
Jul 2023	EK	AMS	BKK	DXB		Europe	Asia	4,101	375.82
Jul 2023	LH	AMS	BKK	MUC		Europe	Asia	969	348.29
Jul 2023	TK	AMS	BKK	IST		Europe	Asia	969	675.36
Jul 2023	WY	AMS	BKK	MUC	MCT	Europe	Asia	41	325.41

3.1 Model Set-Up

The aim of the model is to simulate the operations of an airline in a world-wide network of airports. When thinking about simulating the operations of an airline, it is important to consider the two operating principles an airline can follow: Point-to-Point (P2P), where itineraries are fulfilled by using direct flights, and Hub-and-Spoke (HS), where passengers are routes through a hub airport. In order to model these operation practices, the model must be able to allow for both direct flights and lay-overs. The model that is formulated during this research is based of the Airline Network Design (AND) problem presented by Jaillet et al. (1996) [15]. As presented in section 2, this type of problem does not consider the placement of hubs in the network, however, it only involves the routing of passenger flows in the most cost-efficient manner.

An AND model best fits the aim of this research, as it allows for the evaluation of both passenger and aircraft flows through the network, instead of only focusing on the flows of passengers. This is important as airline operations do include the type of aircraft in the tactical decision making. The second benefit is that this type of model inherently allows for any airport to be connected to any other airport. If this would not be the case, such as in a Hub Location Problem (HLP) all itineraries starting from a given airport must be routed through a set of hubs decided by the model. Such a system would only allow for direct flights to and from a hub airport, and therefore, a P2P network would be more difficult to model.

To be able to use the AND model for this research, some adaptations are implemented to reach the desired level of realism. The most notable adaptation regards the implementation of demand. One shortcoming of the AND model is that all demand must be completely satisfied. However, from the perspective of the airline, it may be more advantageous to not satisfy all demand, in order to maximise their profit. To implement this, the objective of the model must be switched from cost minimisation, to profit maximisation. By doing so, the fares of passengers must be determined as well, instead of only their cost of transportation. The adapted AND will therefore include fares for each itinerary.

Another shortcoming of the AND model is that passengers are seen as a commodity; the passengers do not have a preference in routing. In reality, a passenger can be influenced by the flight and lay-over time of an itinerary. An accurate representation would entail some

sort of elastic demand that is influenced by factors such as the flight time. However, a trade-off must be made between the level of realism and the computational cost of the problem. For the adapted AND model, it is decided to use static demand that is made time sensitive by implementing penalties on non-direct routes. This allows the problem to remain linearly solvable, while implementing more realistic behaviour, regarding the preference between direct and connecting itineraries. However, time sensitivities can vary between types of passenger. Multiple passenger classes will therefore be implemented. This will allow for varying preferences of itinerary type between the passenger classes.

It should be noted that the model does not include cargo flows. Incorporating cargo flows would require additional modelling on for example the handling capacities at an airport. In addition, the it cannot be assumed that the cargo flows are symmetric in the network, which would increase the difficulty of the problem. The effect of omitting cargo could be visible in the choice of aircraft, where in reality larger aircraft could be chosen based on the belly cargo space of aircraft.

This section concludes with an adapted set-up of an AND profit-based model, that includes multiple time sensitive fare classes. The next sections will go into detail on the determination of the inputs of the model. This includes the determination of the demand and the fares, the selection of aircraft and airports, and the set-up of the cost function of the model.

3.2 Demand and Fares

It has been established that the adapted AND model will divide its demand into multiple fare classes. The choice on the number of fare classes is influenced by the computational cost required for each additional fare class. It is decided to use three fare classes in the model: economy class, business class and a third lower class that represents the uncaptured demand. This third class of passengers can be used by the model in case the fares are able to cover the marginal costs on a specific itinerary.

For each itinerary and each fare class, a static demand and a corresponding fare is determined. The data that will be used in this research is obtained from the IATA AirportIS database. This database lists per airline the total number of passengers that were routed through a specific itinerary during a given month. In addition, the average fare on that itinerary is given. A sample of this data is shown in Table 1. This sample

shows two direct and four connecting itineraries. The connecting itineraries also specify the connection airports, in addition to the origin and destination. The dataset of July 2023 will be used in this research, as this month experienced the highest volume of commercial flights at the airports of the European Union [20]

To determine the demand between a city-pair, first, all the passengers of the direct and various connecting itineraries are summed up; this number represents the total flown demand between a city-pair. In addition, there could be connecting itineraries where the first leg corresponds to the given city-pair, but the airport of the second leg is not present in the model. These passengers are included in the demand between the city-pair. The total demand is divided by 31 days to obtain the average demand of one day in July. It is assumed that the flown demand represents the economy and business classes of the model. This flown demand will be divided between these two classes with a set ratio of 4:1 for each city-pair. The ratio has been determined by observing the number seats on various 2-class configurations of the selected aircraft types in this study. The third fare class represents the uncaptured demand, however, the flown demand does not show the uncaptured demand between a city-pair. A set ratio of 1:4 between the uncaptured demand and the economy class is assumed. This leads to a ratio of 1:4:1 between the three fare classes. The effects of this assumption are tested with a sensitivity analysis.

From the same dataset, the fares of this demand can be determined. It should be noted that the dataset does not include the tax and airline fees for each itinerary. These additional costs vary between routes and even between airlines. It is assumed that the tax and fees account for an additional 50% for economy class passengers and 20% for business class passengers. The average fare of all itineraries between a city-pair is calculated and a ratio of 1:2 is assumed between the economy and business fare classes. The fare of the uncaptured demand is assumed to be slightly lower than the economy class. A ratio of 0.8:1 is assumed between the third and the economy fare class. The effects of these assumptions are tested with a sensitivity analysis.

These fares represents a direct itinerary. A non-direct itinerary would result in a lower fare due to the time sensitive penalty. For these three fare classes, different levels of time sensitivity will be assumed. In order to determine the penalty, each passenger class is assigned a Value of Time (VOT). This value represents the perceived value lost by the passenger flying a non-direct route. Several studies have been conducted in order to determine the VOTs for different modes of transport and trip purposes. Wardman e.a. (2016) presents a review of multiple studies conducted to VOTs in Europe [21]. Two results show that the VOT ratio between leisure and business air travel is around 1:2. The review also shows that the average VOT for non-business travel is around €40 per hour. This results in a VOT of €40 and €80 per hour for economy and business class respectively. The value of the uncaptured demand will be based of the VOT of other modes of transport. The paper shows that other modes, such as car and train travel have half or less than half of the value than air travel. For this research, the third fare class will as-

sume half of the VOT, resulting in €20 per hour. The VOT will also be applicable to the transfer time at the airport, however, only half of the VOT is added to take into account the out-of-vehicle time that can be spent on leisure. For connections, an average of 2 hours will be assumed in the model.

An overview of the characteristics of each passenger class presented in this section is shown in Table 2.

Table 2: Assumptions on the three passenger classes in the model.

	Budget	:	Economy	:	Business
Demand Ratio	1	:	4	:	1
Fare Factor	0.8		1		2
Tax Rate	50%		50%		20%
VOT	€20.00		€40.00		€80.00

3.3 Aircraft

One of the decision variables in the model is the number of aircraft that is placed between a city-pair. The model is able to choose between multiple types of aircraft. By implementing multiple types of aircraft, the model is able to optimise for the number of seats, the aircraft range, and the flight cost. A trade-off must be made when selecting the aircraft types and the number of aircraft types that is implemented in the model. More aircraft types will increase the complexity of the problem. For this scenario, it was decided to implement the five aircraft types shown in Table 3. This table shows the seating capacity in a 2-class lay-out and the aircraft range at MTOW.

Table 3: Set of aircraft types and characteristics implemented in the model [22].

	Seats [-]	Range [nmi]
Boeing 777-300ER	381	7370
Airbus A350-900	300	8300
Airbus A321neoLR	200	4000
Airbus A320neo	150	3500
Embraer E195-E2	132	2655

The set of aircraft can be divided into two distance categories: long-range (B777 and A350) and short-range (A321, A320 and E195). By allowing different seating capacities within a distance bracket, the model is able to make tactical decisions, such as an upgrade to a bigger aircraft on a certain route. In the short-haul range,

The fuel calculation of these aircraft is performed using the Piano-X analysis tool. The tool takes into account the performance of the aircraft type to calculate the required fuel for a given scenario, with variables such as the block range and the payload weight. For multiple block ranges, the fuel burn is calculated, in order to create a distance based function for the fuel burn in the model. For the calculations, it is assumed that the aircraft have a load factor of 90%. The average payload weight per passenger is assumed to be 99 kg [23]. The fuel functions and corresponding data are presented in Appendix A.

3.4 Airports

The AND model simulates the world-wide airport network, but it is not possible to implement all the airports of the world. A selection of airports needs to be made, while ensuring that the model is still capable of producing useful insights regarding the transfer flows at AAS. This section will discuss the method of determining the airports that will be included.

In the model, a distinction is made between hub and non-hub airports. At hub airports, it is possible to transfer passengers. By only allowing passengers to transfer at hub airports, the number of possible itineraries is reduced drastically. The choice of airports therefore determines the complexity of the problem. For this problem, it was decided to include 20 hub airports in the model. With 20 hubs, it is possible to cover the current busiest hubs in Europe, in addition to smaller hubs in and around the continent. Only hubs around Europe are included, as the research focuses on the traffic flows that go through Europe. The selection of hubs is based on the Air Connectivity Report by ACI Europe, which ranks the hub connectivity of hubs in Europe [1]. In addition, possible gateway hubs at the edge of Europe are included: Reykjavik, Helsinki and Dubai. For each of these hubs, the capacity is determined based on the maximum hourly runway capacity of the airports. With the assumption that an airport is operable at maximum capacity for 12 hours per day, the maximum daily capacity can be determined. The complete list of hubs and the corresponding daily capacities is shown in Table 4.

Table 4: List of the hub airports and the corresponding daily aircraft capacity based on the hourly runway capacity [24][25][26][27].

AMS	1308	VIE	780
IST	1440	DUB	588
LHR	1092	ZRH	768
FRA	1320	CPH	732
CDG	1308	LIS	516
MAD	1068	OSL	852
BCN	864	KEF	360
MUC	1080	HEL	684
FCO	888	BRU	720
ATH	648	DXB	744

Next are the non-hub airports in the model. The number of non-hub airports puts less strain on the complexity of the model than the number of hub airports. However, there still is a trade-off between the number of airports and the computational time. A total of 200 non-hub airports will be included in the scenarios, resulting in a total of 220 airports. Scenarios of this size were able to be solved to near-optimality with an average of 30 minutes. Increasing the number of airports would exponentially increase to solution time.

The 200 non-hub airports were selected by ranking all the itineraries that connect through the 20 hub airports. The itineraries are obtained from the AirportIS database. This results a list of the 200 airports that provide the most connecting passengers to these hubs. The total list of airports is shown in Appendix E. By using this method, airports that mostly provide direct

leisure flights can be filtered. For these itineraries it can be assumed that they would remain a direct flight, and can therefore be omitted from the problem. These local passenger flows should however be kept in mind when analysing the resulting passenger flows.

3.5 Costs

This section concerns the determination of the operational costs in the model. The AND discerns two types of cost: a cost per aircraft and costs based on the number of passengers. The cost per flight includes, for example, take-off and landing fees, and fixed capital costs. The passenger based costs include, for example, the airport security charges. Other non-operating costs, such as administration and promotion, are omitted from the calculations, as they would not influence the routing decisions and aircraft choice.

To determine the flight operating costs, the simplified Direct Operating Cost (DOC) model of the TU Berlin is used [28]. This model uses empirical formulas for determining the fixed and variable costs on a route based on the type of aircraft. Fixed costs include the capital costs of the aircraft and the salaries of the flight and cabin crew. These costs are calculated for a whole year, and then divided by the average yearly utilisation to obtain the fixed costs per block hour. The variable costs include fuel, maintenance and ATC fees. The maintenance costs and ATC fees are calculated based on the flight time of a certain route. The fuel costs are based on the fuel burn calculations from the Piano-X analysis tool. The full method, including aircraft parameters and fuel functions, is presented in Appendix A.

The method of determining the airport specific charges vary per airport. The charges will be categorised in aircraft dependent and passenger dependent charges. For each hub airport, the charges are obtained by consulting the publicly available airport charges guidelines. A summary of the hub airport charges is presented in Appendix A. The charges of all remaining non-hub airports are assumed to be the same as at Amsterdam Airport Schiphol. This assumption can be made as the non-hub charges would not influence the tactical decisions on any transfer operations in the network.

3.6 Model Formulation

This section presents the notation and formulation of the adapted Airline Network Design (AND) model.

Input: parameters and sets

N : Set of airports, indexed by i

K : Set of aircraft types, indexed by k

M : Set of passenger classes, indexed by m

$H \subset N$: Subset of hub airports, indexed by h

- p_{ij}^m : Fare between airports i and j for class m
- b_{ihj}^m : Passenger specific cost between airports i and j via h for class m
- f_{ij}^m : Total demand between airports i and j for class m
- c_{ij}^m : Operational cost of aircraft type k between airports i and j
- q_k : Seating capacity of aircraft type k
- d_{ihj} : Total distance between airports i and j via hub h
- Γ_i : Airport capacity of airport i
- r_k : Range of aircraft type k

Decision Variables

- x_{ihj}^m : Fraction of passengers of class m travelling between airports i and j using hub h
- y_{ij}^k : Number of aircraft of type k utilised between airports i and j
- z_{ihj}^m : = 1 if f_{ij}^m is routed via hub h

Model Formulation

$$\max \sum_i \sum_j \sum_h \sum_m (p_{ij}^m - b_{ihj}^m) x_{ihj}^m f_{ij}^m - \sum_i \sum_j \sum_k c_{ij}^k y_{ij}^k \quad (1)$$

s.t.

$$\sum_m \left(f_{ij}^m x_{i0j}^m + \sum_h (f_{ih}^m x_{ijh}^m + f_{hj}^m x_{hih}^m) \right) \leq \sum_k q_k y_{ij}^k \quad \forall i, j \quad (2)$$

$$x_{ihj}^m \leq z_{ihj}^m \quad \forall i, j, m, h \neq 0 \quad (3)$$

$$\sum_h z_{ihj}^m \leq 1 \quad \forall i, j, m \quad (4)$$

$$\sum_j \sum_k y_{hj}^k \leq \Gamma_h \quad \forall h \quad (5)$$

$$y_{ij}^k = y_{ji}^k \quad \forall i, j, k \quad (6)$$

$$x_{ihj}^m \geq 0 \quad \forall i, j, h, m \quad (7)$$

$$y_{ij}^k \in \mathbb{W} \quad \forall i, j, k \quad (8)$$

$$z_{ihj}^m \in \{0, 1\} \quad \forall h \quad (9)$$

The objective function, shown in Equation 1, shows the maximisation of the profit in the network based on the passenger fares and the operational costs per passenger and per aircraft. Equation 2 shows the first constraint, which ensures that the number of passengers

between a given city pair is able to fit within the available seats on that route. Equation 3 and 4 ensure that a given passenger class is not divided between multiple routes. Equation 5 ensures that the number of aircraft departing from a given hub is within the departure capacity of the airport. No constraint regarding arrival capacities is needed as Equation 6 ensures symmetric flows of aircraft. Equation 7, 8 and 9 define the domain of the decision variables.

3.7 Solution Method

The AND model is formulated as a Mixed Integer Linear Program (MILP), which can be solved using a Branch-and-Bound (BnB) procedure. A commercial solver can be used to find a solution for a given problem in a shorter time by using additional techniques to converge to a solution. For this study, Gurobi version 10.0.1 is used on two AMD EPYC 7713 64-core processors with a frequency of 2.0 GHz and 512 GB of RAM. With this set-up, an optimality gap of around 6% could be reached within an hour. The optimality gap represents the difference between the upper bound of the problem and the current incumbent solution. The convergence of the optimality gap slowed down exponentially after this limit. Therefore, this limit was kept for all scenarios to obtain usable results within a reasonable amount of time.

To reduce the size of the problem, constraint that would not affect the problem were fixed. Routes with a demand of less than 50 passengers per day are not able to be flown using a direct flight. In addition, routes which exceed the range of a certain aircraft are also not able to be flown by the given aircraft type. The constraint controlling these itineraries could therefore be fixed to 0.

The result of the optimisation procedure is a set of values for all the decision variables. Several analyses can be performed using the results. The analyses will be divided into three categories. First, it is possible to describe the network quality and traffic figures of an airport. This includes the number of destinations that can be reached from an airport, the frequencies they are flown to and the number of each aircraft type that is utilised. In addition, it is possible to find the number of local and transfer passengers that pass through a given airport. Next are the results regarding the environment. From the results, it is possible to calculate the CO₂ emissions based on the fuel burned. At last are the economic results. From the output it is possible to find the total amount of taxes that have been paid at a certain airport, for example.

3.8 Verification and Validation

During the research, it is important to perform verification and validation steps in order to determine any errors that might be present in the model. The verification steps entail determining if the simulation results correspond with the expected output of the model. A set of scenarios is created for various aspects of the model, where the outcome could be determined analytically. The scenarios are created with a simple network of 1 hub and 2 non-hub airports. An example scenario

puts a demand between the 2 non-hub airports that is too small to be performed by a direct flight. The result should be that passengers are routed through the hub, if the fares would still result in increased profit. These scenarios were tested and confirmed to correspond with the predetermined results. An overview of the verification tests is presented in Appendix C.

The validation step of the model is more difficult to perform. The aim of the model is to identify the effects of policy changes in a world-wide airport network. Validation with historic data would be impossible, as there would be too many variables to consider to link historic policy changes to the perceived effects. Similarly, validating if the fare inputs are realistic, would require knowing the composition of passengers on all operated flights. A specific flight could accommodate many different itineraries where each passenger contributes a different amount to the cost of the aircraft. For example, business class passengers may offset most of the cost, while other passengers may only cover their marginal cost of flying.

Instead, more focus is given towards validating the costs of the model. The operational costs are not directly obtained from data, but are determined from several models. These costs were validated by comparing the hourly costs of operating the various types of aircraft with the recommended values for economic analyses, published by Eurocontrol. The used method for determining the operational costs shows an overestimation of the capital costs of aircraft. The used method for determining the operational costs shows a small underestimation of the hourly costs for the short-haul aircraft. This underestimation in the short-haul aircraft could be explained by the block time assumption of the DOC method. The method assumes a block time of 1.83 hours for all aircraft. If it is assumed that the short-haul aircraft have only a block time of 1 hour, the costs correspond with the data. The difference in hourly costs should not be an issue as the total flight cycle cost would still be comparable. An overview of this validation is presented in Appendix C.

4 Case Study: Transfer Tax

This section will focus on one of the possible policy changes that can be evaluated using this model; the introduction of a transfer tax at Amsterdam Airport Schiphol (AAS). Passengers flying from AAS pay a tax for each departure. In 2023 this tax was €26.43 and in 2024 this tax is €29.05 [29]. However, this tax is omitted for passengers transferring or in transit at AAS. Multiple proposals have been made by the Dutch government to stop this exemption, in an attempt to reduce the number of flights at AAS.

The Dutch government has already commissioned a study into the effects of introducing a transfer tax [7]. This study examines the effects of including transfer passengers in the air passenger tax for two price levels. A low fare that charges each transfer passenger €13.215 per departure, which results in a tax of €26.43 per round-trip flight, and a high fare of €26.43 per departure, resulting in €52.86 per round-trip flight. This change in air passenger tax is evaluated using the AEOLUS model, owned by the Ministry of Infrastructure

and Water Management [8]. This model implements a different approach compared to the AND model of this study. Instead of optimising all the traffic flows in the network, the focus is put on the traffic flows in and out of the Netherlands. Destinations are merged together to create geographic zones. In addition, the AEOLUS model is capable of accounting for current market shares and incorporates the effects of policy changes by changing the utility functions of certain routes.

On the contrary, the AND model uses a greenfield approach with no existing market shares. In order to analyse the results, it is needed to create a baseline scenario that can be used to compare the scenarios with policy changes with. The next subsection will show the results of a baseline scenario. This scenario reflects the current situation without an air passenger tax for transfer passengers. Next, the results of the scenarios including the transfer tax are shown. The transfer tax will be modeled in multiple price-levels. A range of price levels between €0.00 and €26.43 will be simulated to be able to spot any possible tip-off points in the data. A total of 7 scenarios are created, including the low and high fares of €13.215 and €26.43.

4.1 Baseline

To find the effects of the introduction of a transfer tax, a baseline scenario is created to compare the outputs of the various scenarios with. These scenarios all have only one variable input, the price level of the transfer tax, in order to have a fair comparison. The transfer tax will be included in the passenger fixed costs for passengers transferring at AAS. For transfers at AAS the fixed cost is indicated as b_{ij}^m in the objective function. The transfer tax will be applied at the same price level to the different fare classes.

The other inputs of the model will remain the same, as presented in section 3. With these inputs the simulation is performed using the designed Python program. The solving algorithm was not able to find an optimal solution within the given time constraint of 1 hour. Instead, a sub-optimal solution with an optimality gap of 6.6% is reached.

An overview of the network and traffic figures of AAS is given in Table 5. The published traffic figures for July 2023 of AAS will be used to compare the results with [30]. AAS serves a total of 168 destinations in the baseline scenario, of the available 200 airports. Compared to the actual conditions, AAS serves a total of 305 destinations for passenger traffic in 2023. However, there are some destinations with little traffic. For example, from the dataset of passenger flows in 2023 it can be found that there are only 258 destinations with more than 25.000 annual passengers arriving at AAS.

The simulation shows that in the baseline there are a total of 732 aircraft movements at AAS. This combines arriving and departing aircraft. The calculated capacity is quite a bit lower than the input capacity, which was set at 1308 movements. The calculated capacity did compare with the actual utilisation of July 2023, which was on average 1321 aircraft per day. However, the average load of the model is more comparable to the actual data. By dividing the total departing passengers by half of 732, the number of departing aircraft, an av-

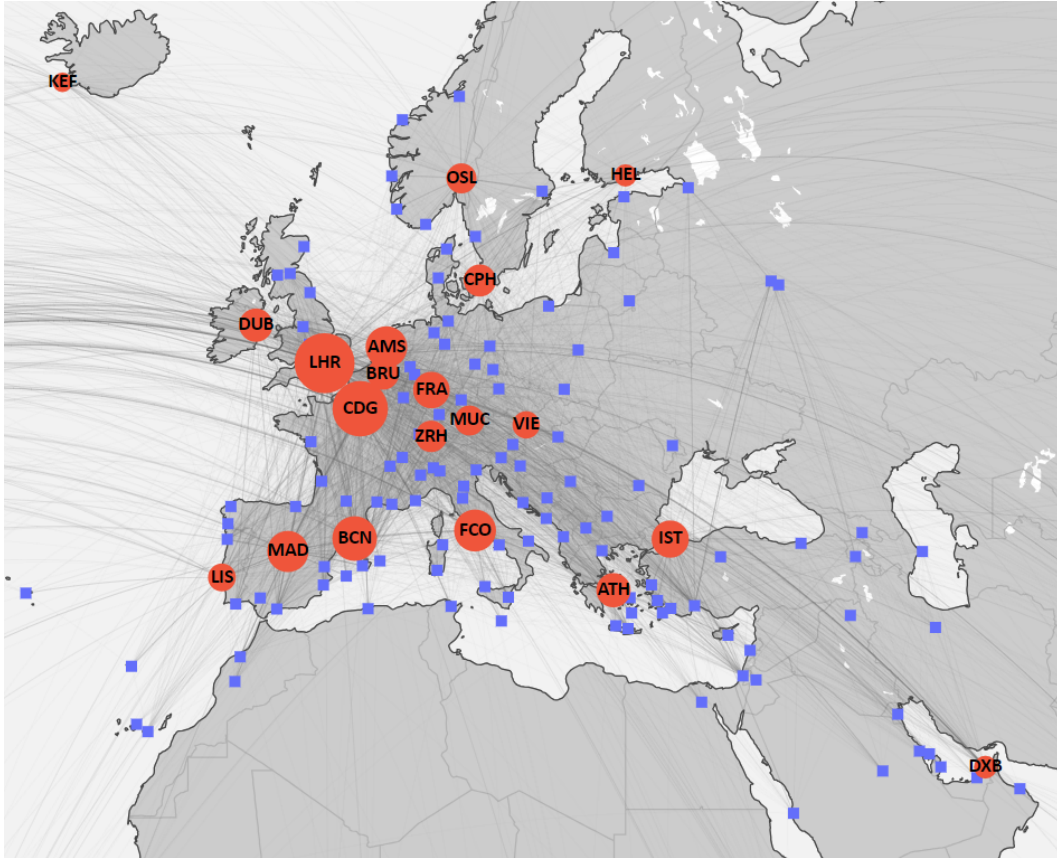


Figure 1: Relative size of hub traffic volume in the baseline scenario. Hub airports are indicated by red dots and non-hub airports by blue squares.

verage load of 186 passengers is obtained. The actual load factor was on average 147 passengers in July 2023.

The total number of passengers passing through AAS would be double the local departures added to the transfer passengers, which results in a total flow of 125.896 passengers. The actual numbers show an average of 193.853 passengers passing through AAS in a day. This difference is mostly due to varying numbers of transfer passengers. The simulation shows a total of 57.746 departing passengers, which is similar to the actual daily average is 62.960 departing passengers.

In addition to the key traffic figures of AAS, a map indicating the traffic flows through the hubs is shown in Figure 1. In this map, the traffic volume of each hub is indicated by the relative size of the dots in the map. The non-hub airports of the model are indicated by squares.

Table 5: Key figures about Amsterdam Airport Schiphol in the baseline scenario.

Europe Destinations	103
Intercontinental Destinations	65
# Aircraft	732
# Local Departing Pax.	57.746
# Transfer Pax.	10.404

Regarding the other hubs in the airport, an overview of the ratios between local and transfer passengers is shown in Figure 2. Most hubs only have a small share

of transfer traffic. Only five hubs have a larger than 25% share attributed to transfer traffic. Four of these, OSL, KEF, HEL and DXB have relatively low airport fees and are situated on the edge or outside of the European continent, which allows them to act as a gateway for the continent.



Figure 2: Share of local (blue) and transfer (red dotted) traffic at the hub airports of the model.

To get an indication of the effects of the assumptions on the baseline scenario, a sensitivity analysis is performed. The complete results of the sensitivity analysis

is shown in Appendix D. The analysis is performed for the main assumptions of the model: the Value of Time (VOT) per passenger class, the fare ratios, the ticket tax, and the passenger class ratios. Multiple scenarios were created to find the effects of these assumptions. The results confirm that the business passenger class has the biggest influence on the number of other passengers on flights. By decreasing the fares or reducing the demand of business class, the number of passengers in other classes are increased by a larger factor. The number of destinations did remain fairly constant between the scenarios, however, small trends due to the assumptions were visible. For example, the number of transfers increased with a lower VOT or the number of destinations slightly increased with more total passengers. The results of the sensitivity analysis need to be taken into account when analysing the results of the simulations.

4.2 Results

The results of the scenarios including a transfer tax are presented in this section. The variable in this case study is the price level of the transfer tax at AAS. The baseline assumes a price level of €0.00. The other scenarios will have a range of price levels between €0.00 and €26.43 per departure. A range of price levels is simulated in order to visualise possible tip-off points in the outputs. The number of scenarios is chosen by a trade-off between the computational time of all the scenarios and the level of detail of the tip-off points. In total seven scenarios are generated between the price levels of €0.00 and €26.43, resulting in steps of around €4.41. This range includes the low and high scenario of €13.22 and €26.43 proposed by the Dutch government. An overview of the scenarios and the corresponding simulation performances, objective value, runtime and the optimality gap, are presented in Table 6. The different scenarios are numbered from 0 to 7, including the baseline scenario. For all scenarios, the simulation reached the time limit of 3600 seconds. This means that the problems are not solved to optimality. Therefore, the optimality gap is given as well for these simulations.

Table 6: Transfer tax scenarios with input transfer tax level and simulation performance figures.

	Tax [€]	Network Profit [€]	Runtime [s]	Gap [%]
0	0.00	482 mln	3600	6.56
1	4.41	485 mln	3600	5.84
2	8.81	482 mln	3600	6.50
3	13.22	487 mln	3600	5.45
4	17.62	481 mln	3600	6.56
5	22.03	482 mln	3600	6.53
6	26.43	481 mln	3600	6.59

In Table 6, the obtained network profits are presented as well. For all simulations the profit remains relatively stable around €482 million. In some scenarios, the profit of the network is higher compared to the baseline without a transfer tax at AAS.

To find the effects that occur specifically at AAS, more outputs of the model are necessary. The outputs that will be presented can be divided in three categories, as have been established in section 3. These categories

are: network and traffic, CO₂, and economic. First, the network and traffic outputs of the simulations will be presented. These outputs include traffic flows of local and transfer passengers through AAS, the shift of passengers to other hubs, the fleet composition, and figures on the network quality of the hub.

The following graphs show the size of the traffic flows of passengers at AAS. The model assumes three types of passenger classes: budget, economy and business. These passenger classes will be indicated in the results as class 0, 1 and 2 respectively. An overview of the characteristics of the passenger classes is shown in Table 2.

In Figure 3, the number of transfer passengers passing through AAS can be seen for the range of transfer tax prices. In the baseline scenario, the number of transfer passengers equals to 10.404. The graph shows that there is a downward trend in transfer passengers when the transfer tax is increased. There are however some anomalies; scenario 1 and scenario 3 have a larger flow in transfer passengers than the preceding scenarios. Scenario 1 even has a total of 10.546 passengers, which is larger than in the baseline.

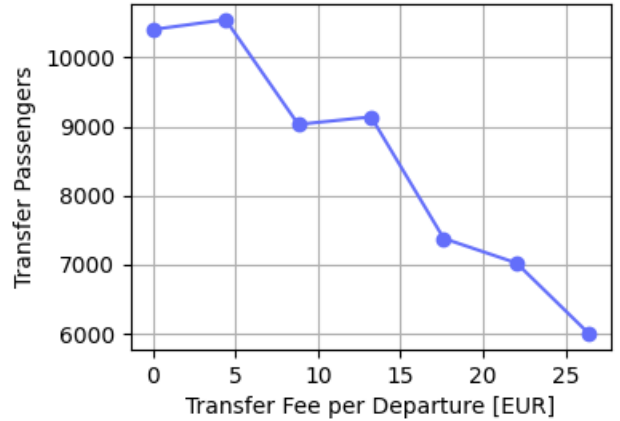


Figure 3: Number of transfer passengers at AAS against the transfer tax.

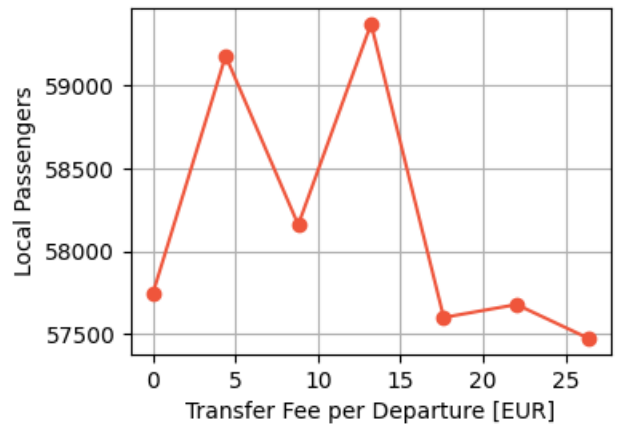


Figure 4: Number of local passengers at AAS against the transfer tax.

In Figure 4, the number of local passengers departing from AAS are shown for the range of transfer tax prices. The graph does not show a clear trend in the number of passengers. Instead, the number of passengers remains around 58.500 passengers for all scenarios.

In Figure 5 and 6, the number of local and transfer passengers through AAS are shown again, but divided into the three fare classes in the model. The graphs show that the ratio between the fare classes remains constant for the range of transfer tax prices. However, the ratio between transfer and local passengers do differ. The demand input assumes a ratio of 1 : 4 : 1 between the three fare classes. For the local passengers from AAS, this ratio is around 0.6 : 3.6 : 1. When comparing this ratio with the input ratio, it can be seen that the higher the class, the more available demand is fulfilled. For the transfer passengers through AAS, this ratio is around 1.0 : 4.4 : 0.9. The traffic flows of transfer passengers follow a different ratio than that of the local passengers. The transfer flows cover more of the middle class and less of the higher class of passengers.

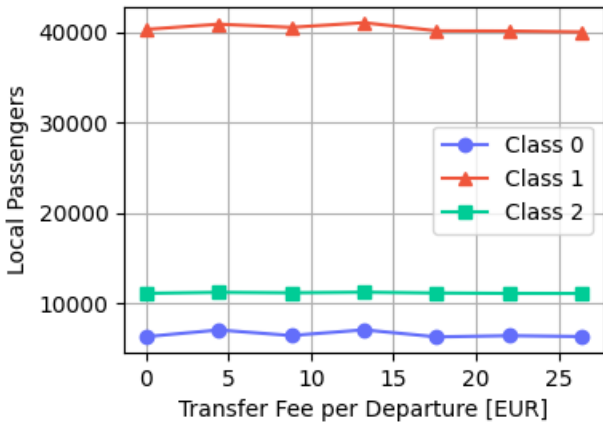


Figure 5: Number of local passengers departing from AAS split up in the three passenger classes against the transfer tax.

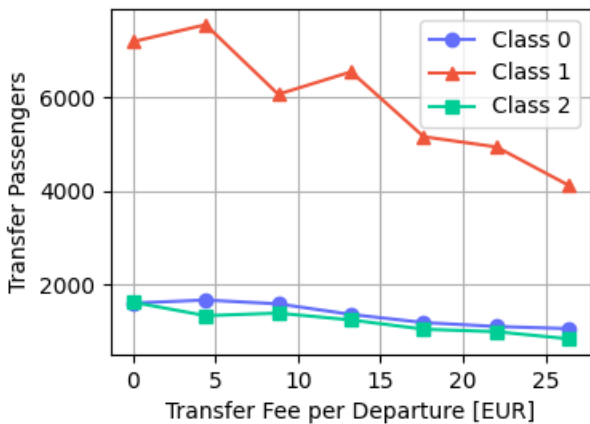


Figure 6: Number of transfer passengers departing from AAS split up in the three passenger classes against the transfer tax.

When increasing the price level of the transfer tax, the number of transfer passengers at AAS decreases. Some of this traffic is captured by surrounding hub airports in the network. In Table 7, the top five airports that capture the most traffic are shown for the low and high scenario. The table shows the number of passengers that used to be routed through AAS in the baseline, but are now routed through another hub airport. The table also gives the remaining passengers that are routed through other hubs outside of the top five. In both the low and the high scenario, the top five consists of the same airports. Four of these hubs are also the closest neighbours of AAS and these are: BRU, FRA, CDG and LHR.

Table 7: Top five airports in the low and high scenario that capture the lost transfer traffic of AAS. The number of captures passengers is shown between the brackets.

	€13.22	€26.43
1	BRU (1253)	FRA (1171)
2	FRA (704)	BRU (933)
3	CPH (473)	CDG (401)
4	CDG (438)	CPH (346)
5	LHR (355)	LHR (295)
remainder	(1780)	(1422)

The network quality of AAS will be described using the number of destinations reachable via direct flight from AAS and the flight frequencies at the airport. In Figure 7, the number of destinations in each transfer tax scenario is graphed. A distinction is made between destinations in Europe and Intercontinental (ICO) destinations. In the baseline scenario, there are 103 European and 65 ICO destinations. Both sets remain relatively stable when increasing the transfer tax price level: the number of European destinations vary between 107 and 103 destinations and the number of ICO destinations varies between 65 and 60. The number of ICO destinations does show a slight trend downward when increasing the transfer tax.

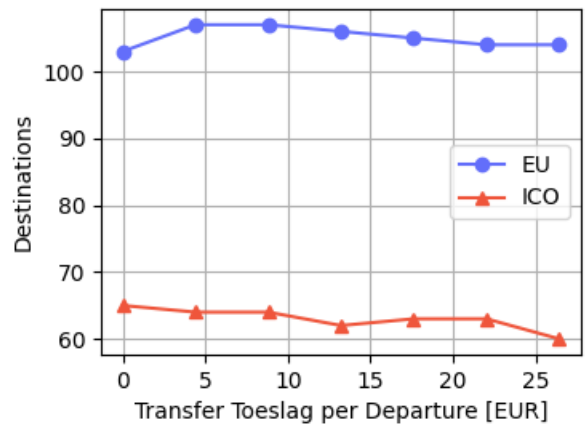


Figure 7: The number of European and intercontinental destinations served from AAS against the transfer tax.

For these destinations, a histogram is made to show with what frequency these destinations are flown to. In Figure 8, the histogram is shown for the destinations in the baseline and the high and low transfer tax scenarios. Most destinations only have a frequency of 1 round-trip per day. When the transfer tax is increased, the frequency of some destinations is reduced, which leads to an increase in the number of destinations being served with a frequency of 1.

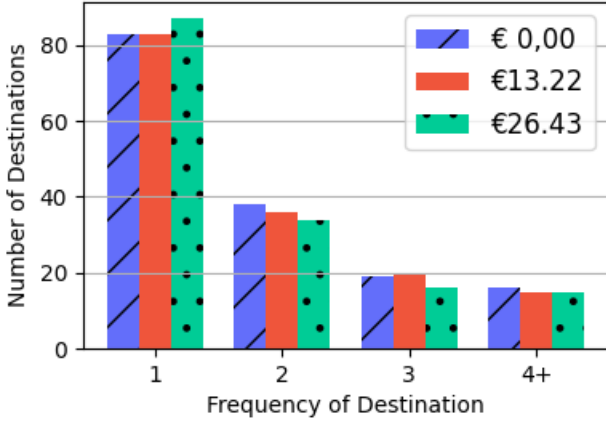


Figure 8: Histogram of the number of destinations that is served for a given frequency for the baseline, low and high scenarios.

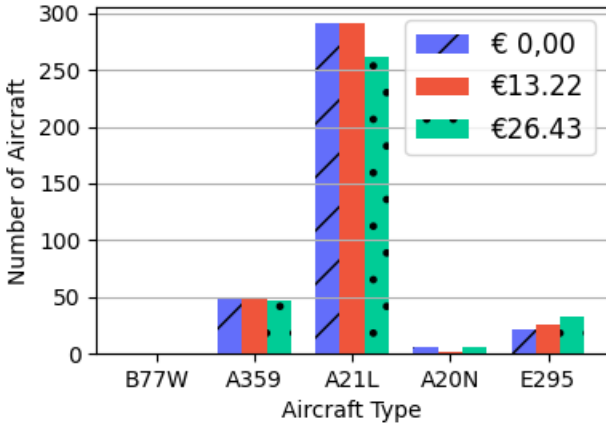


Figure 9: Histogram on the number of aircraft of the five aircraft types in the model for the baseline, low and high scenarios.

The last result about the traffic figures regards the number of aircraft deployed per aircraft type. Figure 9 shows a histogram of the five aircraft types of the model for the baseline, low and high scenario. The first observation is that there is a large share of A321neoLRs in the scenarios. In the short-range segment, there are also some E195-E2s. This share increases when the transfer tax is increased, and there are slightly less passenger flows through AAS. The large share of A321neoLRs indicates that the aircraft is the most efficient type in the model for most routes. In certain cases where the range of the A321neoLR is not sufficient, an A350 is chosen. In the long-range segment, all flights are performed by

the A350. A similar comparison in the long-range segment can be made; the A350 is more efficient than the B777 and the range of the A350 is sufficient for the destinations in the results. As this model does not take into account cargo flows, the advantage of more belly space in larger aircraft are also not taken into account. This also adds to the lack of any B777s in the results.

The next category is CO₂. The CO₂ emissions can be calculated from the fuel burn by the aircraft. The emissions are calculated for the set of flights flying in or out of AAS and the total set of flights in the network. In Figure 10, the emissions of flights passing through AAS are shown. The data shows a clear downward trend, as there are less flights flown from the airport. However, from the data in Figure 11 it can be seen that the global emissions are not affected by the reduction at AAS. The number of flights passing through AAS is relatively small compared to the total number of flights in the network. In addition, some flights are still flown, but via another hub.

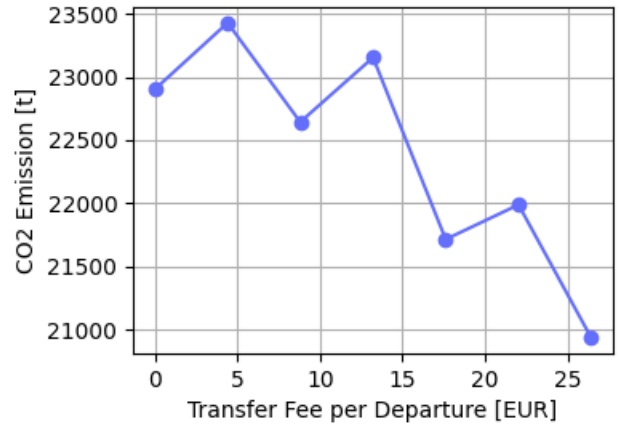


Figure 10: CO₂ emissions of flight passing through AAS against the transfer tax.

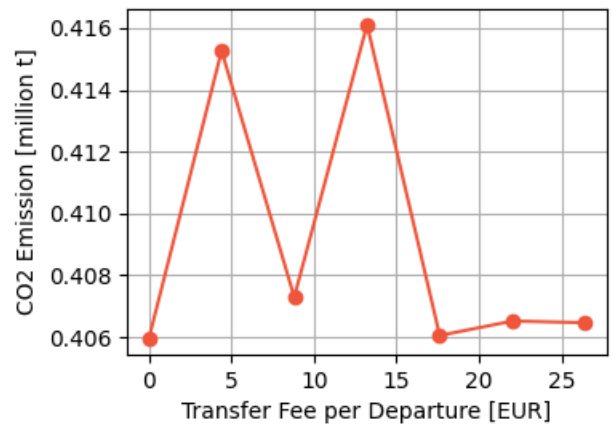


Figure 11: CO₂ emissions of the total set of flights in the network against the transfer tax.

The tax revenue is the last category of outputs of the model. Passengers departing from AAS pay an air passenger tax of €26.43 and this case study introduced this air passenger tax for transfer passengers as well. The

total air passenger tax for the various tax levels is presented in Figure 12. The graph shows an upward trend when the tax level is increased. While the number of transfer passengers is reduced, the tax collected is still able to increase.

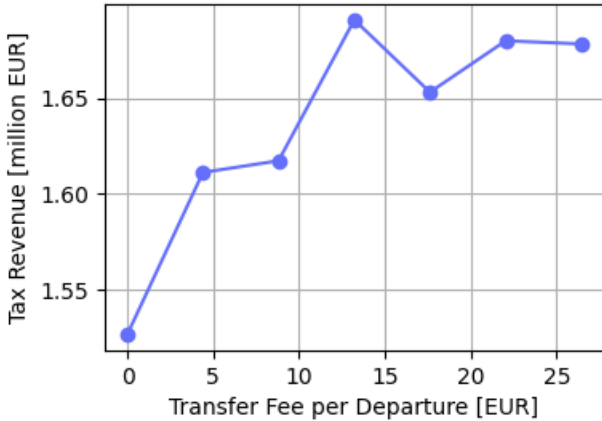


Figure 12: Tax revenue collected at AAS against the transfer tax.

5 Discussion

This paper presents a case study with the aim of gaining more insights into the effects that introducing a transfer tax at Amsterdam Airport Schiphol (AAS) may have on the traffic flows through the airport. The results of various scenarios with differing tax-levels are presented in the previous section. The scenarios start from a baseline that assumes no existing market shares between airlines. The results of the simulations show that implementing a transfer tax reduces the number of transfer passengers at AAS, but does not affect the local passengers. It should be noted that the number of transfer passengers at AAS is relatively small compared to the number of local passengers. Another observation is that the number of destinations remains fairly stable with respect to the baseline scenario. In addition, the total tax revenue increases when implementing a transfer tax. From these outcomes, it can be stated that the network quality of AAS barely degrades with respect to the baseline scenario. Another important conclusion, however, is that the results show that AAS would not be as large of a hub as it is in real-life, if a scenario without pre-existing market shares is assumed. In this discussion, the significance of these conclusions will be established by putting the scenarios in the context of real-life conditions, as well as results of the case-study presented by CE Delft [7].

5.1 Differing Baseline Scenario

One of the conclusions of the results is that AAS would not be a major hub when optimising the network using a greenfield approach, without any existing market shares. This is a different result than what could be expected when looking at the actual traffic flows at AAS. In reality, transfer passengers account for 37% of the total passenger flow at AAS, instead of the 15% that is obtained from the simulation [3]. This also applies to the other current major hubs, such as LHR, CDG and

FRA. The results show that most hubs have transfer flows that account for less than 25% of their departing traffic.

In addition, the results show that most destinations are flown with a daily frequency of one round-trip. Such operations also differ from what is expected at AAS, where there is at often at least a frequency of two trips per day to accommodate an incoming and outgoing wave at the start and end of the day. A possible explanation of this difference could be that the model does not take into account the number of frequencies in the model objective. Instead, the frequencies are only determined on the desired capacity of a route.

One important factor of the difference between the simulation results and the actual traffic flows is the use of a greenfield approach in the simulation. The model does not assume any current market shares, and instead only focuses on optimising for profit. By doing so, the tactical decisions are more influenced by the location of an hub airport and its landing and take-off fees. This would result in airports that are more centrally located and having cheaper airport fees being more desired for transfers. Only five hubs have a larger than 25% share attributed to transfer traffic. Four of these, OSL, KEF, HEL and DXB have relatively low airport fees and are situated on the edge or outside of the European continent, which allows them to act as a gateway for the continent.

Another explanation of the lower share of transfer passengers may be due to the cost of transfer itineraries. The costs of transfer itineraries are usually higher than that of direct itineraries, regarding fuel costs and airport fees. As there are no existing market shares in the model, passengers are flown in the most optimal and profitable manner as possible, which results in more direct flights. Transfer itineraries are still utilised in cases where a direct flight is not viable, and the transfer passengers are able to cover the marginal cost on the specific flights.

From these explanations, the significance of the conclusion can be established. The results show that, in reality, it is not a given for certain airports to act as a hub. Additional strategies, such as lower prices for transfer itineraries, could have been used to attract more transfer traffic. Otherwise, hubs would be better placed at the gateways of the continent for optimal passenger flows.

5.2 Network Quality of AAS

The second conclusion of the results is that increasing the transfer tax at AAS does not have a big impact at the network quality of the hub airport. It should be kept in mind that the share of transfer passengers at the hub was already low in the baseline scenario. Still, the effects of increasing the transfer tax was visible in the results of the simulations. The number of transfer passengers decreased at AAS and a large number of passengers were routed through nearby hubs.

The transfer tax case study can be compared with the study commissioned by the Dutch government with the same purpose of examining the effects of introducing a transfer tax at AAS. This study, performed by CE Delft [7], approaches the problem by simulating the

introduction of transfer fees using the AEOLUS-model. This model is capable of accounting for current market shares, which allows for a better representation of the current situation. Multiple scenarios are created with varying economic growth factors and varying restrictions in aircraft movements at AAS. The results show a similar trend regarding the number of passengers at AAS: the number of local passengers could either slightly decrease due to lower frequencies or slightly increase due to more available capacity, and the number of transfer passengers would decrease due to higher costs. In the low and high transfer tax scenarios, the expected decrease in transfer passengers would be around 18% and 33% respectively. In the results of this study, the decrease in these scenarios would be 12% and 42%. There is however a difference in the number of daily flights between the results. The study of CE Delft predicts a decrease of 5% and 10% in the low and high scenario, whereas this study only sees a minimal reduction of flights, as can be seen in Figure 9. The difference could be explained by the different shares of transfer passengers at AAS. As the results of this study only show a small share of transfer passengers, a decrease of transfer passengers would be less noticeable in the number of flights.

To perform a more fair comparison between the two models, the baseline scenario of the AND model should be revisited in order to better represent the actual network. However, the results can still be of significance in order to gain insights of the general effects that certain policies may have.

6 Conclusion

This study set out to investigate the effects that the proposed policy changes aiming to reduce the number of passengers at Amsterdam Airport Schiphol (AAS) might have on the network quality of the hub. In order to do so, a profit-based Airline Network Design (AND) model is formulated that is capable of simulating the passenger and aircraft flows through multiple hubs around Europe. As different passengers have different preferences for direct and connecting flights, multiple fare classes are implemented into the demand model. Each passenger class has a different time sensitivity, which affects the attractiveness of connecting flights.

With the AND model, a case study is carried out, investigating the effects of introducing an air passenger tax for transfer passengers. In 2023, passengers at AAS paid a tax of €26.43 per departure, while transfer passengers were exempt from this tax. In order to reduce the number of aircraft movements, the Dutch government proposed to introduce this tax for transfer passengers. Two scenarios were proposed: a tax of €13.22 per departure, resulting in €26.43 per round-trip, or €26.43 per departure, resulting in €52.26 per round-trip. This case study examined these scenarios, including five additional scenarios ranging between €0.00 and €26.43. The scenario with a transfer tax of €0.00 acts as a baseline scenario. These scenarios were optimised with a one-hour time limit, however, only near-optimal solutions were reached with a optimality gap around 6%.

The results of the scenarios show that a transfer tax does lead to a reduction in the number of transfer passengers: 12% and 42% for the low and high scenario respectively. However, the network quality in these scenarios is barely affected. This is explained as the baseline scenario shows a different ratio between the local and transfer passengers than in reality. Instead of 37%, the simulation only shows a share of 15% of transfer passengers at Amsterdam Airport Schiphol (AAS). The conclusion that the transfer tax barely degrades the network quality should therefore be put into context of the given baseline scenario. This result does show that when optimising using a greenfield approach, the hub would not be as large as it is in real-life, based on its location and costs.

To better understand the effects at Amsterdam Airport Schiphol it is recommended to improve the modelling of the baseline scenario. The model currently uses a greenfield approach, however, implementing market shares or by using an offset to calibrate the baseline would allow for a better representation of the actual network. In addition, the effect of the missing time dimension in the model could be investigated, which could affect the flight frequencies needed to fulfill certain itineraries. The last recommendation regards the optimisation method of the problem, which is currently not able to produce an optimal solution. Other optimisation techniques could be applied in order to reduce the computational time.

7 Recommendations

This section will elaborate on the set of recommendations for further research using the AND model. The first recommendation regards the set up of the baseline scenario in the AND model. The baseline scenario differs in certain aspects from reality, such as the sizes of hub airports and the transfer flows. In order to use the AND as a support tool, it is preferred to have a model that represents reality more accurately. An implementation of current market shares and a competitive market could result in a better representation of the market. In addition, a different system of modelling the non-hub airports would be required. Increasing the number of airports, increases the complexity of the model. However, an airline such as KLM operates by connecting many unique locations with its hub. In order to capture this business model, a more efficient method is needed that does not require each node to be modelled separately.

Another recommendation is to investigate the effects that the number of frequencies has on the network design. The frequency of a route can have an influence on the demand that a route has, but also influences the possible connections. The model currently does not take the connecting time into account. Instead, it is assumed that the itineraries on a given day have an average lay-over of 2 hours. This average could vary between itineraries and make some routes less desirable or result in connections that are not possible. Adding a time dimension makes the model more complex, but allows for more insights in the actual needed frequencies to fulfill certain itineraries, instead of only the general flow of passengers through the network.

The third recommendation regards the improvement of the simulation method of the AND model. The model currently is solved using the Gurobi MILP solver, which uses a Branch-and-Bound method combined with heuristics. The created AND problems are not consistently solved to optimality within one hour. Certain improvements have already been implemented to reduce the size of the problem. Further research would benefit from a faster optimisation method. This could, for example, be realised by implementing (meta)heuristic methods.

Finally, some recommendations regarding the possi-

bilities for future research can be given. This study focused on the introduction of a transfer tax at AAS, however, it is possible to test other forms of taxation. For example, levying a distance based tax or implementing a fuel tax. Such policies could also be applied to the European Union as a whole, instead of only applying to AAS. Besides increasing cost, it would also be possible to evaluate non-cost-related changes in the network. For example, it would be possible to evaluate the effects of a closed Russian airspace for certain airlines. The AND model could allow for evaluating a multitude of possible scenarios in further research.

References

- [1] ACI Europe. Airport industry connectivity report, 2023.
- [2] Bart De Jong. Schiphol Airport Amsterdam: to Understand the Past Is to Secure Future Economic Growth. In *46th Congress of the European Regional Science Association: "Enlargement, Southern Europe and the Mediterranean"*. Louvain-la-Neuve: European Regional Science Association (ERSA), 2006.
- [3] Amsterdam Airport Schiphol. Schiphol verwelkomde 61,7 miljoen reizigers in 2023, 2023.
- [4] Stefan Grebe and Marco Kouwenhoven. Effects of an aviation tax on aviation in the Netherlands. 2019.
- [5] Jasper Faber and Lisanne van Wijngaarden. Economic and sustainability impacts of an aviation tax: New variants. 2019.
- [6] Stefan Grebe and Christiaan Meijer. Effecten van een verhoging van de vliegbelasting. 2022.
- [7] Christiaan Meijer. Effecten includeren transferpassagiers in de vliegbelasting. 2023.
- [8] Significance. AEOLUS Documentatie versie 2.0.
- [9] Rui Neiva, Aleix Pons, Gareth Horton, Christian Lutz, Martin Distelkamp, Raquel de Luis Iglesias, Olivia Brajterman, Andre van Velzen, and Alice Pirlot. Study on the taxation of the air transport sector. 2021.
- [10] Morton E. O’Kelly. The Location of Interacting Hub Facilities. *Transportation Science*, 20(2):92–106, May 1986.
- [11] Morton E. O’kelly. A quadratic integer program for the location of interacting hub facilities. *European Journal of Operational Research*, 32(3):393–404, December 1987.
- [12] Luiza Bernardes Real, Morton O’Kelly, Gilberto de Miranda, and Ricardo Saraiva de Camargo. The gateway hub location problem. *Journal of Air Transport Management*, 73:95–112, October 2018.
- [13] James F. Campbell. Locating transportation terminals to serve an expanding demand. *Transportation Research Part B: Methodological*, 24(3):173–192, June 1990.
- [14] Andreas T. Ernst and Mohan Krishnamoorthy. Efficient algorithms for the uncapacitated single allocation p -hub median problem. *Location Science*, 4(3):139–154, October 1996.
- [15] Patrick Jaillet, Gao Song, and Gang Yu. Airline network design and hub location problems. *Location Science*, 4(3):195–212, October 1996.
- [16] Sibel A. Alumur, James F. Campbell, Ivan Contreras, Bahar Y. Kara, Vladimir Marianov, and Morton E. O’Kelly. Perspectives on modeling hub location problems. *European Journal of Operational Research*, 291(1):1–17, May 2021.
- [17] Chieh-Yu Hsiao and Mark Hansen. A passenger demand model for air transportation in a hub-and-spoke network. *Transportation Research Part E: Logistics and Transportation Review*, 47(6):1112–1125, November 2011.
- [18] Lie Han and Ning Zhang. P-Hub Airline Network Design Incorporating Interaction Between Elastic Demand and Network Structure. In W. Eric Wong and Tinghuai Ma, editors, *Emerging Technologies for Information Systems, Computing, and Management*, Lecture Notes in Electrical Engineering, pages 89–96, New York, NY, 2013. Springer.
- [19] Morton E. O’Kelly, Henrique Pacca L. Luna, Ricardo S. de Camargo, and Gilberto de Miranda. Hub Location Problems with Price Sensitive Demands. *Networks and Spatial Economics*, 15(4):917–945, December 2015.
- [20] Eurostat. Commercial flights by reporting country, 2024.
- [21] Mark Wardman, V. Phani K. Chintakayala, and Gerard de Jong. Values of travel time in Europe: Review and meta-analysis. *Transportation Research Part A: Policy and Practice*, 94:93–111, December 2016.

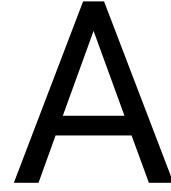
- [22] Airfinance Journal. Air investor 2023, 2023.
- [23] EASA. Review of standard passenger weights - EASA.2021.C24, October 2022.
- [24] Eurocontrol. Airport capacity imbalance study, 2020.
- [25] Airline Route & Ground Services. Turkey's istanbul airport ready to rise together with third independent runway, 2020.
- [26] Isavia. Runway and technical information, 2024.
- [27] Airport Coordination Limited. Slot performance committee & slot adherence policy for airlines & aircraft operators at dubai international airport, 2020.
- [28] J. Thorbeck and Z. Scholz. DOC - assesment method, 2019.
- [29] de Belastingdienst. Aviation tax, 2024.
- [30] Amsterdam Airport Schiphol. Schiphol Airport traffic figures, 2024.

This page is intentionally left blank.

II

Appendix

This page is intentionally left blank.



Determining Operational Costs

This appendix will show the calculation methods used to determine the operational costs in the [Airline Network Design \(AND\)](#) model. The TU Berlin DOC method is used to calculate the operational costs and is presented in [section A.1](#). This method does not differentiate between airports for take-off and landing fees. The determination of the airport fees is therefore presented separately in [section A.2](#). The fuel burn calculations needed to determine the fuel costs are presented in [section A.3](#).

A.1. Aircraft Operational Costs

The aircraft operational costs are determined using the TU Berlin DOC method presented by J. Thorbeck and D. Scholz (2013) [7]. The method uses empirical formulas to estimate the elements of the operational costs. The operational costs are divided into fixed and variable costs. The next two subsections will look into the method of determining these costs.

A.1.1. Fixed Costs

The fixed costs of a flight represent the capital costs, depreciation and insurance of the aircraft, but also the salaries of the crew. The capital costs, C_{CAP} , are determined based on a linear function of the [Operational Empty Weight \(OEW\)](#). The formula for the capital costs is shown in [Equation A.1 - A.2](#). The aircraft specific inputs of the formula are the [OEW](#), the aircraft engine weight (W_{Eng}), and the number of engines (N_{Eng}). The parameters of the formula are as follows:

- P_{OEW} : price per kg OEW of 1150 [€/kg]
- P_{Eng} : price per engine weight of 2500 [€/kg]
- IR: interest rate of 5%
- DP: depreciation period of 14 years
- f_{RV} : residual value of 10%
- f_{ins} : insurance rate of 0.5%

$$C_{CAP} = [P_{OEW}(OEW - W_{Eng}N_{Eng}) + W_{Eng}N_{Eng}P_{Eng}] (a + f_{ins}) \quad (A.1)$$

$$\text{with } a = IR \frac{1 - f_{RV} \left(\frac{1}{1+IR}\right)^{DP}}{f_{RV} \left(\frac{1}{1+IR}\right)^{DP}} \quad (A.2)$$

The determination of the crew costs is based on the number of seats on the aircraft. The formula for the crew cost is shown in [Equation A.3](#). There is one flight attendant for each 50 passengers. The total number of flight attendants is given as n_{FA} . The cost per flight attendant, S_{FA} , is €60.000 per year, and the cost for a flight crew of two pilots, S_{FC} , is €300.000 per year. The crew complement, CC , indicates the number of crew per aircraft and is assumed to be 5.

$$C_{crew} = CC(S_{FA}n_{FA} + S_{FC}) \quad (A.3)$$

The total fixed costs per year can be represented as $C_1 = C_{CAP} + C_{crew}$. To determine the fixed costs per operational hour, an average number of operational hours is determined per aircraft. First, the method assumes a yearly number of operational days of 353.6, which removes time dedicated to C- and D-checks, as well as a statistical number of days for repairs. The average block hours per day is obtained from the Airline Data Project of MIT [2]. The hourly fixed costs are calculated by dividing the yearly fixed costs by the average yearly block hours. The input data for the equations specified per aircraft are shown in Table A.1.

A.1.2. Variable Costs

The second part of the operational cost is the variable or route dependent cost. This cost consists of the following elements: fuel, handling, airport fees, air traffic control, and maintenance. The handling costs and airport fees calculations are omitted as the airport specific costs are calculated separately per airport and is discussed in section A.2. The resulting costs are calculated using the formula shown in Equation A.4. The first part of the formula is the fuel cost. The fuel cost per liter, P_f , is assumed to be €0.541. The calculations for the total fuel per flight, TF, are presented in section A.3. The next part of the formula is the air traffic control costs, which is based on the **Maximum Take-Off Weight (MTOW)** of the aircraft and a price factor, $f(R)$, which is assumed to be 1. The third element is the maintenance cost, MC. The maintenance cost is determined using Equation A.5 - A.8.

$$C_2 = P_f \cdot TF + f(R) \cdot \sqrt{\frac{MTOW}{50}} + MC \quad (A.4)$$

The maintenance costs are split into three parts: the airframe material costs, MC_{MAT} , the airframe personnel costs, MC_{PER} , and the engine maintenance costs, MC_{ENG} . The inputs of these empirical formulas are: the **OEW**, the flight time, FT, the sea-level static thrust of one engine, SLST, the number of engines, N_{ENG} , and the labor rate, LR, of €50 per hour.

$$MC = MC_{MAT} + MC_{PER} + MC_{ENG} \quad (A.5)$$

$$MC_{MAT} = OEW \cdot (0.21 \cdot FT + 13.7) + 57.5 \quad (A.6)$$

$$MC_{PER} = LR \cdot 3 \cdot [(0.655 + 0.01 \cdot OEW) \cdot FT + 0.254 + 0.01 \cdot OEW] \quad (A.7)$$

$$MC_{ENG} = N_{ENG} \cdot (1.5 \cdot SLST + 30.5 \cdot FT + 10.6) \quad (A.8)$$

The total costs of a flight be found by combining the fixed and variable costs. The parameters per aircraft type used in the model are shown in Table A.1. The fixed costs per hour that are obtained from these inputs are shown in Table A.2.

Table A.1: Input data for the DOC method of the aircraft used in the model.

	MTOW [to]	OEW [to]	W_{eng} [kg]	N_{eng}	Seats	Avg. Block Hours	SLST [to]
Boeing 777-300ER	352	168.6	8282.6	2	381	13	52.2
Airbus A350-900	245	126.1	7277.0	2	300	13	38.2
Airbus A321neoLR	97	51.1	3071.5	2	210	11	15.0
Airbus A320neo	79	44.8	3071.5	2	150	11	12.3
Embraer E195-E2	49	28.9	2177.0	2	132	9	10.3

Table A.2: Fixed costs per hour, allocated to depreciation and crew, for the aircraft used in the model.

	Fixed	Depreciation	Crew
Boeing 777-300ER	€5,792	€4,969	€824
Airbus A350-900	€4,498	€3,780	€718
Airbus A321neoLR	€2,529	€1,819	€710
Airbus A320neo	€2,242	€1,625	€617
Embraer E195-E2	€2,015	€1,295	€720

A.2. Airport Fees

The method of determining the airport specific charges vary per airport. The charges will be categorised in aircraft dependent and passenger dependent charges. For each hub airport, the charges are obtained by consulting the publicly available airport charges guidelines. An example cost table of [Amsterdam Airport Schiphol](#) is shown in [Figure A.1](#) and [Figure A.2](#) [3]. The table shows the landing and take-off fees per 1000kg for different periods of the day and for different aircraft noise categories. The minimum charge is based of a *MTOW* of 20.000 tonnes and additional surcharges are applied for noisy aircraft in category s1 and s2. There is also a NOx charge based on aircraft data of NOx emissions during a standardised landing and take-off cycle. Besides the aircraft specific charges, there are also passenger specific charges, which are shown in [Figure A.2](#). [Amsterdam Airport Schiphol](#) has different fees for local and transfer passengers. Certain airports also charge different security fees based on the origin or destination of passengers, such as when entering or leaving the Schengen zone.

Landing and take-off (€) as per April 1, 2023 (Charge per 1,000 kg)	Category S1			Category S2		
	Day	Night		Day	Night	
	landing/ take-off	landing	take-off	landing/ take-off	landing	take-off
Connected	10,90	27,25	32,70	7,90	12,26	13,63
Disconnected	8,72	21,80	26,16	6,32	9,81	10,90
Cargo flight	5,67	14,17	17,00	4,11	6,38	7,09

Figure A.1: Landing and take-off fees for different periods of the day and 2 aircraft noise categories. There are in total 7 categories.

Nox charge		
per kg Nox emission		€ 4,00

Passenger charges		
Passenger Service Charge	Schiphol Centre	Schiphol East
per departing local passenger	€ 20,62	€ 16,50
per departing transfer/transit passenger	€ 8,65	€ 6,89
Security Service Charge		
per departing local passenger	€ 15,12	€ 15,12
per departing transfer/transit passenger	€ 8,46	€ 8,46

Parking charge	
per 1.000 kg per full day	€ 2,33

Figure A.2: NOx charges, passenger charges, and parking charges at [Amsterdam Airport Schiphol](#).

To implement the airport fees into the model, the costs have been divided between aircraft and passenger specific costs. Certain airports have different fees for departures and arrivals. To ensure that the costs in the network remain symmetric, the arrival and departure costs are averaged per airport. The passenger charges are added for each additional passenger on a given route. The passenger charges are again averaged between departing and arrival passengers to ensure symmetry. The passenger fees are specified for intra-Europe and inter-Europe travel, as well as for local and transfer passengers. A summary of the charges is shown in [Table A.3](#).

Table A.3: Landing/take-off charges specified per aircraft type and passenger charges specified for inter/intra Europe travel and local/transfer passengers.

	B777	A350	A321	A320	E195	OD Europe	OD non Europe	Transfer Europe	Transfer non Europe
AMS	€2,776.85	€668.85	€264.81	€172.22	€106.38	€17.87	€17.87	€8.56	€8.56
IST	€1,743.44	€1,215.20	€481.12	€391.84	€242.05	€6.72	€6.72	€6.72	€6.72
LHR	€1,131.17	€863.47	€795.66	€799.17	€767.26	€22.21	€22.21	€16.66	€16.66
FRA	€1,235.78	€801.25	€380.18	€316.75	€253.93	€10.72	€14.60	€7.62	€7.62
CDG	€1,485.44	€1,001.26	€462.15	€396.61	€286.66	€5.46	€12.57	€3.28	€7.54
MAD	€1,494.80	€1,062.10	€460.80	€387.67	€264.97	€8.16	€10.79	€4.89	€6.47
BCN	€1,326.69	€942.52	€408.65	€343.72	€234.79	€7.72	€9.04	€4.63	€5.42
MUC	€1,066.44	€700.41	€394.84	€358.84	€288.88	€11.37	€12.01	€7.82	€8.25
FCO	€931.09	€767.39	€415.69	€365.29	€244.89	€14.67	€18.11	€4.02	€6.96
ATH	€886.13	€713.58	€375.88	€306.13	€170.31	€7.45	€9.10	€0.00	€0.00
VIE	€703.00	€490.00	€194.00	€158.00	€97.60	€11.37	€12.01	€7.82	€8.25
DUB	€3,083.38	€1,714.70	€769.80	€645.60	€486.02	€6.15	€6.15	€1.25	€1.25
ZRH	€1,278.05	€1,083.05	€356.20	€356.20	€356.20	€12.00	€12.00	€7.50	€7.50
CPH	€1,018.13	€709.65	€280.96	€228.83	€141.35	€9.22	€9.22	€5.01	€5.01
LIS	€3,335.74	€1,707.69	€763.30	€562.10	€333.41	€8.00	€12.84	€6.48	€10.15
OSL	€467.21	€399.42	€254.61	€225.97	€136.22	€4.92	€4.92	€1.57	€1.57
KEF	€1,315.98	€991.16	€531.11	€473.83	€304.33	€10.30	€10.30	€2.49	€7.81
HEL	€1,414.25	€1,161.32	€371.36	€316.28	€223.87	€7.71	€7.71	€5.08	€5.08
BRU	€2,776.85	€668.85	€264.81	€172.22	€106.38	€17.87	€17.87	€8.56	€8.56
DXB	€885.32	€614.29	€237.64	€191.83	€114.97	€15.13	€15.13	€5.04	€5.04

A.3. Fuel Calculations

The fuel calculation of these aircraft is performed using the Piano-X analysis tool. The tool takes into account the performance of the aircraft type to calculate the required fuel for a given scenario, with variables such as the block range and the payload weight. Quadratic functions are created with the program for the five different aircraft types, which are implemented in the AND model in order to determine the fuel burn for a given flight. The results of these functions will be compared with published data on the fuel burn of these aircraft and is presented in [subsection B.2.1](#). The terms of the quadratic equation are presented in [Table A.4](#).

Table A.4: Generated fuel equations from Piano-X for the five aircraft in the model.

	ad^2	bd	c
Boeing 777-300ER	0.0005	11.903	2783.2
Airbus A350-900	0.0003	8.4066	1829.3
Airbus A321neoLR	0.0002	5.0145	623.32
Airbus A320neo	0.0002	4.1638	578.28
Embraer E195-E2	0.0002	3.8673	663.23

B

Verification and Validation

This appendix will show the verification and validation procedure that has been applied to the [Airline Network Design \(AND\)](#) model. The purpose of the model verification is to ensure that the results of the simulations correspond with the expected results. The verification procedure is discussed in [section B.1](#). The purpose of the model validation is to determine if the model results are able to represent the real world. The validation procedure is presented in [section B.2](#).

B.1. Verification

The purpose of verification is to ensure that the simulation results correspond with the expected results of the model. The [AND](#) will be tested by simulating multiple small scenarios that can be solved analytically, in order to verify the results. The scenarios assume a set of three dummy airports with one hub where transfers can occur. A map of the airport network is shown in [Figure B.1](#), which includes the distances. Airport 0 is the hub in the network. Two aircraft types are used in the scenarios: type 0 with a capacity of 100 passengers, a range of 800 km, and a cost of €50 per km, and type 1 with a capacity of 200 passengers, a range of 1200 km, and a cost of €90 per km. Additional inputs are specific for each test

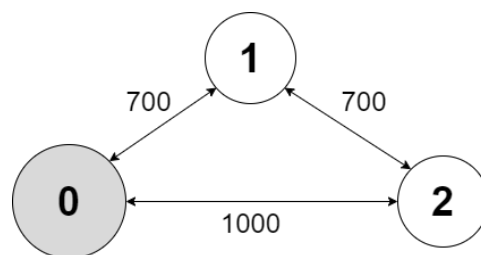


Figure B.1: Map with distances between dummy airports. Airport 0 is indicated as hub.

B.1.1. Aircraft Capacities

The first set of tests regards the capacities of aircraft in the model. These test verify whether the model correctly takes into account the seating capacity of aircraft, when choosing the number of aircraft on a route. Test set 1 only uses aircraft type 1 with a capacity of 100 seats. Test set 2 uses both aircraft type 1 and 2 with capacities of 100 and 200 seats respectively.

#	Test	Explanation	Expected Output	Passed
1.1	There is a demand of 50 passengers between airport 0 and 1	This demand is not enough to cover the cost of the aircraft	No passengers are transported	Yes
1.2	There is a demand of 51 passengers between airport 0 and 1	This demand covers the cost of the aircraft	All 51 passengers are transported	Yes
1.3	There is a demand of 151 passengers between airport 0 and 1	This demand covers the cost of the first and second aircraft	All demand is transported and two aircraft are utilised	Yes

#	Test	Explanation	Expected Output	Passed
2.1	There is a demand of 141 passengers between airport 0 and 1	There is more demand than what could be transported with aircraft type 1. The demand covers the cost of aircraft type 2	All passengers are transported with aircraft type 2	Yes
2.2	There is a demand of 251 passengers between airport 0 and 1	There is more demand than what could be transported with aircraft type 2. The demand covers the cost of aircraft type 1 and 2	All passengers are transported with one aircraft of both type 1 and 2	Yes
2.3	There is a demand of 341 passengers between airport 0 and 1	The demand covers the cost of two aircraft of type 2	All passengers are transported using 2 aircraft of type 2	Yes

B.1.2. Aircraft Range

The third set tests whether the ranges constraint of aircraft is correctly implemented in the model. The tests focus on the route between airports 0 and 2, which is outside the range of aircraft 1.

#	Test	Explanation	Expected Output	Passed
3.1	There is a demand of 90 passengers between airport 0 and 2	The distance between airport 0 and 2 would require aircraft type 2, but the demand would not cover the operational costs	No passengers are transported	Yes
3.2	There is a demand of 91 passengers between airport 0 and 2	The distance between airport 0 and 2 would require aircraft type 2 and the demand covers the operational costs	All passengers are transported using 1 aircraft of type 2	Yes

B.1.3. Implementing Non-Direct Routes

The fourth set tests the behaviour of selecting non-direct routes. Connections can only be done through selected hubs.

#	Test	Explanation	Expected Output	Passed
4.1	There is a demand of 1 passenger between airports 1 and 2 and there are flights between airport 0-1 and 0-2	The demand is not enough for a flight between 1 and 2, but the demand can be flown with a connection at airport 0	The demand between airports 1 and 2 is fulfilled through hub 0	Yes
4.2	There is a demand of 1 passenger between airports 0 and 1, a demand of 90 between airports 1 and 2, and there is a flight between 0 and 2	There is no spoke to airport 1 from hub 0, but the demand between 1 and 2 could make a spoke possible in addition to the demand between 0 and 1	All passengers are routed through hub 0	Yes

B.1.4. Airport Capacity

The fifth set tests the implementation of the airport capacity constraint

#	Test	Explanation	Expected Output	Passed
5.1	There is a demand of 300 between airports 0 and 1, which have a capacity of 2 departures. Only small aircraft are available.	There is more demand than aircraft capacity on the route	Only 200 passengers are transported on 2 aircraft each way	Yes
5.2	There is a demand of 300 between airports 0 and 1, which have a capacity of 2 departures. The small and large aircraft are available.	To fulfill the demand within 2 departures, both a small and a large aircraft are needed	All passengers are transported using 1 aircraft of type 1 and 2	Yes

B.1.5. Airport Fees

The sixth set tests whether the airport fees are correctly implemented in the cost function. These tests assume a fee of €50 per departure. For transfer itineraries there is a discount: instead of €100 for two departures, the cost is set at €75. This is to reflect the reduced fee for transfer passengers at hub airports.

#	Test	Explanation	Expected Output	Passed
6.1	There is a demand of 100 between airports 0 and 1	This test shows if the profit takes into account the airport fee on a direct route	The total profit should be 100*50 less than in the case without fees	Yes
6.2	There is a demand of 54 between airports 0 and 1, and a demand of 95 between airports 0 and 2	Due to higher costs, the required demand is slightly higher than the previous case of 51 and 91	All the demand is transported and the profit is 700	Yes

B.1.6. Passenger Classes

The seventh set test the effect of the passenger classes in the model. The tests assume an economy and business class, where the business class has doubled fares.

#	Test	Explanation	Expected Output	Passed
7.1	There is a demand of 100 economy passengers and 20 business passengers between 1 and 2	An all economy demand of 120 would not be sufficient for a larger aircraft on the route, but the higher fares covers the costs	All the demand is transported using 1 aircraft of type 2	Yes
7.2	There is a demand of 60 economy and 60 business passengers between 1 and 2, and there are flights to hub 0 with available space for 60 passengers	A passenger class does not split itself on multiple routes, but the 120 passengers do not fit on one aircraft.	Only 40 economy and all 60 business passengers are transported between airport 1 and 2 using an aircraft of type 1, as an of aircraft type 2 would cost more money	Yes
7.3	There is a demand of 30 economy and 90 business passengers between 1 and 2, and there are flights to hub 0 with available space for 60 passengers	There is not enough space for all 120 passengers on one aircraft. The 30 economy passengers can either be routed with a connection, or only 10 tickets are offered	The 30 economy passengers are routed with a connection and the 90 business passengers fly direct between airports 1 and 2	Yes

B.2. Validation

The validation step of the model entails determining if the results of the model are able to represent the physical problem. The validation step of the model is more difficult to perform. The aim of the model is to identify the effects of policy changes in a world-wide airport network. Validation with historic data would be impossible, as there would be too many variables to consider to link historic policy changes to the perceived effects. Similarly, validating if the fare inputs are realistic, would require knowing the composition of passengers on all operated flights. Instead, more focus is given towards validating the costs of the model. The operational costs are not directly obtained from data, but are determined from several models. Two different methods are used: one for the fuel calculation and one for the direct operational costs. The following sections will show the validation of these methods.

B.2.1. Fuel Calculation

The fuel calculation of these aircraft is performed using the Piano-X analysis tool. The tool takes into account the performance of the aircraft type to calculate the required fuel for a given scenario, with variables such as the block range and the payload weight. Quadratic functions are created with the program for the five different aircraft types, which are implemented in the [AND](#) model in order to determine the fuel burn for a given flight. The results of these functions will be compared with published data on the fuel burn of these aircraft.

The data that will be used is published in the Airfinance Journal [1], which shows estimates of the fuel burn for different block ranges for a large set of commercial aircraft. The set did not cover the Airbus A321neoLR, which is used in the [AND](#) model. Therefore, the data of the Airbus A321neo will be used to compare the calculations.

The published fuel data and the calculated fuel burn for the various block ranges are shown in [Table B.1 - B.5](#). When comparing the calculations and the fuel data, it can be seen that the fuel burns are quite similar. The differences are around 10% or less. The biggest difference is seen in the Airbus A321neoLR. The large difference could be explained by the use of data of a slightly different aircraft, the Airbus A321neo. The results also show that the for most aircraft the difference is greatest at the lower block ranges. This difference could be explained by the use of a standard range for the reserve fuel in all flights. For shorter flights, this could be overestimated slightly.

All the results do show a slight underestimation of the fuel burn. However, the ratios between the fuel burns of the aircraft are similar to that of the data. The impact on the tactical decision making regarding the type of aircraft should therefore not be affected. This method of fuel calculation will therefore be maintained.

Table B.1: Fuel burn data for different block ranges compared to calculated fuel burn for the Boeing 777-300ER.

Boeing 777-300ER			
Block Range [nmi]	Fuel Data [kg]	Fuel Calculated [kg]	Difference
1000	15,610	15,186	-3%
2000	29,840	28,589	-4%
4000	60,900	58,395	-4%

Table B.2: Fuel burn data for different block ranges compared to calculated fuel burn for the Airbus A350-900.

Airbus A350-900			
Block Range [nmi]	Fuel Data [kg]	Fuel Calculated [kg]	Difference
1000	11,810	10,536	-12%
2000	22,010	19,842	-11%
4000	42,410	40,256	-5%

Table B.3: Fuel burn data for different block ranges compared to calculated fuel burn for the Airbus A321neoLR.

Airbus A321neoLR			
Block Range [nmi]	Fuel Data [kg]	Fuel Calculated [kg]	Difference
200	1,960	1,634	-20%
500	3,600	3,181	-13%
1000	6,450	5,838	-10%

Table B.4: Fuel burn data for different block ranges compared to calculated fuel burn for the Airbus A320neo.

Airbus A320neo			
Block Range [nmi]	Fuel Data [kg]	Fuel Calculated [kg]	Difference
200	1,570	1,419	-11%
500	2,880	2,710	-6%
1000	5,170	4,942	-5%

Table B.5: Fuel burn data for different block ranges compared to calculated fuel burn for the Embraer E195-E2.

Embraer E195-E2			
Block Range [nmi]	Fuel Data [kg]	Fuel Calculated [kg]	Difference
200	1,260	1,445	13%
500	2,440	2,647	8%

B.2.2. Direct Operational Costs

The direct operating costs in the model are calculated using the **Direct Operational Cost (DOC)** method of the TU Berlin. This method calculates the operational costs of a certain aircraft type using empirical formulas based on certain characteristics of the aircraft and the block distance. The calculated costs of the **DOC** method will be compared with standard economic data published by Eurocontrol, which states estimates of operational costs per flight hour [5].

The data set contains a small set of aircraft families. Three of the five aircraft of the **AND** model are present in the data: the Boeing 777, the Airbus A320, and the Embraer 190. For these aircraft, an average flight time per cycle is given. These are 6, 2, and 1.5 hours for the given aircraft types. The operational costs in the model are calculated based on a distance. Therefore, to obtain the operational costs, the average cruise speed of each aircraft type is multiplied by the average flight time of Eurocontrol. In addition, the **AND** model adds a block time of 1.83 to flight cycle, which accounts for the fixed costs of the aircraft, such as crew costs.

The data of the hourly flight costs and the calculated hourly costs are presented in **Table B.6 - B.8**. The table shows the different components of the **DOC** method that result in the total calculated cost. The results show that the costs of the Boeing 777 is similar, whereas the costs of the short-range aircraft is underestimated in the calculations. A possible explanation could be the implementation of the block time per aircraft. All aircraft are assumed to have the same block time, however, it could be expected that the short-range aircraft have a shorter block time. If the block time for the short-range aircraft is assumed to be only 1 hour, the hourly costs are changed to around €4500 and €4000 for the Airbus A320 and the Embraer E195. This corresponds better with the data. This difference should not have an influence in the model, as the total flight cycle cost would still result in the same cost per flight cycle.

Table B.6: Operational cost per hour from data compared to the calculated costs for the Boeing 777-300ER.

Boeing 777-300ER	
Data	€9,507
Calculated	€10,150
- Fuel	€2,719
- Maintenance	€706
- ATC	€932
- Fixed	€5,792
- Depreciation	€4,969
- Crew	€824

Table B.7: Operational cost per hour from data compared to the calculated costs for the Airbus A320neo.

Airbus A320neo	
Data	€4,829
Calculated	€3,478
- Fuel	€611
- Maintenance	€341
- ATC	€284
- Fixed	€2,242
- Depreciation	€1,625
- Crew	€617

Table B.8: Operational cost per hour from data compared to the calculated costs for the Embraer E195-E2.

Embraer E195-E2	
Data	€4,097
Calculated	€2,967
- Fuel	€501
- Maintenance	€270
- ATC	€180
- Fixed	€2,015
- Depreciation	€1,295
- Crew	€720

C

Sensitivity Analysis

This appendix will show the sensitivity analysis that has been performed on the [Airline Network Design \(AND\)](#) model. The purpose of the sensitivity analysis is to gain insight into the effects that the assumptions on the inputs may have on the results of the model. The assumptions of the model mostly regard the set-up of the demand and fares in the network: the implementation of the [Value of Time \(VOT\)](#), the ratio between the fares, the level of ticket tax, and the ratio of demand between the passenger classes. In the sensitivity analysis, multiple scenarios with varying inputs will be simulated, after which an analysis of the results is given. The results of the scenarios will be presented in a table of the key traffic figures of [Amsterdam Airport Schiphol \(AAS\)](#), in addition to the results of the baseline scenario.

C.1. Value of Time

The [Value of Time \(VOT\)](#) represents the perceived value lost by the passenger by flying a non-direct route, instead of a direct route. The [VOT](#) is added into the cost model in order to take into account the effect of time sensitivity of the multiple types of passengers in the model. The current method assumes that budget, economy and business class passengers perceive a value of 20, 40 and 80 per hour in the air respectively. Only half of the value is perceived during a lay-over.

Three scenarios are tested in the sensitivity analysis. The first scenario (A) assumes no [VOT](#) at all for all passengers. This would mean that a transfer flight and a direct flight would be equal in cost for a passenger. The next two scenarios will assume a low and a high [VOT](#): scenario (B) assumes a very low [VOT](#). Budget, economy and business class would perceive a value of 1, 2 and 4 per hour in the air respectively. Scenario (C) assumes double the [VOT](#) than the base values. The last scenario will look at the influence of halving the perceived value during lay-overs. Scenario (D) will not include the halved perceived values during a lay-over. An overview of the scenarios is shown in [Table C.1](#)

Table C.1: Changed [Value of Time](#) values in the air and during a lay-over in the sensitivity scenarios compared to the baseline inputs.

	Value of Time		
	Budget	Economy	Business
Baseline	€20 / €10	€40 / €20	€80 / €0
A	€0 / €0	€0 / €0	€0 / €0
B	€1 / €0.5	€2 / €1	€4 / €2
C	€40 / €20	€80 / €40	€160 / €80
D	€20 / €20	€40 / €40	€80 / €80

The results of the simulations are shown in [Table C.2](#). The optimality gaps of the simulations are given as well, as there was no optimal solution reached within the simulation limit of one hour. There are a few observations that can be made: the first thing that can be noticed, is that there is not much fluctuation between the different scenarios. The total number of local and transfer passengers during the simulated day deviate by less than

a thousand passengers. The number of destinations also only vary by a few. This shows that the monetary value in each scenario does not greatly affect the simulation outcome. However, one trend is still visible in the data: the number of transfer passengers decreases when the VOT is increased. This was expected, as a higher VOT, would discourage transfers. In addition, it can be seen that not halving the VOT during lay-overs results in comparable figures as in scenario C. This may indicate that most transfer itineraries are mostly influenced by the transfer time, rather than the additional flight time of a non-direct itinerary. It should be noted that the slight differences between the scenarios could be attributed to not having reached the optimal solution during the simulation.

Table C.2: Key figures of the sensitivity analysis on the Value of Time.

	Base	A	B	C	D
Optimality Gap	6.56 %	3.56 %	4.72 %	3.94 %	3.97 %
Europe destinations	103	106	105	108	107
Intercontinental Destinations	65	65	63	67	69
# Aircraft	732	756	734	758	756
# Local Passengers	57746	58944	57174	59108	59070
- Class 0	6340	6826	6295	6938	6914
- Class 1	40280	40737	39780	40964	40882
- Class 2	11126	11381	11099	11206	11274
# Transfer Passengers	10404	11614	11410	11165	10976
- Class 0	1598	1564	2030	1805	1911
- Class 1	7188	7830	7392	7596	7423
- Class 2	1618	2220	1988	1764	1642

C.2. Fare Ratio

The demand model assumes that there are three passenger classes in the network: budget, economy and business. Each of these classes has its own fare. The fares are determined using the AirportIS dataset from [International Air Transportation Organisation \(IATA\)](#), where average fares are presented for a given city-pair market. From this average fare, a base fare is determined for the economy class. The base model assumes that business class passengers pay 200 % of the base fare, and budget passengers pay 80% of the base fare. This gives a ratio of 0.8 : 1 : 2 between the three classes.

Three scenarios are created to get insights into the effect of the share that each fare class pays. The first scenario (A) assumes that budget class passengers are only able to pay a small amount. The budget fare is set to 20 % of the base fare. The second scenario (B) assumes that business class passengers are able to pay a larger share. The business fare is set to 400 % of the base fare. The third scenario (C) combines both the smaller and larger share that budget and business class passengers are able to pay. An overview of the scenarios is shown in [Table C.3](#)

Table C.3: Changed fare ratio variables in the sensitivity scenarios compared to the baseline inputs.

	Fare Ratio		
	Budget	Economy	Business
Baseline	0.8	1.0	2.0
A	0.2	1.0	2.0
B	0.8	1.0	4.0
C	0.2	1.0	4.0

The results of the simulates are shown in [Table C.4](#). The first observation of the results is that it can be seen that the number of business class passengers remains fairly constant or even grows in the simulations. From the results, it can be concluded that the fares of business class passengers determine the number of lower classes needed. In the case that it is assumed that the business class has a higher fare, there are less passengers of the other classes needed to cover the costs of a flight. When the fares of the budget class are reduced, the

result is that most passengers are dropped, except for some budget class passengers that might cover the marginal costs of a flight.

Table C.4: Key figures of the sensitivity analysis on the ratio between the fares.

	Base	A	B	C
Optimality Gap	6.56 %	4.15 %	4.33 %	4.07 %
Europe destinations	103	107	101	99
Intercontinental Destinations	65	62	60	59
# Aircraft	732	694	562	536
# Local Pax.	57746	51935	43205	40121
- Class 0	6340	505	3615	361
- Class 1	40280	40103	28265	28456
- Class 2	11126	11327	11325	11304
# Transfer Pax.	10404	11862	8350	9431
- Class 0	1598	55	1215	15
- Class 1	7188	9102	5080	6730
- Class 2	1618	2705	2055	2686

C.3. Ticket Tax

The fares are determined using the AirportIS dataset from [IATA](#). This dataset includes average fares on a given city-pair market, however, these fares do not include the taxes and fees that passengers had to pay for the tickets. The additional fees can contribute a considerable amount to the final price of a given itinerary. The baseline model assumes that the budget and economy passengers pay an additional 50% of the average fare on taxes and fees. For business class passengers, it is assumed that an additional 20% of the fare is added.

For this analysis, three scenarios are created that will vary the additional taxes and fees for the three passenger classes. The first scenario (A) assumes that there are no additional costs to the determined fare for each passenger class. The second scenario (B) assumes the same low percentage of 20% for all passenger classes. The last scenario (C) assumes the same high percentage of 50% for all passenger classes. An overview of the scenarios is shown in [Table C.5](#)

Table C.5: Changed tax rate variables in the sensitivity scenarios compared to the baseline inputs.

	Tax Rate		
	Budget	Economy	Business
Baseline	50%	50%	20%
A	0%	0%	0%
B	20%	20%	20%
C	50%	50%	50%

The results of the simulations are shown in [Table C.6](#). The results show that a reduction of the ticket tax to 20% or 0% would reduce the passenger flows of the network. This is to be expected as this additional tax on top of the fares also includes airline fees that are used to cover the airlines operating costs. By reducing these fees, the routes become less profitable for the airline. The local traffic flows of the baseline were already comparable to the actual local traffic flows of the network. Observations regarding business class show that if there is no tax, the share of business transfers is almost doubled, and if the tax is increased, there is almost no significant change. This could show that the business class already covers most part of the operational costs of a flight, and if its share is reduced, more passengers are needed to cover the costs of a flight.

Table C.6: Key figures of the sensitivity analysis on the ticket tax.

	Base	A	B	C
Optimality Gap	6.56 %	3.85 %	4.83 %	6.2 %
Europe destinations	103	92	101	103
Intercontinental Destinations	65	53	60	66
# Aircraft	732	460	598	722
# Local Pax.	57746	34068	47038	57273
- Class 0	6340	2572	4371	6068
- Class 1	40280	20622	31545	40005
- Class 2	11126	10874	11122	11200
# Transfer Pax.	10404	8812	8292	9374
- Class 0	1598	1384	1445	1468
- Class 1	7188	4471	5431	6344
- Class 2	1618	2957	1416	1562

C.4. Passenger Demand Ratio

The demand model assumes a fixed ratio between the three different passenger classes. The demand is determined using the AirportIS dataset from IATA, which includes the number of passengers that were flown on a given itinerary. The demand model assumes that the flown demand between two cities consists of 80 % economy class passengers and 20 % business class passengers. In addition, there could also be uncaptured demand. This assumption is based on the number of seats that are available on typical 2-class aircraft configurations. The budget passenger class of the demand model is assumed to be an additional 20 % of the demand shown in the dataset. This results in the class ratio of 2 : 8 : 2 between the budget, economy and business class respectively.

The sensitivity analysis looks at varying ratios of these three passenger classes. The first scenario (A) assumes a higher percentage of economy passengers, resulting in 90 % and 10 % economy and business class passengers. The second scenario (B) assumes that there is more uncaptured demand than in the baseline. A share of 40 % is assumed for the budget class passengers. The third scenario (C) combines both of these cases. An overview of the scenarios is shown in Table C.7

Table C.7: Changed demand ratio variables in the sensitivity scenarios compared to the baseline inputs.

	Demand Ratio		
	Budget	Economy	Business
Baseline	20%	80%	20%
A	20%	90%	10%
B	40%	80%	20%
C	40%	90%	10%

The results of the simulations are shown in Table C.8. It can be seen that varying the ratios between the passenger demand classes has an immediate effect on the ratios between the flown passengers. A doubling of the budget demand results in a around a doubling of the local and transfer budget passenger flows and a halving of the business class demand results in around a halving of the local and transfer business passenger flows. The results also show that less business class demand results in more total passengers. More passengers are needed to cover the operational costs. In addition, as there are more passengers, there are also more aircraft and slightly more destinations with less business class demand. This could indicate that the number of business class seats in the baseline scenario could be reduced as the same routes are still operable without such a large business class demand.

Table C.8: Key figures of the sensitivity analysis on the ratio between the demand classes.

	Base	A	B	C
Optimality Gap	6.56 %	6.09 %	5.77 %	5.55 %
Europe destinations	103	110	107	109
Intercontinental Destinations	65	66	68	70
# Aircraft	732	790	818	874
# Local Pax.	57746	62008	66249	70950
- Class 0	6340	7947	14535	17161
- Class 1	40280	48477	40515	48274
- Class 2	11126	5584	11199	5515
# Transfer Pax.	10404	11018	9742	10083
- Class 0	1598	1928	2767	2655
- Class 1	7188	8487	5583	6814
- Class 2	1618	603	1392	614

This page is intentionally left blank.

D

Airport List

This appendix presents the airports that have been included in the [Airline Network Design \(AND\)](#) model. The tables show the [IATA](#) airport code and its latitude and longitude. [Table D.1](#) presents the 20 hub airports. These hubs have been selected as they cover the current busiest hubs in Europe, in addition to smaller hubs in and around the continent. [Table D.2](#) presents the 200 non-hub airports of the model. This selection of airports is determined by ranking the destinations by the number of connecting passengers for the selected hubs.

Table D.1: Selection of 20 hub airports indicated by [IATA](#) code and latitude and longitude.

Airport	Latitude	Longitude	Airport	Latitude	Longitude
AMS	52.3086	4.7639	VIE	48.1103	16.5697
IST	41.2613	28.7420	DUB	53.4287	-6.2621
LHR	51.4706	-0.4619	ZRH	47.4581	8.5481
FRA	50.0365	8.5613	CPH	55.6179	12.6560
CDG	49.0128	2.5500	LIS	38.7813	-9.1359
MAD	40.4719	-3.5626	OSL	60.1939	11.1004
BCN	41.2971	2.0785	KEF	63.9850	-22.6056
MUC	48.3538	11.7861	HEL	60.3172	24.9633
FCO	41.8045	12.2520	BRU	50.9014	4.4844
ATH	37.9364	23.9445	DXB	25.2528	55.3644

Table D.2: Selection of 200 non-hub airports indicated by [IATA](#) code and latitude and longitude.

Airport	Latitude	Longitude	Airport	Latitude	Longitude
PDL	37.7412	-25.6979	NCE	43.6584	7.2159
KIV	46.9277	28.9310	VCE	45.5053	12.3519
STN	51.8850	0.2350	DUS	51.2895	6.7668
GRZ	46.9911	15.4396	MAN	53.3494	-2.2795
AES	62.5625	6.1197	MXP	45.6306	8.7281
TZX	40.9951	39.7897	GVA	46.2381	6.1090
OLB	40.8987	9.5176	ARN	59.6519	17.9186
VGO	42.2318	-8.6268	HAM	53.6304	9.9882
KRS	58.2042	8.0854	BER	52.3622	13.5007
LED	59.8003	30.2625	ALA	43.3543	77.0428
EVE	68.4913	16.6781	CAN	23.3924	113.2990
LCG	43.3021	-8.3773	MCT	23.5933	58.2844
DLM	36.7131	28.7925	TAS	41.2579	69.2812
LEJ	51.4239	12.2364	EBL	36.2376	43.9632
DRS	51.1341	13.7678	FRU	43.0613	74.4776

Table D.2: Selection of 200 non-hub airports indicated by IATA code and latitude and longitude.

Airport	Latitude	Longitude	Airport	Latitude	Longitude
RHO	36.4054	28.0862	LAS	36.0834	-115.1518
CAG	39.2515	9.0543	ADD	8.9779	38.7993
MPL	43.5762	3.9630	LHE	31.5216	74.4036
MAH	39.8626	4.2187	KIX	34.4273	135.2440
TFN	28.4827	-16.3415	HAV	22.9892	-82.4091
AAL	57.0928	9.8492	SGN	10.8188	106.6520
DME	55.4088	37.9063	BAH	26.2673	50.6376
CHQ	35.5317	24.1497	DMM	26.4712	49.7979
CGN	50.8659	7.1427	CLT	35.2140	-80.9431
SKP	41.9616	21.6214	KHI	24.9065	67.1608
BOO	67.2692	14.3653	KWI	29.2266	47.9689
GDN	54.3776	18.4662	CUN	21.0394	-86.8743
TOS	69.6833	18.9189	PHL	39.8719	-75.2411
LJU	46.2237	14.4576	TPE	25.0777	121.2330
ABZ	57.2019	-2.1978	RAK	31.6069	-8.0363
FNC	32.6979	-16.7745	SCL	-33.3930	-70.7858
VNO	54.6341	25.2858	AUH	24.4438	54.6517
SJJ	43.8246	18.3315	HAN	21.2212	105.8070
TRN	45.2008	7.6496	BNE	-27.3842	153.1170
BJV	37.2506	27.6643	DOH	25.2731	51.6081
EVN	40.1473	44.3959	YYC	51.1139	-114.0200
FAO	37.0144	-7.9659	MAA	12.9900	80.1693
RIX	56.9236	23.9711	ISB	33.5490	72.8257
LPA	27.9319	-15.3866	JED	21.6796	39.1565
BRI	41.1389	16.7606	DAC	23.8433	90.3978
JMK	37.4351	25.3481	ACC	5.6052	-0.1668
GYD	40.4675	50.0467	CGK	-6.1256	106.6560
SVQ	37.4180	-5.8931	MLE	4.1918	73.5291
BSL	47.5900	7.5292	NRT	35.7647	140.3860
JTR	36.3992	25.4793	GIG	-22.8100	-43.2506
NUE	49.4987	11.0781	CMN	33.3675	-7.5900
BRE	53.0475	8.7867	MRU	-20.4302	57.6836
DBV	42.5614	18.2682	CPT	-33.9648	18.6017
TLL	59.4133	24.8328	DSS	14.6700	-17.0733
HER	35.3397	25.1803	PTY	9.0714	-79.3835
MLA	35.8575	14.4775	LOS	6.5774	3.3212
NCL	55.0375	-1.6917	BLR	13.1979	77.7063
TBS	41.6692	44.9547	CMB	7.1808	79.8841
ESB	40.1281	32.9951	MEL	-37.6733	144.8430
TRD	63.4578	10.9240	MNL	14.5086	121.0200
NTE	47.1532	-1.6107	DPS	-8.7482	115.1670
LUX	49.6233	6.2044	RUH	24.9576	46.6988
ALC	38.2822	-0.5582	LIM	-12.0219	-77.1143
PMO	38.1760	13.0910	MSP	44.8820	-93.2218
ADB	38.2924	27.1570	SYD	-33.9461	151.1770
BLL	55.7403	9.1518	KUL	2.7456	101.7100
SPU	43.5389	16.2980	TUN	36.8510	10.2272
SOF	42.6967	23.4114	DEN	39.8617	-104.6730
ZAG	45.7429	16.0688	DTW	42.2124	-83.3534
CTA	37.4668	15.0664	ALG	36.6939	3.2145
SKG	40.5197	22.9709	BOG	4.7016	-74.1469
AYT	36.8987	30.8005	AMM	31.7226	35.9932
BOD	44.8283	-0.7156	EZE	-34.8222	-58.5358

Table D.2: Selection of 200 non-hub airports indicated by IATA code and latitude and longitude.

Airport	Latitude	Longitude	Airport	Latitude	Longitude
IBZ	38.8729	1.3731	IKA	35.4161	51.1522
SVG	58.8767	5.6378	NBO	-1.3192	36.9278
TIA	41.4147	19.7206	PEK	40.0801	116.5850
VLC	39.4893	-0.4816	YVR	49.1939	-123.1840
LCA	34.8751	33.6249	IAH	29.9844	-95.3414
BEG	44.8184	20.3091	HKG	22.3089	113.9150
VKO	55.5915	37.2615	DFW	32.8968	-97.0380
KRK	50.0777	19.7848	SEA	47.4492	-122.3111
ORY	48.7233	2.3794	MEX	19.4354	-99.0824
BIO	43.3011	-2.9106	JNB	-26.1392	28.2460
STR	48.6899	9.2220	PVG	31.1434	121.8050
GLA	55.8719	-4.4331	ICN	37.4691	126.4510
BGO	60.2934	5.2181	HND	35.5523	139.7800
HAJ	52.4611	9.6851	ATL	33.6367	-84.4281
LIN	45.4451	9.2767	BEY	33.8209	35.4884
BHX	52.4539	-1.7480	CAI	30.1115	31.3967
PMI	39.5517	2.7388	MIA	25.7932	-80.2906
TLS	43.6291	1.3638	BOM	19.0887	72.8679
FLR	43.8100	11.2051	EWR	40.6925	-74.1687
BLQ	44.5354	11.2887	YUL	45.4706	-73.7408
MRS	43.4393	5.2214	BKK	13.6811	100.7470
NAP	40.8860	14.2908	SIN	1.3502	103.9940
GOT	57.6628	12.2798	DEL	28.5556	77.0952
EDI	55.9501	-3.3723	GRU	-23.4319	-46.4678
OTP	44.5711	26.0850	SFO	37.6190	-122.3750
AGP	36.6749	-4.4991	BOS	42.3643	-71.0052
OPO	41.2481	-8.6814	YYZ	43.6772	-79.6306
LGW	51.1481	-0.1903	TLV	32.0114	34.8867
WAW	52.1657	20.9671	IAD	38.9445	-77.4558
LYS	45.7256	5.0811	LAX	33.9425	-118.4080
BUD	47.4298	19.2611	ORD	41.9786	-87.9048
PRG	50.1008	14.2600	JFK	40.6394	-73.7793

This page is intentionally left blank.

III

Literature Study
previously graded under AE4020

This page is intentionally left blank.

Literature
Review

AE4020

Research into World-Wide Airport Network Models

Winand Mathoera

4775848



Literature Review

Research into World-Wide Airport Network Models

by

Winand Mathoera

Student Number: 4775848
Course Code: AE4020
Supervisor: Ir. P. C. Roling
Datum: April 3, 2024

Cover image made by Winand Mathoera

Executive Summary

Schiphol Airport characterises itself as a large hub airport in the European market. The Dutch catchment area is however not able to support the whole route network of the airport. Instead, the airport fulfills a gateway function: in 2022 transfer passengers occupy 37 % of the total 52.5 millions passengers at Schiphol Airport¹. This dependency creates a vulnerability to changes in the aviation market, affecting the cost of transferring at Schiphol Airport. Such what-if scenarios are currently analysed using a network model of 60 airports. The aim of this research is to improve this model by increasing the handling capabilities of larger networks and increasing the realism. The research question of the problem is formulated as follows:

How can a large scale world-wide airport network be modelled in order to analyse the traffic flows and emergence of hubs due to changes in cost?

The literature review approaches this question from four angles: the formulation of the model, the method of optimising the problem, the airport and aircraft characteristic, and the dynamics of cost and demand in the network. Four sub-questions were formulated and are discussed next.

The first question regards the formulation of the model: how can an airport network with hubs be modelled to show the effects of cost? Several types of models are presented, where the differences were mainly based on the structure of the network. In this case, there are models that inherently assume a hub-and-spoke network or models that show the emergence of hubs based on cost benefits on the consolidation of flows. Different formulations were presented that can improve the computational efficiency. For example, path-based and flow-based formulations were reviewed, where the latter is capable of reducing the size of the problem, but also introduces weaker LP bounds to the problem.

The second question entails the optimisation process: what are possible optimisation methods which allow for solving large scale problems? Exact and heuristic procedures are reviewed. Meta-heuristic methods display their ability to solve large-scale problems. Specialised exact methods are however also able to solve large-scale problems, given that several optimisation techniques are combined. Some of the largest networks of hub location problems that have been reviewed vary between 100 and 500 nodes.

The third question regards the incorporation of airport and aircraft characteristics: what methods are available to model the airport and aircraft characteristics in the model? The desired characteristics are the capacities, range and fuel burn. The review presents methods of incorporating these in the model, however, these increase the complexity of the model.

The last question considers the cost and demand dynamics: how can the dynamics of cost and demand be incorporated into the model? The focus is on implementing the effects of flow consolidation, also known as economies of scale, and the effects of price sensitivity into the model. In addition, estimating demand remains a complex task due to the many influences, such as price, level of service, and network design. Further research should be performed in order to better understand implementations of real-life data into such models.

This literature review presents a good basis for the next phases of the research. Some decisions will need to be made based on the desired level of detail of the model. If more complex methods are desired, such as a better implementation of aircraft characteristics, it is important to analyse the effects it may have on the computational efficiency of the model.

¹Retrieved on 11-04-2023: <https://nieuws.schiphol.nl/verdubbeling-aantal-reizigers-schiphol-in-2022/>

Contents

Executive Summary	i
List of Figures	iii
List of Abbreviations	iv
1 Introduction	1
2 Review of Airport Network Model Approaches	3
2.1 Overview of Hub Location Models	3
2.2 p-Hub Location Problems	4
2.3 Uncapacitated Hub Location Problem	6
2.4 Flow-Based Variations	7
2.5 Airline Network Design model	8
2.6 Other Variations	10
2.6.1 P-Hub Center Location Problem	10
2.6.2 Hub Covering Location Problem	10
2.7 Discussion	11
3 Review of Problem Optimisation Methods	13
3.1 Exact Methods	13
3.1.1 Branch and Bound	13
3.1.2 Branch and Cut	14
3.1.3 Column Generation	14
3.1.4 Branch and Price	15
3.1.5 Benders Decomposition	16
3.2 Meta-Heuristic Methods	17
3.2.1 Tabu Search	18
3.2.2 Simulated Annealing	18
3.2.3 Genetic Algorithm	19
3.2.4 Ant Colony Optimisation	19
3.3 Discussion	20
4 Review of Airport and Aircraft Modelling	21
4.1 Airport Modelling	21
4.1.1 Overview of Capacity	21
4.1.2 Empirical Approach	23
4.1.3 Runway Capacity Model	24
4.1.4 Airport Capacity Model	26
4.1.5 Simulation	27
4.1.6 Airport Capacity Implementation	28
4.2 Aircraft Modelling	28
4.2.1 Aircraft Range Determination	28
4.2.2 Payload-Range Characteristics	30
4.2.3 Implementing Aircraft Characteristics	31
4.3 Discussion	33
5 Review of the Dynamics of Cost and Demand in Airport Networks	34
5.1 Economies of Scale	34
5.1.1 Discounted Arc Cost	34
5.1.2 Piece-Wise Arc Cost	35
5.1.3 Multi-Aircraft Arcs	36
5.2 Price Sensitivity	37
5.3 Demand Modelling	38
5.3.1 Supply-Side	39
5.3.2 Demand-Side	40
5.4 Discussion	41
6 Conclusion	43
Bibliography	44

List of Figures

3.1	Visualisation of the procedure of the Column Generation (CG) algorithm [22]	15
3.2	Visualisation of the procedure of the Branch-and-Price (BnP) algorithm [61]	16
4.1	Departure-arrival capacity chart constructed by four different operating strategies [39].	22
4.2	Example table lookup for the determination of the runway capacities of two different runway configurations [25]	23
4.3	Example chart for the determination of the runway capacity [25]	24
4.4	Empirical determination of the arrival-departure capacity curve [29].	24
4.5	Opening and closing case between arriving aircraft with different approach speeds [34].	25
4.6	Visualisation of the components of the Integrated Airport Capacity Model (IACM), including the model inputs [39].	27
4.7	Payload-range diagram visualising the three limiting cases of the payload. [63]	31
5.1	Cost function diagram based on the flow between cities i and j : A regular cost-function and its discounted form by factor α [2].	35
5.2	Cost function diagram based on the flow between cities i and j : A non-linear cost-function and a piece-wise approximation [2].	35
5.3	Cost function diagram based on the flow between cities i and j : A piece-wise cost-function representing the minimum cost between a small and a large vehicle [2].	36

List of Abbreviations

- ACM** Airport Capacity Model. 26, 27
ACO Ant Colony Optimisation. 18–20
AND Airline Network Design. 3, 11, 28, 32, 33
ATC Air Traffic Control. 23
- BADA** Base of Aircraft Data. 30, 33
BD Benders Decomposition. 13, 16, 17, 20
BnB Branch-and-Bound. 11, 13–15
BnC Branch-and-Cut. 13, 14
BnP Branch-and-Price. iii, 13, 15, 16
- CFP** Corner-Point Feasible. 13
CG Column Generation. iii, 13–15
CHLP Capacitated Hub Location Problem. 20, 32, 33
- EA** Evolutionary Algorithm. 14
- FAA** Federal Aviation Administration. 22, 26
- GA** Genetic Algorithm. 18, 19
GDP Gross Domestic Product. 40
GHLP Gateway Hub Location Problem. 32
- HCFP** Hub Covering Flow Problem. 32
HCV Hub Covering Problem. 10, 32
HLP Hub Location Problem. 3
HS Hub-and-Spoke. 3, 11, 31, 34, 37, 41, 43
- IACM** Integrated Airport Capacity Model. iii, 27
IFR Instrumental Flight Rules. 21, 22
IMC Instrument Meteorological Conditions. 22
- MILP** Mixed Integer Linear Programming. 14
MIP Mixed-Integer Problem. 16
MP Master Problem. 14, 16, 17
MTOW Maximum Take-Off Weight. 30–33
- OD** Origin-and-Destination. 3–8, 10, 14, 19, 34, 36–41
OEW Operational Empty Weight. 30, 31
- p-HCP** p-Hub Center Problem. 4, 10
p-HLP p-Hub Location Problem. 3–5
p-HMP p-Hub Median Problem. 5–8, 11, 14, 19, 28, 34, 37
P2P Point-to-Point. 37
- RCE** Runway Configuration Estimator. 26
RCM Runway Capacity Model. 26

RMP Restricted Master Problem. 14–16

SA Simulated Annealing. 18–20

SP Sub-Problem. 16, 17

TAAM Total Airspace and Airport Modeller. 27

TCM Terminal Capacity Model. 27

TS Tabu Search. 18–20

UHLP Unconstrained Hub Location Problem. 3, 6, 7, 11, 19, 20, 28

UMAHLP Unconstrained Multiple-Allocation Hub Location Problem. 6

USAHLP Unconstrained Single-Allocation Hub Location Problem. 6, 18

VFR Visual Flight Rules. 21

VMC Visual Meteorological Conditions. 22

WTC Wake Turbulence Category. 22, 23, 26

1

Introduction

Schiphol Airport characterises itself as a large hub airport in the European market. The Dutch catchment area however is not able to solely support the route network present at Schiphol [21]. Transfer passengers are the key in enabling this network. This dependency on transfers originated from the increased competition in the aviation market due to deregulations. In order to gain a prominent place in the market, the concept of *mainport* was introduced [21]. The aim of this concept is to fulfill a gateway function by expanding intercontinentally to primary and secondary destinations [21]. This focus on transfer passengers is still visible today: in 2022 transfer passengers occupy 37 % of the total 52.5 millions passengers at Schiphol Airport¹.

This dependency on transfer passengers could be a vulnerability of the airport, in case of changes in the aviation market, such as an introduction of penalties on emission in the Dutch airspace. In order to be better prepared for uncontrollable changes in the future, it is important to consider various what-if scenarios that can occur in the aviation market. In order to predict the outcome of the various scenarios, Schiphol uses a network model to analyse the changes in the traffic flows due to changes in cost or policies. However, this model can only handle up to 60 airports, 3 different types of aircraft, and lacks realism in the modeling of costs.

The aim of the research is to formulate a new model that is able to predict the changes in traffic flows in the global aviation market and the effect on the market position of Schiphol as a hub for various scenarios. Such scenarios could include changes in fuel prices (taking into account either global or local effects), emission penalties, port charges, or changes in policies, such as utilising at least a certain percentage of sustainable fuels when departing from a certain airport. These effects can be expressed in costs, enabling them to be incorporated in a cost-based traffic flow model. This research aim results in the following research objective:

To formulate a cost-based model that is able to locate hubs in a world-wide airport network by minimising the cost of the global airport network.

The literature review is the first phase of the research project, which aims at reviewing the state-of-the-art of the subject and finding the information necessary in order to achieve this objective. The main research questions defines the main issue of this problem and can be formulated as follows:

How can a large scale world-wide airport network be modelled in order to analyse the traffic flows and emergence of hubs due to changes in cost?

This research question will be split up into four sub-questions in this literature review. These questions regard the formulation of the model, the method of optimising the problem, the airport and aircraft characteristic, and the dynamics of cost and demand in the network. These four sub-questions are formulated as follows:

¹Retrieved on 11-04-2023: <https://nieuws.schiphol.nl/verdubbeling-aantal-reizigers-schiphol-in-2022/>

- **How can an airport network with hubs be modelled to show the effects of cost?:** A formulation of the problem needs to be found. The literature review aims at presenting various methods that are capable of modelling the world-wide airport network in order to capture the effects on the traffic flows based on the costs in the network.
- **What are possible optimisation methods which allow for solving large scale problems?:** It is desired to be able to solve large-scale world-wide networks with a model. Different optimisation methods exist that need to be applied to the problem. The literature review aims at presenting different methods that are available, in addition to their ability to solve large-scale problems.
- **What methods are available to model the airport and aircraft characteristics in the model?:** The model needs to be adapted to the characteristics of the nodes and vehicles in the world-wide airport network. In this case, these are airports and aircraft. Both of these have characteristics, such as capacity restrictions, that need to be taken into account in the model. The review aims at presenting the different methods of determining the characteristics and the implementation of them in the model.
- **How can the dynamics of cost and demand be incorporated into the model?:** In order to implement the effects of cost into the model, it is needed to understand the dynamics between cost and demand in an airport network. The literature review aims at presenting the implementation of cost and demand into the model, and the effects of cost on demand.

The literature review is divided into these four sub-questions. First, in chapter 2, the approaches to modelling the airport network are reviewed. Next, in chapter 3, the possible optimisation methods for the problem are reviewed. In chapter 4, a review of the determination and implementation of the airport and aircraft characteristics is given. In chapter 5, the dynamics of cost and demand in airport networks are reviewed. At last, in chapter 6, a conclusion of the literature research is given.

Review of Airport Network Model Approaches

This chapter gives a review on approaches to modelling airport networks with hubs. The aim is to give an answer to the sub-question: **How can an airport network with hubs be modelled to show the effects of cost?** This chapter will review mathematical models that are able to show the traffic flows in an airport network including hubs based on cost factors. To model a network with hubs, it is useful to consider the Hub Location Problem (HLP), as they inherently assume a HS network based on the cost benefits. There also exists other models that do not assume such a network, but determine the hubs in a network based on the characteristics of the traffic flows through the network. This chapter starts with an overview of the hub location models, in section 2.1. Next, in section 2.2 - 2.6, the different models are reviewed. At last, in section 2.7, a discussion on the review is given.

2.1. Overview of Hub Location Models

One of the approaches of modelling an airport network is to make use of Hub Location Problem (HLP). Early research into this type of problem is motivated by locating the central facilities in a Hub-and-Spoke (HS) network as the location and throughput of the facility influence the total transportation cost [56]. The Hub Location Problem (HLP) has many applications, such as air transportation systems [5], post delivery services [73] and telecommunication networks [11]. This chapter will elaborate on a few key hub location model formulations. Before this is done, a some definitions are introduced in order to classify the different hub location problems. In a review of the state-of-the-art of hub location problems, Farahani et al. (2013) stated some definitions that can be used to classify hub location problems [26]. Some of the key definitions are as follows:

- **Solution domain:** is the available selection of nodes of the model. This can be all the nodes in the network, a discrete set of nodes, or a continuous domain on a plane
- **Objective criterion:** Examples are a mini-sum objective that minimised the total transportation cost, a mini-max objective that minimised the total maximum transportation cost between each two nodes, and a maximisation of the total profit in the network.
- **Source of number of hubs:** The determination of the number of hubs is exogenous if it is a required input, otherwise, if it is an output of the model, it is endogenous.
- **Allocation Type:** a model has single-allocation if a spoke is connected to one hub, otherwise, multiple-allocation for more connections.
- **Hub capacity:** the hubs in the network are either capacitated or uncapacitated.

These definitions are used to classify the varieties of the models. The following sections will elaborate on five categories of hub location problems. The first category is the p-Hub Location Problem (p-HLP), which solves a network for a exogenously determined number of hubs. On the other hand, the Unconstrained Hub Location Problem (UHLP) determines the number of hubs endogenously. Both of these models are described using a path-based formulation. This implies that the decision variables in the problem indicate the flow over a given path between an Origin-and-Destination (OD) city pair. Besides the path-based formulations, there are also flow-based formulations of these model types, where the decision variables denote the flow between individual legs of a complete itinerary. An advantage of these types of models is the reduction in problem size as not all individual paths needs to be described by a decision variable, however, it does weakens the bounds of the problem. Next, the Airline Network Design (AND) model is presented that has

decision variables based on the number of aircraft, instead of working with flows of passengers. This model does not determine the number of hubs implicitly, but does encourage consolidation of flows. At last, models with other objectives than minimising the total operational cost are reviewed, such as the p-Hub Center Problem (p-HCP), where the objective is to minimise the maximum link cost of the network.

2.2. p-Hub Location Problems

One of the earliest hub location models is introduced by O'Kelly (1986); a programming formulation for the single and two hub location problem [55]. The aim of this research entailed bringing together spatial interaction models, where the focus has been placed on travel behaviour, and location theory, which focuses on the facility locations. Farahani et al. (2013) presents a compact formulation of the single hub location problem and it is shown in Equation 2.1 - 2.4 [26]. The model is locates a single hub in the network, such that the total cost of transporting the passengers through the network is minimised.

In this model, h_{ij} is the amount of flow between OD pair i and j , C_{ij} is the cost of transporting a passenger from node i to node j , and Y_{ij} is a binary number, being 1 if node i is connected to node j and 0 otherwise. Y_{ii} is equal to 1 if i is the hub node and 0 otherwise. Constraint 2.2 assures that there is only one hub and constraint 2.3 assures that nodes are only connected to the hub.

$$\min \sum_i \sum_j \sum_k h_{ik} (C_{ij} + C_{jk}) Y_{ij} Y_{kj} \quad (2.1)$$

s.t.

$$\sum_j Y_{jj} = 1 \quad (2.2)$$

$$Y_{ij} - Y_{jj} \leq 0 \quad \forall i, j \quad (2.3)$$

$$Y_{ij} \in \{0, 1\} \quad \forall i, j \quad (2.4)$$

Besides a single and two hub location model, it is also possible to model networks with multiple hubs. O'Kelly (1987) presented the p-Hub Location Problem (p-HLP), which is able to model networks with p hubs. In this problem the number of hubs is defined exogenously [56]. A compact formulation of the p-HLP has been presented by Farahani et al. (2013) and is shown in Equation 2.5 - 2.9 [26]. The objective of this formulation is split into three parts: the cost of transporting passengers on the spoke-hub leg, hub-spoke leg, and the inter-hub leg.

The variables are similar to the single hub location problem. However, constraint 2.7 is added to ensure that a node is only connected to one hub, resulting in a single-allocation network. In addition, constraint 2.6 restricts the number of hubs to P , instead of 1.

$$\min \sum_i \sum_k C_{ik} Y_{ik} \left(\sum_j h_{ij} \right) + \sum_k \sum_i C_{kj} Y_{ik} \left(\sum_j h_{ji} \right) + \alpha \sum_i \sum_j \sum_k \sum_m h_{ij} C_{km} Y_{ik} Y_{jm} \quad (2.5)$$

s.t.

$$\sum_j Y_{jj} = P \quad (2.6)$$

$$\sum_j Y_{ij} = 1 \quad \forall i \quad (2.7)$$

$$Y_{ij} - Y_{jj} \leq 0 \quad \forall i, j \quad (2.8)$$

$$y_{ij} \in \{0, 1\} \quad \forall i, j \quad (2.9)$$

A downside of both of these formulations is that the objective is quadratic. Quadratic models require other methods to be solved exactly than linear problems. However, linearising a model increases the number of variables in the problem, but the computation time can be reduced by using heuristic solving methods [10].

A linear model of the p-HLP has been presented by Campbell (1994) [10]. The approach taken is to combine the quadratic term $Y_{ik}Y_{jm}$ into a single term X_{ijkm} to indicate the flow of passengers between OD pair i and j using hubs k and m . The formulation of the model is shown in Equation 2.10 - 2.16. This problem is similar to the p-median problem, where each node must be allocated to a hub. In this linear formulation of the p-Hub Location Problem (p-HLP), each OD city pair must be allocated to a hub pair. This type of model is also known as the p-Hub Median Problem (p-HMP).

besides X_{ijkm} , the other variables of this model are: the cost to transport a passenger between city pair i and j using hubs k and m , C_{ijkm} , the amount of flow between OD city pair i and j is W_{ij} , and Y_k , which is 1 if city k is a hub and 0 otherwise. Constraint 2.11 is similar to the previous models, as it limits the number of hubs to P . Constraints 2.12 - 2.15 ensure a valid connection between the replacement of $Y_{ik}Y_{jm}$ with X_{ijkm} . There are also other sets of constraint that try to ensure this connection. For example, Skorin-Kapov et al. (1996) introduced another set of constraints that creates a tighter model [66]. This is useful when solving the model; when solving the model with relaxation on the integrality of the Y_k variable, the model still mostly produced integral solutions. This new set of constraints replace constraints 2.13 and 2.14 with constraints 2.17 and 2.18. Next to the tighter model, the number of constraints is reduced by $2n^3(n-1)$ constraints.

$$\min \sum_i \sum_j \sum_k \sum_m W_{ij} X_{ijkm} C_{ijkm} \quad (2.10)$$

s.t.

$$\sum_k Y_k = P \quad (2.11)$$

$$\sum_k \sum_m X_{ijkm} = 1 \quad \forall i, j \quad (2.12)$$

$$X_{ijkm} \leq Y_m \quad \forall i, j, k, m \quad (2.13)$$

$$X_{ijkm} \leq Y_k \quad \forall i, j, k, m \quad (2.14)$$

$$X_{ijkm} \geq 0 \quad \forall i, j, k, m \quad (2.15)$$

$$Y_k \in \{0, 1\} \quad \forall k \quad (2.16)$$

$$\sum_m X_{ijkm} \leq Y_k \quad \forall i, j, k \quad (2.17)$$

$$\sum_k X_{ijkm} \leq Y_m \quad \forall i, j, m \quad (2.18)$$

The p-HMP models are present in various studies. For example, García et al. (2012) applies a p-HMP to the Australian Post dataset, a common dataset used to evaluate hub location models [27]. García et al (2012) present a specialised exact algorithm to solve the model and is evaluated on networks up to 200 nodes. However for large network, the model is only able to give an optimal solution within a 10 hour limit when a large number of hubs is chosen. For example, 180 hubs for 200 airports. Another study, presented by Ishfaq and Sox (2011), evaluates the effectiveness of the tabu-search metaheuristic on the p-HMP [36]. This study evaluates networks up to 100 nodes. Networks with 100 nodes and 6 hubs are solved within 3 seconds, compared to 83 seconds solved using CPLEX, a commercial solver. The metaheuristic is much faster, however, the solution gap with the exact solution increases with network size. For the networks with 100 nodes, the average solution gap was 8.3 %. [36]

2.3. Uncapacitated Hub Location Problem

The Unconstrained Hub Location Problem (UHLP) is another variation on hub location problems. Compared to p-hub location problems, the number of hubs are decided endogenously, instead of exogenously. To prevent all the nodes from becoming hubs, a fixed price will be charged when allocating a node as a hub in the network. A basic formulation of the problem is presented by Campbell (1994) and is shown in Equation 2.19 - 2.24 [10]. This formulation is based on the p-HMP shown in Equation 2.10 - 2.16 and also produces a multi-allocation network.

The objective function 2.19 defines the cost to transfer the passengers and the cost to allocate a node as a hub. This model again uses the four-indexed variable X_{ijkm} , similar to p-HMPs, to indicate the flow fraction between OD pair i and j , using hubs k and m , as well as the variables C_{ijkm} , W_{ij} , and Y_k . A new variable, F_k indicates the cost to locate a hub at node k . The constraints of the UHLP are identical to the p-HMP formulation, except constraint 2.11, which determines the number of hubs, is no longer needed.

$$\min \sum_i \sum_j \sum_k \sum_m W_{ij} X_{ijkm} C_{ijkm} + \sum_k F_k Y_k \quad (2.19)$$

s.t.

$$\sum_k \sum_m X_{ijkm} = 1 \quad \forall i, j \quad (2.20)$$

$$X_{ijkm} \leq Y_m \quad \forall i, j, k, m \quad (2.21)$$

$$X_{ijkm} \leq Y_k \quad \forall i, j, k, m \quad (2.22)$$

$$X_{ijkm} \geq 0 \quad \forall i, j, k, m \quad (2.23)$$

$$Y_k \in \{0, 1\} \quad \forall k \quad (2.24)$$

The basic formulation of the UHLP is for multiple-allocation networks, also known as Unconstrained Multiple-Allocation Hub Location Problem (UMAHLP). The problem can also be rewritten to solve for a single-allocation network or Unconstrained Single-Allocation Hub Location Problem (USAHLP). This change is achieved by replacing some constraints of the original problem. The formulation of the USAHLP is shown in Equation 2.25 - 2.31. [10]

$$\min \sum_i \sum_j \sum_k \sum_m W_{ij} X_{ijkm} C_{ijkm} + \sum_k F_k Y_k \quad (2.25)$$

s.t.

$$Y_k \in \{0, 1\} \quad \forall k \quad (2.26)$$

$$0 \leq X_{ijkm} \leq 1 \quad \forall i, j, k, m \quad (2.27)$$

$$\sum_k \sum_m X_{ijkm} = 1 \quad \forall i, j \quad (2.28)$$

$$Z_{ik} \in \{0, 1\} \quad \forall i, k \quad (2.29)$$

$$Z_{ik} \leq Y_k \quad \forall i, k \quad (2.30)$$

$$\sum_j \sum_m (W_{ij} X_{ijkm} + W_{ji} X_{jimk}) = \sum_j (W_{ij} + W_{ji}) Z_{ik} \quad \forall i, k \quad (2.31)$$

However, other formulations exist that make use of the properties of the multiple-allocation network to pre-process the problem [14]. One of the properties is that the demand between a given OD pair i and j will always travel in one direction between hubs k and m ; the direction with the lowest cost will be chosen [31].

This cost is represented as the undirected flow cost C_{ije} , where e are all the edges $(k, m) \in E$ in the network. The undirected flow cost is then found using: $C_{ije} = \min\{C_{ijkm}, C_{ijmk}\}$.

Another reduction in variables can be achieved by defining a restricted set of hub arcs, E_{ij} , for a given OD pair [15]. Boland et al. (2004) present properties of UHLP that can be used to restrict the set of hub arcs. For example, in an uncapacitated problem, no flow will be routes through two hubs if the routing through one hub is cheaper [8]. Combining these properties will result in the formulation of the UHLP shown in Equation 2.32 - 2.36 [15]. This formulation is similar to the original UHLP formulation, however this formulation has less constraints and this formulation gives tighter LP bounds [31].

$$\min \sum_i \sum_j \sum_e W_{ij} X_{ije} C_{ije} + \sum_k F_k Y_k \quad (2.32)$$

s.t.

$$\sum_e X_{ije} = 1 \quad \forall i, j \quad (2.33)$$

$$\sum_{e \in E_{ij}: k \in e} X_{ije} \leq Y_k \quad \forall i, j, k \quad (2.34)$$

$$X_{ije} \geq 0 \quad \forall i, j, e \in E_{ij} \quad (2.35)$$

$$Y_k \in \{0, 1\} \quad \forall k \quad (2.36)$$

This formulation has been used in several studies and is solved using different techniques, such as by Marín (2005) using a Lagrangian relaxation in combination with a branching method [48], or Cánovas et al. (2007) using a dual-ascent based heuristic [17]. A comparison between the basic and new formulation of the UHLP is presented by Mokhtar et al. (2017), where the computational times of the basic UHLP formulation are compared to the new formulation analysed in Contreras et al. (2011) for the same dataset [50][15]. Both studies solve the model using Benders decomposition method, an exact algorithm that can be used to solve large instances of UHLP. However, Mokhtar et al. (2017) uses a modified version of the algorithm, which improves the computation times. The analysis is performed up to 200 nodes and shows that the basic formulation is faster in computation times in two thirds of the tests. However, the higher efficiency is mostly noticed in smaller networks, whereas the new formulation performs better in larger networks.[50]

2.4. Flow-Based Variations

The p-HMP and UHLP models are both path-based models, where a single decision variable indicates the complete path of a passenger. A variation on these types of models can be made by treating the problem as a multi-commodity flow problem, where the sources and sinks are the hub nodes. Ernst and Krishnamoorthy (1998) present a formulation for an uncapacitated multi-allocation p-HMP [24]. This section will elaborate on this flow-based variation.

The motivation of this type of model was to find a new formulation that is able to solve larger problems compared to what is possible with path-based formulations, such as the formulation of Skorin-Kapov et al. (1996) [66], shown in section 2.2. To achieve this, the new formulation reduces the number of variables and constraints by not considering every flow between each OD city pair individually. The formulation of this model is given in Equation 2.39 - 2.47. For this formulation, the passenger flow W_{ij} is divided into origin i , O_i , and destination i , D_i , using Equation 2.37 and 2.38.

$$O_i = \sum_{j \in N} W_{ij} \quad (2.37)$$

$$D_i = \sum_{j \in N} W_{ji} \quad (2.38)$$

In the model, Z_{ik} is the flow from city i to hub k , X_{ijk} is the flow from OD city pair i and j using hub k , Y_{ikm} is the flow from city i using hubs k and m , H_k is an integer indicating if city k is a hub, d_{ij} is the distance to travel between cities i and j , and χ , α and δ are the collection, transfer and distribution cost respectively. Again, P indicates the number of hubs in the network.

$$\min \sum_{i \in N} \left[\sum_{k \in N} \chi d_{ik} Z_{ik} + \sum_{k \in N} \sum_{m \in N} \alpha d_{km} Y_{ikm} + \sum_{m \in N} \sum_{j \in N} \delta d_{jm} X_{ijm} \right] \quad (2.39)$$

s.t.

$$\sum_k H_k = P \quad (2.40)$$

$$\sum_k Z_{ik} = O_i \quad \forall i \quad (2.41)$$

$$\sum_m X_{ijm} = W_{ij} \quad \forall i, j \quad (2.42)$$

$$\sum_m Y_{ikm} + \sum_j X_{ijk} - \sum_m Y_{imk} - Z_{ik} = 0 \quad \forall i, j \quad (2.43)$$

$$Z_{ik} \leq O_i H_k \quad \forall i, j \quad (2.44)$$

$$X_{ijm} \leq W_{ij} H_m \quad \forall i, j, m \quad (2.45)$$

$$X_{ijm}, Y_{ikm}, Z_{ik} \geq 0 \quad \forall i, j, k, m \quad (2.46)$$

$$H_k \in \{0, 1\} \quad \forall k \quad (2.47)$$

This formulation reduces the problem size compared to the path-based p-HMP. However, a disadvantage of this formulation is that it has weaker bounds [24]. When solving the problem with LP relaxation, the solution usually is not integral, which does occur for the p-HMP presented in Skorin-Kapov et al. (1996) [66]. To combat this, constraints are added during the optimisation process to create tighter bounds. For example if a problem is symmetric, the constraints based on Equation 2.48 are added, which states that the flow between city pair i and j is symmetric. These cuts are added for all the city pairs that are not symmetric in the solution. From the computational study presented by Ernst and Krishnamoorthy (1998) it was concluded that this approach for the flow-based method was more efficient than the path-based method presented in Skorin-Kapov et al. (1996) [24].

$$Z_{ik} = \sum_j X_{ijk} \quad \forall i, k \quad (2.48)$$

2.5. Airline Network Design model

A different type of flow-based model is proposed by Jaillet et al. (1996). This model does not assume a priori a hub-and-spoke structure and is therefore not focused on locating hubs [37]. It is however intended that cost-efficient cities can cause consolidation of flows, which results in hubs of the network. Another point of this model is that it is formulated to regard multiple aircraft types, and their corresponding capacities, in the optimisation. At last, the formulation allows for different route-options to be taken between one origin and destination pair. This is the result of capacity restrictions on the aircraft and possible cheaper alternatives for the remaining passengers.

Three different formulations of the model are given by Jaillet et al. (1996). The differences between them are the maximum number of stops that are considered in the optimisation: one-stop, two-stop and unlimited stops for an origin and destination pair. The one-stop and two-stop connection models are useful as they are the most common type flown by airlines, whereas the unlimited stop connections are more common for other applications, such as telecommunications and air cargo. The unlimited stop connection models, however, can serve as a lower bound for the other two models. First, the formulation of the single-stop model is shown in Equation 2.49 - 2.53. [37]

$$\min \sum_{i \neq j} \sum_{k \in K} d_{ij} c_k y_{ij}^k \quad (2.49)$$

s.t.

$$f_{ij} \sum_{t \neq i, j} (f_{it} x_{ijt} + f_{tj} x_{tij} - f_{ij} x_{itj}) \leq \sum_{k \in K} b_k y_{ij}^k \quad \forall i \neq j \quad (2.50)$$

$$\sum_{t \neq i, j} x_{itj} \leq 1 \quad \forall i \neq j \quad (2.51)$$

$$x_{itj} \geq 0 \quad i \neq t \neq j \quad (2.52)$$

$$y_{ij}^k \geq 0 \text{ and integer} \quad \forall i \neq j, k \in K \quad (2.53)$$

The objective function of the model is to minimise the total transportation cost. The inputs in the model are: the distance between node i and node j , d_{ij} , the cost per unit distance for aircraft type k , c_k , the capacity for aircraft type k , b_k , and the flow between node i and node j , f_{ij} . In this model, it is assumed that both the distances and the flows are symmetric. The decision variables of the model are: the number of aircraft of type k that fly between node i and node j , y_{ij}^k , and the fraction of the flow of passengers between cities i and j that is connected through node l , x_{ilj} .

Constraint 2.50 ensures that the flow between cities i and j does not exceed the capacity of the total available seats between i and j . Constraint 2.51 ensures that the fraction of the connecting flows between i and j are non-negative. The other constraints ensure that the decision variables are non-negative.

The two stop variation of this model replaces constraint 2.50 with constraint 2.54. This equation again ensures that the flow between cities i and j does not exceed the total available number of seats. However, now it needs to take into account more types of combinations, as there are more cities involved in a path. A new variable is introduced to represent the flow using two hubs: x_{iltj} is the fraction of the flow of passengers between cities i and j that is connected through hubs l and t .

$$f_{ij} + \sum_{t \neq i, j} (f_{it} x_{ijt} + f_{tj} x_{tij} - f_{ij} x_{itj}) + \sum_{l, t \neq i, j} (f_{lj} x_{ltij} + f_{it} x_{ijlt} + f_{lt} x_{lijt} - f_{ij} x_{iltj}) \quad (2.54)$$

A benefit of this model compared to the hub location problems described in section 2.1, is the focus on available capacity per arc in the network. This method produces the number of aircraft needed for the network, and is also able to differentiate between different models of aircraft. In addition, multiple paths between origin-and-destinations are possible to emerge as limited capacity on an arc and opportunities for consolidation may lead a fraction of the passenger flow on a different route [37].

A possible downside of the approach of the model is that there is no hub-and-spoke structure assumed in the simulation. Hubs emerge in a simulation using this type of model by consolidating flows through certain hubs. A possible outcome could be that direct connections between nodes are more economical, which results in no hubs being present in the network.

2.6. Other Variations

The previously described models try to minimise the total cost of the network, however, there are also other variations that can be used to locate hubs in a network. One variation on the hub location problem aims to minimise the maximum distance or cost of each spoke to a hub. This problem is called the p-Hub Center Problem (p-HCP). Another variation is the Hub Covering Problem (HCV), which locates hubs based on the ability to cover a certain OD pair. For example, this coverage can be based on a maximum cost that cannot be exceeded to connect a city to hub. This section will elaborate on these two variations.

2.6.1. P-Hub Center Location Problem

The p-Hub Center Problem (p-HCP) aims at minimising the maximum cost of each link in the network. This type of model is useful in emergency facility location or for networks with perishables. A formulation of the model has been presented by Farahani et al. (2013) and is shown in Equation 2.55 - 2.61 [26]. The decision variables in this model are as follows: X_{ijkm} is the flow of passengers between OD pair i and j using hubs k and m , and Y_k is an integer indicating if city k is a hub. The other variables are: C_{ijkm} , the cost to transport a passenger between OD pair i and j using hubs k and m , and P , the number of hubs in the network.

$$\min \max_{i,j,k,m} \{X_{ijkm}C_{ijkm}\} \quad (2.55)$$

s.t.

$$\sum_k Y_k = P \quad (2.56)$$

$$\sum_k \sum_m X_{ijkm} = 1 \quad \forall i, j \quad (2.57)$$

$$X_{ijkm} \leq Y_m \quad \forall i, j, k, m \quad (2.58)$$

$$X_{ijkm} \leq Y_k \quad \forall i, j, k, m \quad (2.59)$$

$$X_{ijkm} \geq 0 \quad \forall i, j, k, m \quad (2.60)$$

$$Y_k \in \{0, 1\} \quad \forall k \quad (2.61)$$

2.6.2. Hub Covering Location Problem

The Hub Covering Problem (HCV) aims at covering all nodes in the network based on a coverage condition. For example, the cost to cover a OD pair using hubs k and m must not exceed a specified value γ_{ij} . This condition is shown in Equation 2.62 [10]. This can be extended by specifying a maximum value on each individual link cost c_{ij} of a path. This condition is shown in Equation 2.63 [10]. Other types of coverage could also be based on the distance between the nodes [38].

$$C_{ijkm} \leq \gamma_{ij} \quad (2.62)$$

$$\max\{c_{ik}, c_{mj}, \alpha c_{km}\} \leq \gamma_{ij} \quad (2.63)$$

A formulation of the HCV is presented by Campbell (1994), which is shown in Equation 2.64 - 2.68. This formulation aims to minimise the total cost of locating hubs in the network, while covering all the demand in the network. The decision variables in the model are: Y_k , an integer indicating if city k is a hub, and X_{ijkm} , the flow of passengers between OD pair i and j using hubs k and m . Other variables are: F_k , the cost of locating a hub at node k , and V_{ijkm} , an integer indicating if OD pair i and j is able to be covered by hub pair k and m . [10].

$$\min \sum_k F_k Y_k \quad (2.64)$$

s.t.

$$\sum_k \sum_m V_{ijkm} X_{ijkm} \geq 1 \quad \forall i, j \quad (2.65)$$

$$X_{ijkm} \leq Y_m \quad \forall i, j, k, m \quad (2.66)$$

$$X_{ijkm} \leq Y_k \quad \forall i, j, k, m \quad (2.67)$$

$$Y_k \in \{0, 1\} \quad \forall k \quad (2.68)$$

2.7. Discussion

This chapter presented a review of models that could be capable of modelling airport networks, in order to show the effects of cost on the placement of hubs. Each of the models has its own advantages and disadvantages. This section will briefly compare the different distinctions between the models.

The first distinction between the models is the method of defining the number of hubs in a network. The p-HMP models define the number of hubs exogenously and therefore a decision needs to be made before the simulation is started. This method would require performing an initial analysis on the network to determine the desired number of hubs in the network. On the other hand, UHLP models define the hubs endogenously. This method requires an additional variable in the model: the fixed cost of setting up a hub. This would require determining the fixed cost of setting up a hub for each airport separately or assuming the same cost for all airports.

The second distinction between the models is the use of path-based or flow-based decision variables. It has been shown in section 2.4 that the flow-based counterparts of the path-based models have a smaller problem size. This is due to the use of three-indexed variables, instead of four-indexed variables, which describe all the possible paths in the network. However, these models are shown to have weaker LP bounds, which slow down the optimisation [24]. The proposed solution involved tightening the problem by adding cuts during a Branch-and-Bound algorithm. This resulted in a more efficient optimisation compared to the path-based models for medium sized problem. Other solutions have been proposed for larger networks. When the flow-based models are chosen, it is necessary to identify the possible solutions to handle the weak LP bounds. In addition, the compatibility of these solutions with different optimisation methods should be tested, such as when using metaheuristics instead of the current Branch-and-Bound method.

The third point of consideration is the adaptability of the model to the problem. This could include the use of capacities of airport facilities and the use of different aircraft types. The incorporation of multiple aircraft increases the realism of the problem, for example by including the maximum range or capacity on a given route. The Airline Network Design (AND) model, introduced in section 2.5, already incorporates the use of different aircraft types for example, whereas the conventional hub location problems assume a single aircraft type. However, a downside of the AND model is that it does not assume the benefits of a Hub-and-Spoke network. This becomes apparent from the analysis of the model performed by Jaillet et al. (1996). From a computational study comparing the results of the p-HMP model of Skorin-Kapov et al. (1996) and the AND model, it could be concluded that the AND model mostly places the hubs in central locations [37]. This solution does not correspond with the solution of the conventional model, that places hubs at cities that already have large origin or destination flows to benefit from the consolidation of flows.

A last point of consideration is the presence of variations on the objective function of the model. In section 2.6, a few variations have been given on the conventional hub location problems. The conventional hub location problems emphasised on minimising the cost of the total network. It is also possible to minimise

the maximum cost of each leg or to change to objective to covering all demand by hubs with a set criteria. Both of these variations include the effect of cost in the model and could be useful for certain applications. For example, the method of implementing the coverage limits could be extended to the conventional hub location problems to implement the same coverage requirements. In addition, coverage penalties could be introduced to allow for solutions that do not contain all the demand in the network.

Review of Problem Optimisation Methods

This chapter will give a review on problem optimisation methods that can be applied to the optimisation problems discussed in chapter 2. The aim of this chapter is to give an answer to the sub-question: **What are possible optimisation methods, which allow for solving large scale problems?** Several optimisation methods will be reviewed in this chapter. Applications of the various methods to hub location problems will be given to show the performance of the methods. In order to solve for large scale problems, it is important to reach an optimal solution within a reasonable amount of time and with a small solution gap. The computation time however is dependent on the hardware that is used by the optimisation program and the formulation of the problem. The review will therefore focus on various implementations of the algorithms and show the performance in these specific cases. The chapter is divided into three parts. First, in section 3.1, exact optimisation methods will be reviewed. In section 3.2, meta-heuristic optimisation methods are discussed. At last, in section 3.3, a discussion of the review is presented.

3.1. Exact Methods

This section will elaborate on exact optimisation methods that can be applied to hub location problems. The selection of optimisation methods is based on the popularity of the methods in hub location models, obtained from a comprehensive study on exact optimisation applications presented by Farahani et al. (2013) [26]. The methods range from a basic enumeration procedure to a specialised exact algorithm for hub location problems. The algorithms are: Branch-and-Bound (BnB), Branch-and-Cut (BnC), Column Generation (CG), Branch-and-Price (BnP), and Benders Decomposition (BD).

Before continuing to the solution algorithms, the simplex solution method will be explained. For most of the methods, the simplex method forms a basis of the solution algorithm, by finding optimal solutions to sub-problems. The simplex method is an algebraic procedure that solves a problem geometrically. The solution space of a problem can be defined by the constraints in the problem. Intersecting constraints in the solution space result in corner-points. The corner-points in the feasible region are called Corner-Point Feasible (CFP) solutions. A property of the CFP solutions is that if no adjacent CFPs provide better solutions, the current CFP is the optimal solution [33]. The simplex method chooses new solutions by selecting the CFP that has the highest rate of increasing the objective function (in a maximisation problem), therefore, not all solutions have to be evaluated. The solution algorithms described increase the efficiency of the optimisation process by building upon this solution method.

3.1.1. Branch and Bound

The Branch-and-Bound (BnB) method is the first exact method that will be discussed in this section. The BnB method is an enumeration procedure to solve an integer problem by using a clever structure, which divides the problem in many sub-problems. The algorithm starts by solving a relaxed version of the problem using the simplex method. This is the bounding step of the algorithm, where the optimal solution of the relaxed problem provides the lower bound in a minimisation problem. The problem is then split into two sub-problems by adding constraints to an individual variable with a non-integer solution. This step is called branching. The sub-problems of each branch again can be optimised and result in another lower bound of the main problem. If the solution consists of only integers, it can be considered to be an upper bound of the main problem. If there is a branch with a lower bound higher than the current upper bound, it is certain that the branch will not result in a better solution, and can therefore be disregarded. This step is

called fathoming. The algorithm is repeated on the branched with the lowest lower bound, in the case of a minimisation problem. This will continue until there are no more branches that are not fathomed. [9]

The BnB method can be slow and requires effort that grows exponentially with the size of the problem [9]. However, the BnB method provides the basis of other methods, such as the Branch-and-Cut (BnC) method, and the method is also used in combination with heuristics. An example is the optimisation algorithm presented in Stanojević et al. (2015). This solution algorithm uses the Evolutionary Algorithm (EA) heuristic method to find initial hub locations in a hub location problem, after which the network is further solved using parallel BnB instances [67]. The BnB method itself is used by the Mixed Integer Linear Programming (MILP) solver `lp_solve` [4].

3.1.2. Branch and Cut

The Branch-and-Cut (BnC) algorithm improves on the Branch-and-Bound (BnB) algorithm by implementing a cutting plane algorithm. Cutting planes can be added to further constrain the problem or lifted to reduce the number of constraints. The addition of a cutting plane algorithm results in a two-phase algorithm. The first phase of the algorithm is concerned with finding the optimal solution of the problem using the cutting plane algorithm. The problem starts by finding the optimal solution to the relaxed problem using the simplex method. If the solution is a feasible integer solution, the algorithm stops. However, if there are non-integer variables, there is at least one inequality in this solution of the relaxed problem compared to the main problem [3]. The cuts that are violated will be added to further constrain the relaxed problem. Cuts can be removed if they produce positive slack variables in the solution [24].

If no more cutting planes can be identified, the second phase consisting of the BnB algorithm is started. If this phase does not result in a feasible solution, the violated cuts during the second phase will be identified and are added to the constraints of the first phase. The first phase is resumed and the cycle is continued until a feasible optimal solution is found. [3]

An implementation of the BnC algorithm to solve a p-HMP model is presented by Ernst and Krishnamoorthy (1998) [24]. The presented algorithm constructs various types of cuts that can be added to the problem. For example, if the network is assumed to be symmetric, a cutting plane restricting the flow out of a node to be equal to the flow into the node can be added. A computational study comparing the efficiency of the BnB and BnC methods on various network sizes shows that the BnC method is significantly more effective. The computation time required for a network of 15 nodes averages around 470 seconds for the BnB algorithm and around 8 seconds for the BnC algorithm.

3.1.3. Column Generation

The Column Generation (CG) algorithm is a method which is typically used for problems with too many variables to be solved explicitly. In the CG algorithm, it is assumed that not all decision variables of the original problem are used. Instead, only a subset of the original problem decision variables are taken and decision variables are added if they are needed. Before starting the algorithm, the original problem is reformulated to the Master Problem (MP) and the sub-problems. The initial subset of decision variables that results in a feasible solution is called the Restricted Master Problem (RMP). An example of a RMP is presented in Contreras et al. (2011), where the RMP restricts the set of potential hubs for the flows between each OD city pair [16].

An overview of the CG algorithm is shown in Figure 3.1 [22]. After having defined an initial RMP, the solution and the dual values of the problem are found using the simplex method. An example of a basic linear problem is given in Equation 3.1 - 3.3. The primal and dual solution of the problem are denoted by $\bar{\lambda}$ and $\bar{\mathbf{u}}$. Instead of solving the pricing step for all the decision variables, this step is only performed over the subset

of columns of the RMP. The aim of the pricing problem is to see if there is a slack in the current decision variables, indicated by the dual values of the RMP, that can be taken by the non-basic decision variables in the problem.

$$z^* := \min \sum_{j \in \mathbf{J}} c_j \lambda_j \quad (3.1)$$

s.t.

$$\sum_{j \in \mathbf{J}} \mathbf{a}_j \lambda_j \geq \mathbf{b} \quad \forall j \in \mathbf{J} \quad (3.2)$$

$$\lambda_j \geq 0 \quad \forall j \in \mathbf{J} \quad (3.3)$$

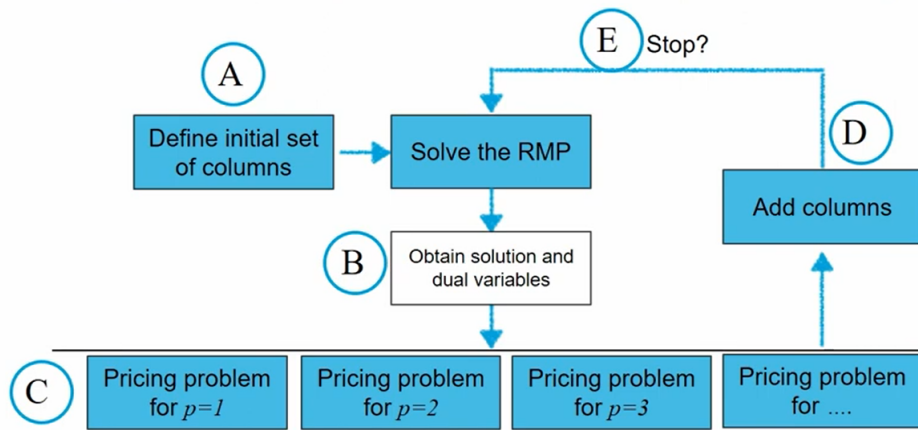


Figure 3.1: Visualisation of the procedure of the Column Generation (CG) algorithm [22]

The pricing problem for the example problem is shown in Equation 3.4, where \bar{c} are the reduced cost coefficients and A is the subset of columns in the RMP [45]. If there is no reduced cost coefficient $\bar{c}_j < 0$, there is no additional column that can improve the problem and the optimal solution is found in the current RMP. Otherwise, the column with a negative reduced price is added to the RMP and the algorithm continues.

$$\bar{c}^* := \min\{c(\mathbf{a}) - \bar{\mathbf{u}}^T \mathbf{a} \mid \mathbf{a} \in A\} \quad (3.4)$$

3.1.4. Branch and Price

The Branch-and-Price (BnP) algorithm is a hybrid between the Column Generation (CG) and Branch-and-Bound (BnB) algorithms. An overview of the BnP algorithm is presented in Ponboon et al. (2016) and is shown in Figure 3.2 [61]. The initialisation of the algorithm is similar as the CG algorithm: first the Restricted Master Problem (RMP) is constructed that is able to produce a feasible solution. However, in the BnP algorithm, the RMP is relaxed before finding the optimal solution. The pricing problems are then solved and column candidates are identified and added to the RMP. If there are no new columns to add to the problem and the RMP has an integer optimal solution, the optimal solution of the original problem is obtained. If there is a non-integer optimal solution, then a new branch is generated on the RMP. The branching scheme is similar to the BnB algorithm described in subsection 3.1.1.

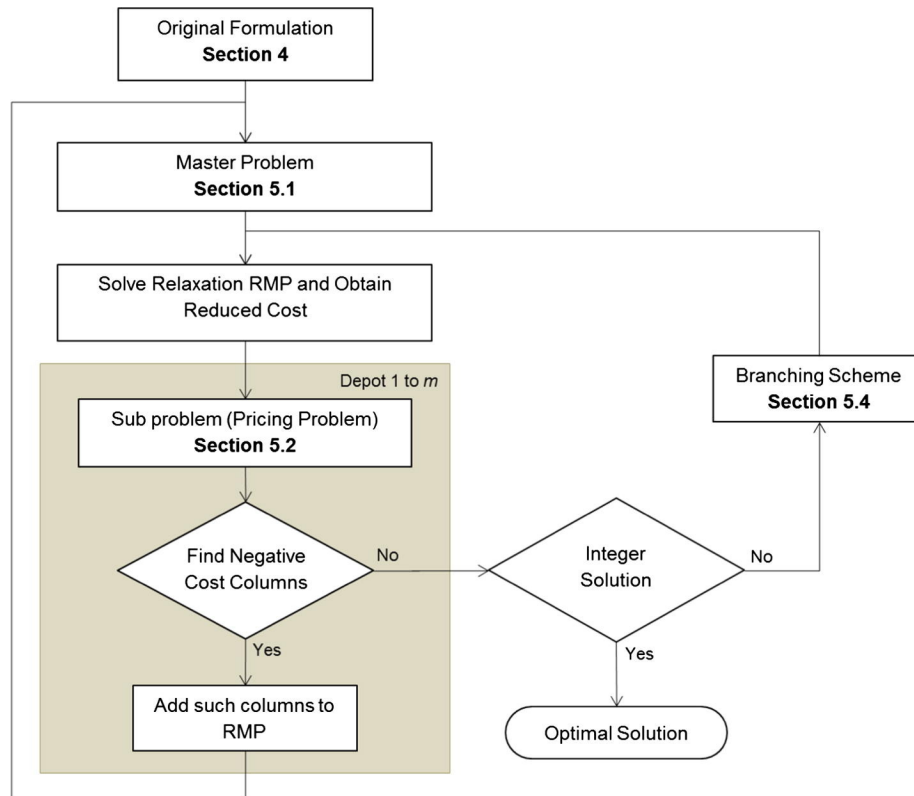


Figure 3.2: Visualisation of the procedure of the Branch-and-Price (BnP) algorithm [61]

An implementation of the BnP algorithm for a capacitated single-allocation hub location problem is presented in Contreras et al. (2011) [16]. The problem is solved using the BnP algorithm, however, instead of using LP relaxation, the model is solved using Lagrangean relaxation. It is shown that the Lagrangean formulation is able to solve formulations based on four indices faster than LP relaxations of similar formulations with four, but also three indices. The efficiency of the algorithm is also increased by extending the termination criteria of the model by comparing the solution of the current RMP with lower bounds obtained from different methods. The final algorithm has been evaluated for networks up to 200 nodes and was able to solve them optimally.

3.1.5. Benders Decomposition

The Benders Decomposition (BD) algorithm is an exact method that can be applied to mixed linear and non-linear integer models. Instead of solving the model directly, the algorithm iterates between a linear model that gives an upper bound and a cut in the search space, and a more manageable integer model that gives a lower bound and integer solution [52]. In the algorithm, the original problem is divided into the Master Problem (MP) and the Sub-Problem (SP). The MP is the relaxed version of the original problem, together with the original integer variables and the constraints. The SP is the original problem where the integer variables are fixed based on the results of the MP. After every iteration of solving the MP and the SP, a new constraint based on the dual values of the SP is added to the MP. This additional constraint is called a Benders cut. [20]

Najy and Diabat (2020) present the construction of the MP and SP for a simple Mixed-Integer Problem (MIP) [52]. The original problem is shown in Equation 3.5 - 3.7. This equation minimises z^* , has decision variables x and y , and the constraints are given by Equation 3.6. This minimisation problem can also be written as Equation 3.8. This equation solves two minimisation problems, one for each decision variable.

$$z^* = \min_{x,y} c^T x + f^T y \quad (3.5)$$

s.t.

$$Ax + By \geq b \quad (3.6)$$

$$x \geq 0, y \in Y \subseteq \mathbb{Z}_+ \quad (3.7)$$

$$z^* = \min_{y \in Y} \{f^T y + \min_{x \geq 0} \{c^T x : Ax \geq b - By\}\} \quad (3.8)$$

The aim of the Sub-Problem is to find the upper bound of the original problem. The first step is to find the dual problem of the minimisation of x . For a each given y , the dual problem can be constructed and is shown in Equation 3.9, where u is the decision variable of the dual problem. If a fixed value \bar{y} is given, the upper bound of z^* is obtained by using Equation 3.10. This is the Sub-Problem of the algorithm.

$$z^* = \min_{y \in Y} \{f^T y + \max_{u \geq 0} \{(b - By)^T u : A^T u \leq c\}\} \quad (3.9)$$

$$z^* = \min_{y, \theta} \{\theta + f^T y : (b - By)^T u \leq \theta, \forall u : A^T u \leq c, u \geq 0\} \quad (3.10)$$

For the Master Problem, the first step is to rewrite the problem shown in Equation 3.9 contain an infinite constraint set, where the constraints are derived from all the points in the search space $\{u : A^T u \leq c, u \geq 0\}$. The new formulation is given in Equation 3.11. For the MP, the constraint set is restricted to some extreme points obtained from the SP. This relaxation of the problem leads to the lower bound of the problem and is shown in Equation 3.12, where U_T is a subset of u .

$$z^* \leq f^T y + \max_{u \geq 0} \{(b - By)^T u : A^T u \leq c\} \quad (3.11)$$

$$z^* \geq \min_{y, \theta} \{\theta + f^T y : (b - By)^T u \leq \theta, \forall u_t \in U_T\} \quad (3.12)$$

The algorithm proceeds by finding an upper bound using the Sub-Problem, in addition a new u^T is obtained and added to the Master Problem. A lower bound is then found using the Master Problem. The value of y is then used in a new iteration starting with the Sub-Problem. The iteration stops when the difference between lower and upper bound is sufficiently small.

The BD algorithm has been used to solve many different versions of hub location problems and has been shown to outperform standard solvers, such as CPLEX. Najy and Diabat (2020) and de Camargo et al. (2008) present implementations of the Benders Decomposition algorithm to multiple-allocation uncapacitated hub location problems. The algorithm is able to solve large scale networks that are out of reach for stander solvers: networks of 100 nodes and even up to 200 nodes are solvable whereas the implementation in CPLEX only handles up to 25 nodes. Other examples include an implementation for a capacitated single allocation problem [19] and a hybrid implementation between BD and an outer-approximation heuristic [18].

3.2. Meta-Heuristic Methods

Heuristic methods are able to produce a solution that is feasible, but in comparison with exact methods, the solutions are likely only near-optimal, however they cannot guarantee it. Heuristic methods are mostly iterative algorithm that search on new solutions that improve on the previous solution. The algorithms are often based on simple ideas on finding a better solution, An advantage of using heuristic methods is the capability of handling large scale problems, however the methods require a formulation that is adapted to the original problem. On the other hand, metaheuristics provide general procedures in order to solve a

problem. This section will elaborate on some of the popular meta-heuristics that have been applied to hub location problems, based on a comprehensive list of heuristic algorithm applications presented by Farahani et al. (2013) [26]. These methods are: Tabu Search (TS), Simulated Annealing (SA), Genetic Algorithm (GA), and Ant Colony Optimisation (ACO).

3.2.1. Tabu Search

The first metaheuristic that will be reviewed is the Tabu Search (TS) algorithm. The Tabu Search algorithm aims at escaping a local optimum of a problem to find the global optimum. After having obtained an initial solution, the algorithm needs to perform a local search procedure. This procedure results changes that can be made to the current solution to reach an improvement. However, when a local optimum is reached, there will be no more moves that can be made to improve the solution. In order to escape the local optimum solution, the principle of the steepest ascent and mildest descent approach is followed; If there are no more improvement possible, the move that results in the smallest loss is chosen. In order to stay away from the previously left local optimum, the move to the local optimum is put on a list of forbidden moves, the tabu list. A move will only be on the list temporarily to allow for better moves to be found. [33]

An example of Tabu Search in hub location problems is presented in Marianov and Serra (2003) [47]. The problem is solved in two phases: first, the construction phase is executed to obtain an initial solution with the location of the hubs. Next is the improvement phase, where new solutions are obtained by exchanging a hub by a non-hub location. In case a non-feasible solution is obtained, a penalty is added. The TS algorithm is used in this phase to avoid cycling back to the same solution. The algorithm was able to solve networks of 30 nodes in 25 seconds on a personal computer.

Another implementation is shown in Silva and Cunha (2009), where a multi-start Tabu Search algorithm is used [65]. This algorithm is used in cases when initial solutions are obtained easily, but improvement are difficult to find, for example when a problem is tightly constrained and will lead to many infeasible moves. The implementation of the algorithm was tested on USAHLP networks with 100 and 200 nodes and had a computation time of 12 seconds and 1112 seconds respectively. The algorithm used was evaluates using 94 benchmark problems of up to 200 nodes and was shown to present optimal solutions to 92 of the problems.

3.2.2. Simulated Annealing

The next metaheuristic that is reviewed is the Simulated Annealing (SA) algorithm. This algorithm again is aimed at escaping a local optimum solution to find the global optimum. However, instead of wasting iterations exploring local optima by performing climbing and ascending moves, the Simulated Annealing algorithm searches more directly for the global optimum. This is enabled by implementing a random component in the selection of the next move. In a given problem, the following parameters can be defined [33]:

- Z_c is the current solution value
- Z_n is the current candidate solution value
- T is a parameter indicating the tendency to accept new solutions

In the case that the new solution improves on the current solution, the move is always taken. However, in the case that the solution is worse, the new move will be taken based on the probability described in Equation 3.13, in the case of a maximisation problem.

$$P\{acceptance\} = e^{-x} \quad \text{where } x = (Z_n - Z_c)/T \quad (3.13)$$

A key principle of the algorithm is that the tendency to take other solutions decreases with each iteration. The parameter T used for this process is determined using a temperature schedule, named based on an analogy with physical annealing where the slowly decrease in temperature results in decreasing fluctuations in atom energy levels. An example temperature schedule for three iterations is as follows: $T_1 = 0.2Z_c$, $T_2 = 0.5T_1$, $T_3 = 0.5T_2$.

An application of this algorithm is presented by Chen (2007), who introduces a hybrid between the SA and TS algorithms for a UHLP problem [12]. This hybrid improves the solution finding method of the SA algorithm by avoiding cycles using a tabu list. The implementation of the problem is divided into three steps: determining the number of hubs, selecting the hub nodes, and allocating non-hub nodes to hubs. The first step of the algorithm is to increase the number of hubs in the network, until the marginal decrease in transportation cost is smaller than the fixed cost of adding a hub. To find new solutions, the algorithm performs moves that replaces a single hub node with another node. The model has been tested with networks up to 200 nodes with the new hybrid algorithm, a SA algorithm, and a Genetic Algorithm (GA) algorithm. The result show that the SA algorithm is able to solve the large problem to the best known solution within one hour. The hybrid algorithm however still comes out as the best algorithm of the three by solving the problem in 3 minutes.

3.2.3. Genetic Algorithm

Another metaheuristic that can be used is the Genetic Algorithm (GA). This algorithm does not start with one trial solution, instead, a whole population of feasible solutions is created. The basis of the algorithm is to run a population of solutions and to generate new solutions based on the current population. In order to rank the solutions, a fitness score is given to each solution, which is based on for example the objective function value. Of this population, a certain group will be selected as parents of the new population, where the solutions with a better fitness have a higher chance of being selected. These parents produce new solutions by combining different parts of their solution and by introducing some mutations in the solution in order to explore the feasible region of the problem. The main choices that need to be made in order to use this model are: the population size, the manner of selecting the parents, the passing of features, the mutation rate, and the stopping rule. [33]

An implementation of a GA is presented by Lin et al (2012) to solve a p-HMP model [43]. This choice was motivated by the ability to search a vast area of the feasible region and the use of probabilities instead of deterministic rules. In addition, this method was favourable as it does not require continuity or differentiability of the constraints. The implementation uses the different OD paths for the encoding of the genes of the solutions. This allows for feasibility in the solutions, while gradually improving to a local optimum. The model uses a population of 100 and determines the fitness based on the inverse on the total cost of the solution. A Computational study performed on a network of 40 airports with 3 or 4 hubs showed to produce solutions with a reasonably good quality. The local optimal solutions differed less than 0.1% with the lower bounds. The study also showed that the computational time increases with the number of hubs from 60 minutes to 80 minutes for 3 and 4 hubs respectively.

3.2.4. Ant Colony Optimisation

The last metaheuristic that will be discussed is the Ant Colony Optimisation (ACO) algorithm. This metaheuristic uses a colony of artificial ants which cooperate to find optimal solutions to a optimisation problem. The artificial ants are relatively simple agents and converge to a optimal solution by interacting indirectly using stigmergy, which is indirect communication through the use of the environment [23]. To use an ACO algorithm, it is first needed to define the solution components that can be used to construct a solution. Next, a set of pheromone values need to be defined. The total pheromone model is the basis of the ACO algorithm [7].

The algorithm starts by managing an ant colony and letting them construct a solution by choosing different elements based on stochastic decision policies based on a pheromone trail. After a solution is obtained, it is evaluated by an ant and the pheromones on the trail of the solution are updated, either increased if pheromones are deposited or evaporated if there are less ants on the trail. The evaporation of pheromones are useful to avoid a too rapid convergence of the problem and keeping a wide search space. [23]

Four implementations of the ACO algorithm on a CHLP model are presented by Randall (2008) [62]. The simplest approach presented is a hub oriented ACO, which determines which of the nodes should become hubs in the model. This approach is used in combination with a greedy heuristic, which allocates the non-hub nodes to the selected hubs by the ants, where the allocation is based on the traffic flow and distance to the hub. A hub is allocated to a node by choosing the best combination of short distance and low traffic flow. A computational study was performed with this algorithm for networks up to 50 nodes. On smaller networks of 10 and 20 nodes were solvable in less than 1 second, in addition, larger problems with 50 nodes were also solved to optimality relatively quickly, within 100 seconds.

3.3. Discussion

This chapter has reviewed various optimisation methods, either solving a problem using exact or meta-heuristic methods. The aim of the research is to find optimisation methods that are able to solve large scale models. This section will briefly discuss the trade-off between the different types of optimisation methods.

First is the choice between exact and heuristic based methods. Small-scale problems are able to be solved efficiently using exact methods, however, large-scale problems would require the use of heuristic or specialised exact methods, such as the Benders Decomposition (BD) algorithm. Large-scale problems can be considered out of reach of *simple* exact methods due to the computational time needed to solve the problem [20]. However, even though large-scale problems can be solved using specialized exact methods, meta-heuristic methods are capable of solving to optimality or near-optimality within less computational time [26]. As heuristic methods can end up at solutions that are near-optimal, instead of optimal, it is important to analyse the behaviour of the heuristic method by comparing the heuristic against exact methods for smaller networks.

Besides a choice between exact and heuristic based methods, it is possible to combine various techniques; a combination of several algorithmic techniques is of importance when solving large-scale models [2]. Examples of such refinements are introducing elimination tests to reduce the problem size and constructing stronger undominated cuts, known as Pareto-optimal cuts, to improve the convergence of an algorithm. Contreras et al. (2011) uses this combination of these techniques on top of a BD algorithm and was able to optimise UHLP networks of 500 nodes [15]. Other examples of combinations have been presented in the chapter as well, for example, the hybrid between the SA and TS algorithms for a UHLP problem presented by Chen (2007) [12]. The hybrid form is able to solve a network of 200 nodes 20 times faster.

When deciding on a optimisation method, it is important to understand the formulation of the problem as well. A good implementation of the optimisation method can help the performance. This is for example visible in the application of the Ant Colony Optimisation (ACO) algorithm, presented by Randall (2008), who presents four different forms of the algorithm to a CHLP model [62]. One of these models is aimed at determining the nodes that should become hubs in a network, coupled with another heuristic for the node allocation. On the other hand, another model combines these by successively linking nodes to potential hubs in the same algorithm. The result show that different implementations have better qualities regarding the best solution and computation time.

4

Review of Airport and Aircraft Modelling

Much research has been dedicated to using hub location problems for airport networks. To adapt a model to the airport network, it is necessary to know the characteristics of the nodes and the vehicles. The aim of this chapter is to find an answer to the following sub-question: **What methods are available to model the airport and aircraft characteristics in the model?** First, the airport characteristics will be reviewed in section 4.1. This section regards the determination of the capacity of airports and the implementation of the capacity in hub location models. Next, in section 4.2, the determination of the aircraft characteristics are reviewed. This includes the calculation of the range and fuel burn of a flight and a review of the implementation in different models. At last, in section 4.3, a discussion on the review is given.

4.1. Airport Modelling

The determination of airport capacities has two strategic purposes: understand the ability of the components of an airport system to manage the passenger and aircraft flows and to estimate the delays that can occur for different traffic flows [34]. Airport capacity is an important factor to consider in the hub location process. A small airport can emerge as a hub in an uncapacitated model, but the flows at the airport may exceed the capacity that the existing infrastructure allows for. The aim of this section is to present and review the methods that can be used to estimate airport capacities. First, in subsection 4.1.1, an overview is given on the different methods of capacity determination. In subsection 4.1.2 - 4.1.5, the various methods are discussed.

4.1.1. Overview of Capacity

Airport capacity estimation is an important factor in the traffic management process as inaccuracies could lead to delays or under-utilisation of the available capacity. The process of estimating the capacity of an airport is difficult as the process depends on many factors, such as airport operation procedures, runway configuration, the air traffic mix and meteorological conditions [39]. It should be noted that there are two definitions of airport capacity that are being used when talking about airport capacity prediction problems. The first is the *ultimate capacity* of an airport. This capacity indicates the maximum throughput that an airport system is able to handle. The second is the *practical capacity* of an airport. This capacity states the throughput of an airport, which is able to keep the average delay of flights below a specified amount. This concept links the capacity of an airport with the delays of an airport system. [34]

When choosing a method to estimate the airport capacities, it is important to consider the characteristics of the problem. Choi and Kim (2021) present the three characteristics that can be used to describe the airport capacity prediction problem [13].

- **Daily patterns.** Airports have daily patterns in their demand, and usually, the capacity of an airport is dependent on the expected demand levels [13]. The capacity of an airport is low early in the morning and late at night as people do not prefer to fly at these times. The daily pattern of an airport can also consist of peak periods, which can influence the use of priority for arrivals or departures.
- **Weather Conditions.** The capacity of an airport is dependent on the weather conditions of the airport. Flights to and from an airport are operated either under Visual Flight Rules (VFR) or Instrumental Flight Rules (IFR), where the decision is based on the weather conditions at the airport. If there

are bad weather conditions, a flight needs to be operated under IFR, which increases restrictions on flights. One of these restrictions is the minimum separation distance, where an increase would lead to a decrease in capacity. Airports which face a lot of bad weather conditions, can expect a big difference in the capacity between Visual Meteorological Conditions (VMC) and Instrument Meteorological Conditions (IMC). [13]

- **Nonlinear Capacity.** The capacity of an airport is described by two figures: the capacity of arrivals and the capacity of departures. These two capacities are interdependent of each other and are connected with a nonlinear function. This capacity curve can be represented in a graph with the departure capacity against the arrival capacity. An example is shown in Figure 4.1, where the curve is constructed by connecting the capacities at various operating procedures [39]. The end-points of the graph represent the only-arrival and only-departure modes. The points in-between represent mixed modes.

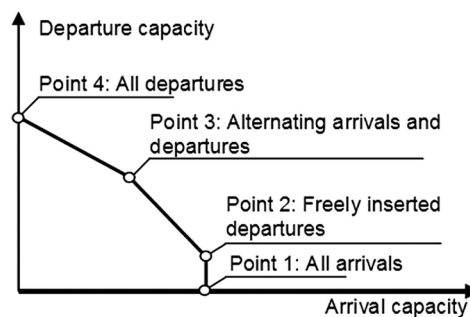


Figure 4.1: Departure-arrival capacity chart constructed by four different operating strategies [39].

These characteristics are useful to taken into account when estimating the airport capacity. Besides the characteristics of the airport capacity problem, it is also useful to know the components of the total airport system capacity. The two main components that can be recognised are the runway and airspace capacity. The runway capacity regards the flow of aircraft that can safely be allocated to a runway. These flows are influence by the runway configuration, operation procedures and the Wake Turbulence Category (WTC) distribution of the aircraft. Early analyses mostly focus on this component of the system [34]. The next component is the capacity of the terminal airspace around an airport. The airspace capacity is influenced by, for example, weather influences on certain zones in the airspace.

Various airport capacity models have been formulated which are able to estimate capacities of an airport system. To organise these models, Mascio et al. presents five different levels of model refinement for airport capacity prediction problems [49]. The different levels are distinguished by the amount of information needed for the model inputs, the number of components considered in the model, and the application of the models. The five categories are as follows:

1. **Table Lookup.** The first level is based on comparing the runway configuration to runway configurations for which the capacity already has been estimated. An example of such a lookup table is generated by the Federal Aviation Administration (FAA). For various runway configurations and flight mixes, there are available hourly capacities for either VMC or IMC. The table generated by the FAA is shown in Figure 4.2. An advantage of this method is that not much data is required for the estimation, however, the method is intended only for runways only and simple airfields. [25]
2. **Charts.** The second level again has the same use-case as the first level, however, if more detailed information is available on the traffic mix and the airport lay-out, it is possible to obtain more accurate estimates by reading off graphs. The FAA has also generated graphs for various runway configurations. An example graph is shown in Figure 4.3. [25]


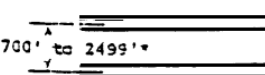
NO.	Runway-use Configuration	Mix Index % (C+3D)	Hourly Capacity Ops/Hr		Annual Service Volume Ops/Yr
			VFR	IFR	
1.		0 to 20	98	59	230,000
		21 to 50	74	57	195,000
		51 to 80	63	56	205,000
		81 to 120	55	53	210,000
		121 to 130	51	50	240,000
2.		0 to 20	197	59	355,000
		21 to 50	145	57	275,000
		51 to 80	121	56	260,000
		81 to 120	105	59	285,000
		121 to 180	94	60	340,000

Figure 4.2: Example table lookup for the determination of the runway capacities of two different runway configurations [25]

- Analytic Models.** The third level regards analytical models based on the runway capacities of airports. Such models are able to connect multiple factors with each other, such as the aircraft Wake Turbulence Category distribution, final approach speeds, separation distances, and Air Traffic Control (ATC) rules.[49]
- Airfield Capacity Simulation.** The fourth level concerns the capacity estimation of complex airfields, which requires more detailed input data. Examples of such inputs may be the flight track geometries, fleet mix per runway and the configuration of the airport itself.
- Aircraft Delay Simulation.** The fifth and last level of models are able to simulate the operations at the airfield and also take the flight schedule into consideration.

These five categories of airport capacity prediction models show the different levels of detail that can be attained for a model. The categories do however lack a category of models that are present in the research field; empirical models. An example is the empirical approach to airport capacity estimation presented by Gilbo (1993), where the non-linear curve of the departures and arrivals is approximated based on data [29]. More recently, data-driven models are being used to estimate airport capacities. Examples are: a decision-tree model, which can predict the runway capacity in real-time [30], a machine learning based application, which is based on historical flight tracks, weather forecasts, and airport operational data [51], and neural-networks which are able to predict the airports capacity and implements transfer learning to adapt the model to other airports [13].

This section gave an overview of the different methods that can be followed to estimate the airport capacity. The following subsections will review some instances of each of the models in the described categories, ranging from the empirical approach to the simulation approach.

4.1.2. Empirical Approach

An empirical approach to the airport capacity prediction problem is presented by Gilbo (1993) [29]. The empirical approach is proposed as it eliminates assumptions based on the distribution functions of random variables in the analytical approaches. The method proposed uses the non-linear relationship characteristic between the arrivals and the departures of a runway to generate a model. In the model, the relationship between the arrival capacity c_a and departure capacity c_d is described by the following function: $c_d = \phi(c_a)$. This function is obtained by fitting a curve based on the traffic flows during peak periods. It is assumed that the peak periods reflect or approach the actual maximum capacity of an airport.

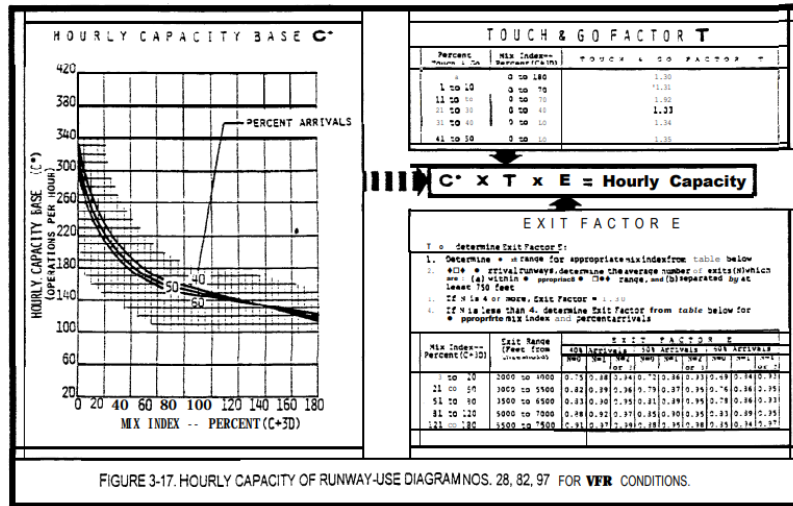


Figure 4.3: Example chart for the determination of the runway capacity [25]

The data obtained during the peak hours is plotted in an arrival-departure capacity graph. This results in the graph shown in Figure 4.4. The dots represent the arrival and departure capacity during peak periods; in this case the peak periods have a time-span of 15 minutes. Around these data points, a piece-wise linear curve is fitted. If all the points are considered, the outer curve is obtained. It can be seen that the envelope obtained from this curve leaves some large areas where there are no data points. To increase the robustness of the model, the outliers in the dataset need to be removed by some rejection criteria. This results in the inner curve in Figure 4.4, which can be used for the capacity estimation of an airport. The obtained curve can be used to optimise the capacity of an airport. For example, Gilbo (1993) presents a model that is able to allocate the airport capacity to the arrival and departure demand for a given time-span [29].

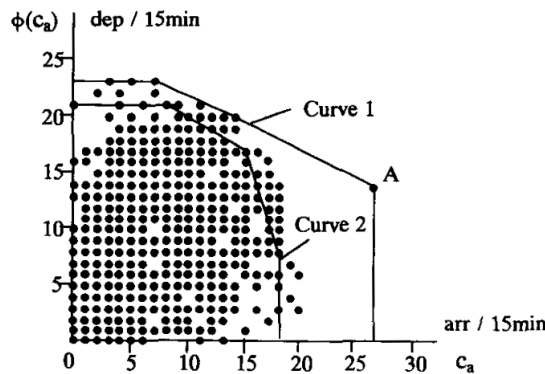


Figure 4.4: Empirical determination of the arrival-departure capacity curve [29].

4.1.3. Runway Capacity Model

The first analytical model reviewed is presented by Hockaday and Kanafani (1974) and is aimed at estimating the ultimate capacity of a runway system for various operating conditions [34]. The main assumption of the model is that aircraft arrive at a certain point before continuing onto the descent path. In addition, any deviations from the mean path are normally distributed and independent of other aircraft. The first step in the capacity calculation consists of finding the interval times between the various aircraft categories for landings and take-offs. Next, the runway capacities can be calculated using the interval times and expected fleet mix for the various operating conditions. At last, the capacity of the runways can be optimised by selecting the best operating strategy.

There are five conditions that describe the minimum separation between aircraft. These conditions are as follows:

- **AROR(i)** Arrival Runway Occupancy Requirement. The time needed for an aircraft to clear a runway after arrival.
- **AASR(ij)** Arrival-Arrival Separation Requirement. The time between two arriving aircraft that needs to be maintained in order to ensure minimum separation distances.
- **DROR(i)** Departure Runway Occupancy Requirement. The time that a departing aircraft occupies the runway.
- **DDSR(ij)** Departure-Departure Separation Requirement. The time between two departing aircraft that needs to be maintained in order to ensure minimum separation distances.
- **DASR(j)** Departure-Arrival Separation Requirement. The time separation between arriving aircraft of class j to ensure the separation rules.

The minimum separation times of the various conditions are assumed to be based on normal distributions around a average time based on the aircraft category. The determination of the Arrival-Arrival Separation Requirement requires an extra step as this time separation is based on the velocities of the two aircraft involved. There are two cases in arrival separation that need to be considered. First is the closing case, where the trailing aircraft is overtaking the leading aircraft, $v(i) \leq v(j)$. The minimum separation is applied to the moment when the leading aircraft lands, as this is the closest the two aircraft will be. The minimum separation time is found by dividing the minimum separation distance between the two aircraft categories, $\delta(ij)$, and the airspeed of the trailing aircraft $v(j)$. This equation is shown in Equation 4.1. In the other case the space between the aircraft opens up, as the leading aircraft has a higher speed, $v(i) > v(j)$. The separation at the runway threshold is now larger than at the entry point. The minimum separation time is now using the formula shown in Equation 4.2, where γ is the length of the final approach path. The opening and closing case are visualized in Figure 4.5, where the time separation between the leading and trailing aircraft is shown with respect to the distance to the runway. [34]

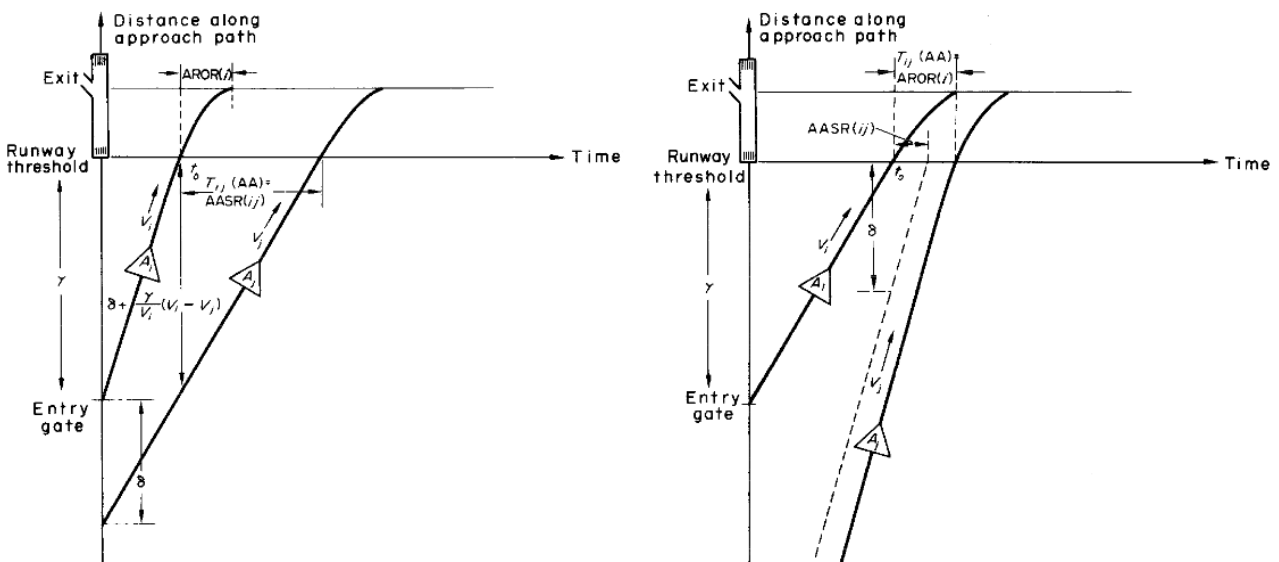


Figure 4.5: Opening and closing case between arriving aircraft with different approach speeds [34].

$$\frac{\delta(ij)}{v(j)} \quad \text{for } v(i) \leq v(j) \quad (4.1)$$

$$\frac{\delta(ij)}{v(j)} + \gamma \left(\frac{1}{v(j)} + \frac{1}{v(i)} \right) \quad \text{for } v(i) > v(j) \quad (4.2)$$

The capacity of a runway is found by dividing the average inter-arrival or departure time of two aircraft by the desired time span. To find the average time, it is first needed to determine the time of a single aircraft pair. For two arriving aircraft, the inter-arrival time, $TAA(ij)$, is the maximum of the $AASR(ij)$ and the $AROR(i)$. The inter-departure time, $TDD(ij)$, is the maximum of the $DDSR(ij)$ and the $DROR(i)$. The average time is based on the fleet mix proportions, where the probability of aircraft i using the runway is $p(i)$. The probability that aircraft i is followed by aircraft j is $p(ij) = p(i)p(j)$. The average inter-arrival and departure time are then found using Equation 4.3 and Equation 4.4.

$$TAA = \sum_{ij} p(ij)TAA(ij) \quad (4.3)$$

$$TDD = \sum_{ij} p(ij)TDD(ij) \quad (4.4)$$

To find the capacity in mixed operation use, Hockaday and Kanafani (1974) use the method of inserting departures into a runway with arrival priority. The number of aircraft that can be inserted is determined by comparing the inter-arrival time between two aircraft of categories i and j with the Departure-Arrival Separation Requirement time $DASR(j)$. When the capacities of these three operating modes are determined, it is possible to select the best operating strategy for an airport based on the expected demand.

4.1.4. Airport Capacity Model

Another analytical based model is the Airport Capacity Model (ACM), produced by the FAA [70]. This model includes weather predictions, such as surface winds and visibility, to find the probabilistic capacity estimates for a runway system [39]. The model consists of two modules; these modules are the Runway Configuration Estimator (RCE) and the Runway Capacity Model (RCM). The inputs to these modules are categorized into four categories and are shown below:

- **Weather Forecasts:** includes the surface winds at the airport, the height of the cloud ceiling, and the visibility range.
- **Predicted Demand:** consists of the hourly arrival and departure estimates and the aircraft Wake Turbulence Category mix.
- **Airport Adaptation:** The runway lay-out, geometry, possible configurations, as well as the runway occupancy times and approach speeds per aircraft category.
- **Operational Standards and Procedures:** state the thresholds for crosswind, tailwind, ceiling and visibility. This also includes the minimum separations for arrivals and departures, and the Wake Turbulence Category (WTC) separations.

These inputs are used by the two modules, the first of which is the Runway Configuration Estimator. There are three main steps that are performed by this module. The first step is to find the possible runway configuration based on the available runways of an airport. Next, the surface winds are used to calculate the expected crosswind and tailwind at each runway. Using the stated thresholds of the airports, the usable runway configurations can be determined.

The second module, the Runway Capacity Model, delivers the runway capacities of the chosen runway configuration of the RCE. The first step in the capacity determination is to determine the meteorological conditions at the airport using the input weather conditions. For each single runway the capacity for the

several operating procedures is estimated, using the predicted demand, airport adaptation, and operational standards. A similar method for determining the minimum time separations is used as presented in subsection 4.1.3 [39]. The last step is to combine the capacities of the single runways to obtain the total airport capacity estimate.

An improvement to the Airport Capacity Model is the Integrated Airport Capacity Model (IACM), presented by Kicingier et al. (2011), incorporates the terminal airspace capacity into the model; a visualisation of the components of this model is shown in Figure 4.6 [40]. Next to the Airport Capacity Model (ACM), the Terminal Capacity Model (TCM) determines the capacity of the terminal airspace around the airport based on the parts of the airspace which are affected by the weather and have an influence on the arrival and departure traffic. Additional inputs to this model are precipitation and echo tops forecast. The capacities of both the ACM and TCM are combined to obtain an improved estimate of the airport capacity. [39]

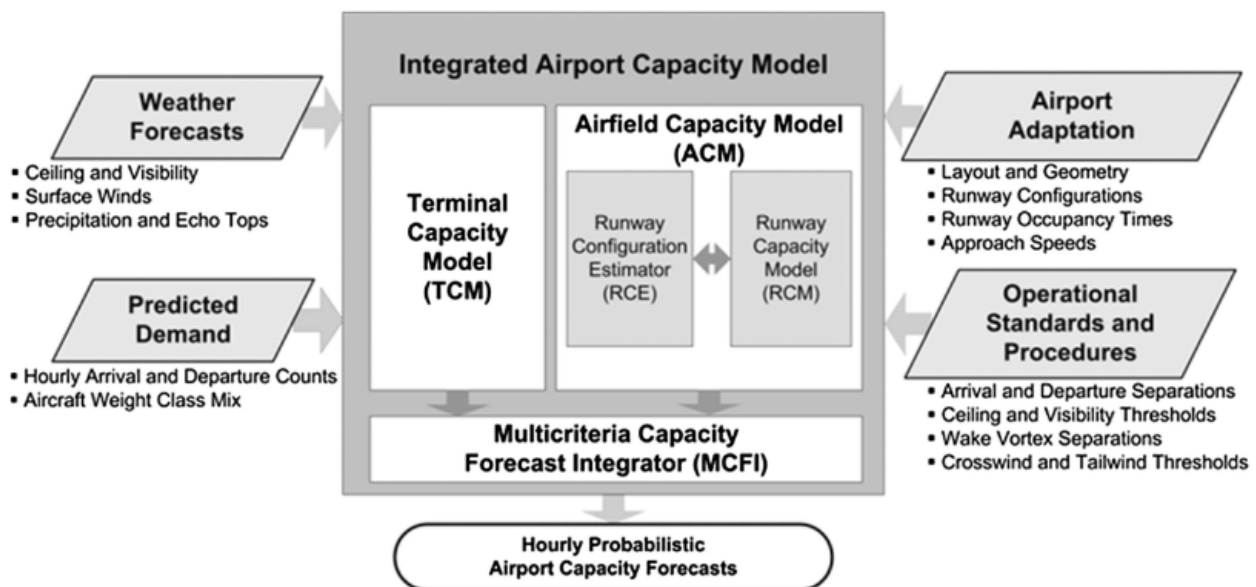


Figure 4.6: Visualisation of the components of the Integrated Airport Capacity Model (IACM), including the model inputs [39].

4.1.5. Simulation

The fourth and fifth level of detail in airport capacity prediction regard the use of simulation models. Compared to analytical models, the simulation models require labor-intensive setups and large data-sets are required per airport in order to estimate the airport capacity [13]. However, a greater level of detail can be achieved by using simulation-methods, whereas analytical models provide approximations of the airport capacity, which is more useful for strategic purposes [39].

An example of a simulation-based model is the Total Airspace and Airport Modeller (TAAM), owned by Jeppesen. The model is a fast-time flight path simulator, which is able to simulate the total air traffic system of an airport. There are many applications of the model, such as estimating the airport capacities, planning airport improvements, designing arrival and departure procedures and assessing the controller workload. The model requires an input file that described the entire air traffic system, but the level of detail required is dependent on the application. The file includes inputs such as the airport layout, the air traffic schedule and flight plans, and airport operational standards. Different aspects of the model have been verified in different scenarios. The simulation model is able to demonstrate being capable of simulating the airport operations closely compared to reality.[68]

4.1.6. Airport Capacity Implementation

The previous subsections elaborated on the determination of the airport capacities. The hub location problems described in section 2.1 all assume that the nodes of the network are uncapacitated, which means that there is no limit on the flow that can pass through a node. In real life however, nodes in a network are limited in capacity by for example the operating conditions of the runways of an airport [34]. This section will elaborate on the different methods that can be applied to hub location problems to incorporate capacity, as well as the method of obtaining the capacity of the airports in the network.

There are various methods that allow for the implementation of capacity in the network. The first of these is setting a limit on the flow that can pass through an airport node. The second limits the maximum flow on a link between two nodes. An example of the first method is given by Campbell (1994) formulates a constraint for the Unconstrained Hub Location Problem (UHLP). This constraint limits the total passenger flow through a node and is shown in Equation 4.5. [10] This constraint can be added to the UHLP given in Equation 2.19 - 2.24. This equation assumes a new variable, Γ_k , which represents the maximum number of units that can pass through the hub node k .

$$\sum_i \sum_j W_{ij} \left(\sum_m (X_{ij}^{km} + X_{ij}^{mk}) - X_{ij}^{kk} \right) \leq \Gamma_k Y_k \quad \forall k \quad (4.5)$$

Another method is to implement a limit on the capacity of an arc between two cities. Campbell (1994) present a constraint that is able to achieve this. A constraint is added that add a minimum and a maximum threshold on an arc. An example constraint is shown in Equation 4.6 for the p-HMP shown in Equation 2.10 - 2.16 [10]. In this equation, the minimum threshold flow between cities i and k is indicated by T_{ik} and the constraint is restricted by using a large number M . The choice of the large number determines the maximum flow on the arc. This is determined using Equation 4.7.

$$T_{ik} - \sum_j \sum_m (W_{ij} X_{ijkm} + W_{ji} X_{jimk}) \leq M(1 - Z_{ik}) \quad \forall i, k \quad (4.6)$$

$$M_{ik} = \sum_j (W_{ij} + W_{ji}) \quad \forall i, k \quad (4.7)$$

A disadvantage of these methods is the use of decision variables that determine the total flow of passengers, instead of putting restrictions on the number of vehicles. The number of vehicles however are used to indicate the runway capacity of an airport. To incorporate the runway capacity into the model, it would be favourable to include a decision variable for the number of vehicles, such as is present in the Airline Network Design (AND) model presented by Jaillet et al (1996) [37]. However, this model does not yet include a method to impose limits on the airport capacity.

4.2. Aircraft Modelling

The previous section elaborated on the airport characteristics. Aircraft also have certain characteristics that need to be taken into account, such as the maximum payload and the possible maximum range, which are dependent on each other. The basic models shown in section 2.1 are currently only formulated for the flow of passengers, without a distance restriction. This section will focus on incorporating the characteristics of aircraft in the models. First, in subsection 4.2.1, the determination of aircraft range is discussed. Next, in subsection 4.2.2, the dynamics between payload and range are explained. At last, in subsection 4.2.3, the implementation of the aircraft characteristics into hub location models are discussed.

4.2.1. Aircraft Range Determination

This subsection will regard the determination of the range and fuel consumption of an aircraft. The method presented in this subsection is obtained from Ruijgrok (2009) [63]. For a model that includes the choice of an aircraft type, it is important to know if an aircraft is able to meet the range requirements of a certain flight.

In addition, the fuel consumption of that aircraft can be used to determine the fuel cost or the amount of emissions. Two distinctions in range will be made in this review: the stage length and cruise range. The stage length, also known as total range, is the total distance that can be flown between take-off and landing. The cruise range however is the distance of the cruise phase.

The maximum total range of an aircraft is dependent on the fuel capacity of an aircraft. An important variable in the range calculation is the fuel consumption per hour, F , which is defined as the difference in fuel weight W_f per unit of time. As the usage of fuel leads to an equal decrease in aircraft weight W , the variable can be rewritten as shown in Equation 4.8. The burned fuel can be determined using the integral shown in Equation 4.9. The range of an aircraft is based on an integral over the velocity. By combining this with the fuel consumption rate, the integral shown in Equation 4.10 can be obtained. In this equation the fraction V/F is also called the specific range.

$$F = \frac{dW_f}{dt} = -\frac{dW}{dt} \quad (4.8)$$

$$W_f \int_{t_1}^{t_2} F dt \quad (4.9)$$

$$R = \int_{t_1}^{t_2} v dt = \int_{W_1}^{W_2} -\frac{V}{F} dW \quad (4.10)$$

In order to determine the stage length of a flight, the calculation will be split in two parts: the cruise phase, and the phases of climb and descent. This distinction is made as different assumption can be made for each phase. First, the cruise phase is considered. In the range determination, there is a distinction between propeller and jet aircraft. The difference is visible in the fuel consumption rate, shown in Equation 4.11 and Equation 4.12. For propeller aircraft, the fuel consumption is based on a specific fuel consumption c_P and the brake power P_{br} , found using the power available P_a and the propulsive efficiency η_j . For propeller aircraft, the specific fuel consumption c_T and the thrust T are used.

$$F = c_P P_{br} = c_P \frac{P_a}{\eta_j} \quad (4.11)$$

$$F = c_T T \quad (4.12)$$

For the determination of the cruise range, it can be assumed that the aircraft will be in steady and level flight. For the propeller aircraft, it can be assumed then that the power available P_a is equal to the power required P_r . The fuel consumption rate can then be rewritten to Equation 4.13, with D as the drag on the aircraft. Using the relationship of $D = C_D/C_L W$, the specific range can be rewritten as shown in Equation 4.14. Inserting this range into Equation 4.10 gives the range equation for propeller aircraft, in Equation 4.15.

$$F = c_P \frac{P_a}{\eta_j} = c_P \frac{P_r}{\eta_j} = c_P \frac{DV}{\eta_j} \quad (4.13)$$

$$\frac{V}{F} = \frac{\eta_j}{c_P} \frac{C_L}{C_D} \frac{1}{W} \quad (4.14)$$

$$R = \int_{W_2}^{W_1} \frac{\eta_j}{c_P} \frac{C_L}{C_D} \frac{dW}{W} \quad (4.15)$$

During cruise, only small variations can be expected in η_j and c_P and at a single of attack during cruise, C_L/C_D is also constant [63]. These assumptions allow the integral to be approximated using Equation 4.16.

$$R = \frac{\eta_j}{c_P} \frac{C_L}{C_D} \ln \frac{W_1}{W_2} \quad (4.16)$$

For the determination of the range of jet aircraft, similar steps can be performed. If steady level flight is assumed, the thrust can be rewritten to Equation 4.17, using the relationship $D = C_D/C_L W$. Combining Equation 4.12, Equation 4.10 and Equation 4.17 gives the range integral shown in Equation 4.18. For steady level flight, it can be assumed that c_T and C_L/C_D remain constant, which allows for the integral approximation shown Equation 4.19.

$$T = D = \frac{C_D}{C_L} W \quad (4.17)$$

$$R = \int_{W_2}^{W_1} \frac{V}{c_T} \frac{C_L}{C_D} \ln \frac{dW}{W} \quad (4.18)$$

$$R = \frac{V}{c_T} \frac{C_L}{C_D} \ln \frac{W_1}{W_2} \quad (4.19)$$

The second part of the total range determination is due to the climb and descent phases. For these phases, the rate of climb, RC , of an aircraft is an important parameter. The rate of climb is defined as the vertical component of the airspeed V and is shown in Equation 4.20, with H as the altitude and γ as the flight path angle. The distance flown during a climb or descent manoeuvre, s , is then calculated by taking the integral over the horizontal part of the velocity, shown in Equation 4.21, which is rewritten to integrate over height using Equation 4.20. The fuel weight burned is found by integrating the fuel consumption rate over time, as shown in Equation 4.22, which is rewritten to be integrated over altitude using Equation 4.20.

$$\frac{dH}{dt} = RC = V \sin \gamma \quad (4.20)$$

$$s = \int_{t_1}^{t_2} V \cos \gamma dt = \int_{H_1}^{H_2} \frac{dH}{\tan \gamma} \quad (4.21)$$

$$W_f = \int_{t_1}^{t_2} F dt = \int_{H_1}^{H_2} \frac{F}{RC} dH \quad (4.22)$$

When solving for the fuel burn, it should be noted that in these integrals the weight reduction due to fuel burn has an effect on the rate of climb. In order to include these effects, the integral could be solved iteratively, while updating the rate of climb to the new aircraft weight after each step. The new weight of the aircraft is then found by subtracting the fuel weight burned in each step. This method requires the use of a graph or an analytic expression between the rate of climb, altitude and weight. Another method is proposed by EUROCONTROL, which uses performance data of the Base of Aircraft Data (BADA) [53]. This method combines a thrust model, which provides the thrust of the aircraft, and a fuel consumption model, which calculates the fuel burned. An advantage of using this method is the availability of many aircraft type specific data

4.2.2. Payload-Range Characteristics

In the last subsection it was established that the range of an aircraft is limited by the fuel capacity of an aircraft. In order to determine the amount of fuel an aircraft can carry, it is important to understand the different components of the weight of an aircraft. The weight of an aircraft can be divided into three main weight categories: the Operational Empty Weight (OEW), the payload weight and the fuel weight. These weights added up are restricted to the Maximum Take-Off Weight (MTOW) of the aircraft. The payload capacity of an important factor in the economic performance of an aircraft. The payload-range diagram is a useful tool to show the payload capacity.

An example payload-range diagram is shown in Figure 4.7 [63]. This diagram shows the payload weight against the maximum range of an aircraft. The diagram can be divided into three segments. The first segment restricts the payload to the available space on the aircraft. In the second segment, in order to increase

the range, the payload needs to be exchanged for fuel weight as the combined weight of the aircraft is limited by the MTOW. The third segment starts when the tank capacity is reached. In order to get any increase in range, the weight needs to be reduced by removing payload.

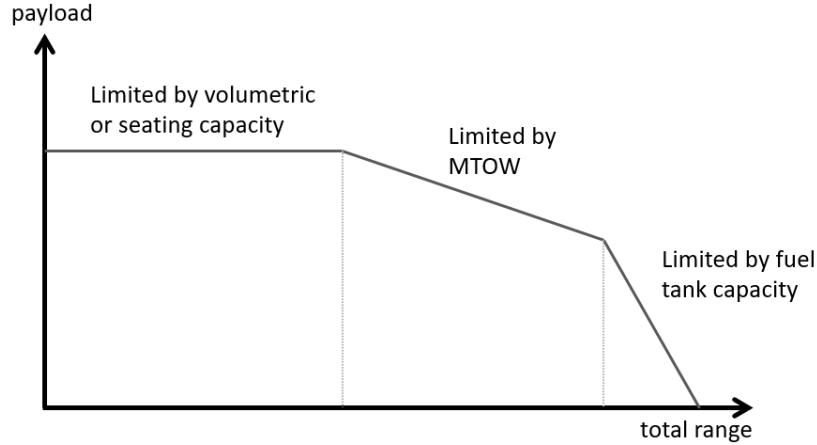


Figure 4.7: Payload-range diagram visualising the three limiting cases of the payload. [63]

The curve of the payload-range diagram indicates the limited payload for each range, however, all points under the curve could be a possible payload. An interesting use of the graph is to determine the additional fuel weight for an increase in payload. To start, the range equation, shown in Equation 4.19, can be rewritten to contain the individual components of weight: the Operational Empty Weight W_0 , the payload weight W_P and the fuel weight W_f . Equation 4.23 shows the individual weight components, assuming that the end of the phase has no fuel left. This equation can be rewritten to solve for W_f , as shown in Equation 4.24. To find the increase in fuel weight for an increase in payload weight, the derivative is taken over the payload weight W_P . The result is shown in Equation 4.25.

$$R = \frac{V}{c_T} \frac{C_L}{C_D} \ln \frac{W_0 + W_P + W_f}{W_0 + W_P} \quad (4.23)$$

$$W_f = (W_0 + W_P) \left(e^{\frac{RC_D c_T}{VC_L}} - 1 \right) \quad (4.24)$$

$$\frac{dW_f}{dW_P} = \left(e^{\frac{RC_D c_T}{VC_L}} - 1 \right) \quad (4.25)$$

4.2.3. Implementing Aircraft Characteristics

Much research has been dedicated to using hub location problems for airport networks. Different approaches are taken to implement the characteristics of aircraft into the model. First, the maximum range of aircraft will be discussed. A common approach is to not regard any characteristics in the model. An example is the analysis performed by O'Kelly (1998) who compares different Hub-and-Spoke networks resulting from three different versions of hub allocation models [57]. The paper states the use of a single and multiple allocation model referenced from Campbell (1994), which are also described in section 2.1, and the FLOWLOC model formulated by O'Kelly and Bryan (1997) [59], which is similar to the multiple allocation model, however it gives a greater discount for larger flows between two hubs. These three models do not take into consideration any distance limitations or capacity constraints.

Another more recent example is the Gateway Hub Location Problem (GHLP) formulated by Bernades Real et al. (2018) [5]. The formulated mathematical model makes a distinction between *standard* hubs and *gateway* hubs, where the former only allows for connections within a region, the latter allows for connections to other regions. This model again does not include any constraints regarding the characteristics of the aircraft in the network. However, longer arc distances are discouraged as the cost of activating an arc between nodes is based on a weighted function of the distance.

The approach taken in the two given examples seem to assume that there will always be an aircraft that is able to fly the route. In addition, there is also no explicit number of aircraft determined for a route, which allows any capacity problems of aircraft to be disregarded. An advantage of this system is that it avoids complicating the model. This approach can be useful if it is certain that there will be no range limitations within a given network. For example, the analysis performed by O’Kelly (1998) simulated a network in the United States of America. If the largest distance between two nodes is smaller than the maximum range at a useful payload, then there would be no need for implementing such a constraint in the model. This does however mean that a payload, or load factor, needs to be assumed for all aircraft to be sure that the range can be met; an aircraft at Maximum Take-Off Weight (MTOW) has a different range than an aircraft with no payload and maximum fuel.

In the case that range is able to be a limiting factor, another approach should be followed. The following approach that will be discussed implements a limit on the maximum arc distance between two nodes. This limit can be imposed in different ways. One method is to directly add a constraint to the model. An example is the model formulated by Oktal and Ozger (2013), which is a multi-allocation Capacitated Hub Location Problem (CHLP) with additional constraints; if a distance between two nodes is greater than the aircraft range, it can not be chosen. The range in this case is chosen to be the maximum range of the considered aircraft at MTOW. [58]

Another method of implementing range of the aircraft into the model has been used by Lowe and Sim (2013). The model presented is a Hub Covering Flow Problem (HCFP), which improves upon the Hub Covering Problem (HCV) by incorporating the transportation costs of the demand flow. Limits on the distance are imposed by using the big-M method on the transportation cost between two nodes. If the distance between two nodes becomes larger than the maximum range of an aircraft, the cost will rise to a large number M, which would counteract the minimisation of the total cost. In addition, this method can be used when multiple types of aircraft are considered in the network. If the maximum range of an aircraft is reached, instead of assuming a cost of M, first the operating cost of the next aircraft is used. This can be repeated for the desired amount of aircraft. [44]

Next, the implementation of capacity is discussed. As most hub location models do not include a decision on the number of aircraft, there is also no need to implement the capacity in the models. The capacity of aircraft does get utilised in the Airline Network Design (AND) model presented by Jaillet et al. (1996), as this model selects the number of aircraft on city pair based on the expected flow. The capacity of aircraft can however also be implemented in hub location models that do not make implicit decisions on the number of aircraft. A solution is presented by Kimms (2016), which uses city arc-costs based on the number of vehicles; an additional fixed cost is incurred for every additional aircraft that is needed to cover the flow. A more detailed review of this method is given in subsection 5.1.3.

4.3. Discussion

This chapter reviewed modelling methods of airports and aircraft. The aim is to find techniques to represent the characteristics of airports and aircraft in the hub location models. For both of these components of the airport networks, the modelling techniques have been reviewed, as well as the method of implementation into hub location models. This section will elaborate on the key-points of the chapter.

First, the method of airport modelling is treated. To better reflect airports in a hub location model, it is useful to include the capacities of the airports. The method of modelling airports therefore focused on determining the capacities of a given airport. Different methods have been discussed that vary in complexity. If more data is available, such as weather forecast and operational standards, it is possible to get more accurate capacity numbers. Before choosing a method for the model, it should be determined what accuracy level is desired. As the capacities are used for a hub location model, rather than a real-time application, it is not beneficial to include current weather forecasts. Instead, the hub location model focuses on the capacities relative to other cities in the model. In such applications, it could suffice to use simple techniques to determine the airport capacities.

If the capacity numbers are determined, it is needed to determine how to implement the capacities into the model. This is dependent on the type of model that is used. What should be taken into consideration is how to adapt the capacity to the formulation of the model; if a model has decision variables based on passenger flows, the airport capacity cannot be directly implemented, as these are generally given as numbers of aircraft.

Next, the method of aircraft modelling is discussed. The main characteristics that can be implemented in hub location models were determined to be range, capacity and fuel use. The basis of determining range and fuel burn have been established in this chapter. When determining these characteristics, it is important to consider the method of determining the performance during climb and descent, as these segments are not described by the Breguet range equation. An example method is the use of the BADA aircraft database in order to iteratively determine the performance during climb and cruise. The interactions between capacity and fuel weight have also been reviewed. An useful tool is the determination of the marginal fuel weight for additional payload. This can be used to get better estimates for the fuel burn for certain load factors, if the model takes this into account.

The method of implementing the aircraft characteristics is found to be lacking in current literature on hub location models. A common approach is to neglect any characteristics of the aircraft in the model, besides incorporating the fuel component in the cost function. Some studies show an implementation of the maximum range of aircraft into the model. For example, a Capacitated Hub Location Problem (CHLP) model formulated by Oktal and Ozger (2013), who limit the distance between two cities to the maximum range at Maximum Take-Off Weight (MTOW) of an aircraft [58]. The model presented by Lowe and Sim (2013) implements range for different aircrafts, by using different range brackets and updating the cost-function based on the aircraft in that range bracket [44]. A direct implementation of aircraft characteristics is only found in the AND model formulated by Jaillet et al. (1996), where the aircraft range and capacity are used to determine the number of aircraft on a given route [37]. In addition, this method allows for multiple types of aircraft to be regarded.

Review of the Dynamics of Cost and Demand in Airport Networks

The final part of the literature research entails the review of cost dynamics and demand modeling in airport networks. These elements of the model are grouped as they have some dependency on each other. The aim of this chapter is to answer the sub-question: **How can the dynamics of cost and demand be incorporated into the model?** The first part of the chapter, section 5.1, will look at the modelling of economies of scale: the cost benefits of consolidating flows in Hub-and-Spoke (HS) networks. In section 5.2, the modelling of price sensitivity is reviewed. This entails the change in demand due to a change in price of a given service. In section 5.3, the various methods of determining the demand in an airport network are reviewed. At last, in section 5.4, a discussion of the review is given.

5.1. Economies of Scale

One of the main benefits that the usage of hubs provides is consolidation of flows. These flow consolidations have a positive effect on the operational cost as larger, more cost efficient, aircraft can be used and higher load-factors can be expected. In addition, the usage of hubs could further reduce the investment cost by focusing on on location only. This effect is called economies of scale. However, a main issue in conventional hub location problems is the inadequate modelling of economies of scale [2]. This section will elaborate on three modelling methods that vary in complexity: discounted arcs, piece-wise arcs, and multi-aircraft arcs.

5.1.1. Discounted Arc Cost

One of the earliest used methods to model economies of scale is to introduce a discount factor for inter-hub transfers. This method models the cost-benefits of inter-hub travel as a discount on the operational cost compared to a non-hub flight. This discount is visualised in Figure 5.1 [2]. This figure shows the total operational cost based on the amount of flow between cities i and j . In the figure c_{ij} described the standard unit costs between cities i and j and α is the discount factor of the flow between two hubs. This method is present in a p-HMP formulated by Campbell (1994) and the total cost of the itinerary is shown in Equation 5.1 [10]. This equation describes the cost between an OD pair i and j using hubs k and m using three cost components: two spoke-hub flights and one discounted inter-hub flight.

$$C_{ijkm} = c_{ik} + c_{mj} + \alpha c_{km} \quad (5.1)$$

This method has been applied in many other hub location models and still is the basis for recent research in the field [2]. For example, it can still be found in studies such as: Mahmoodjanloo et al. (2020) which uses this implementation to formulate a multi-modal hub location pricing problem [46], and Gelareh et al. (2015) which shows a formulation for an uncapacitated multi-allocation hub model with budget constraints for the operator of the network [28].

This implementation allows for less complex models, however, it may not always be a good reflection of real networks [2]. It assumes that the cost is linear compared to the flow between two cities, which could lead to effects of economies of scale being modelled incorrectly. For example, a spoke-hub connection with a large flow benefits of economies of scale by using larger vehicles, but will be priced using the non-discounted cost.

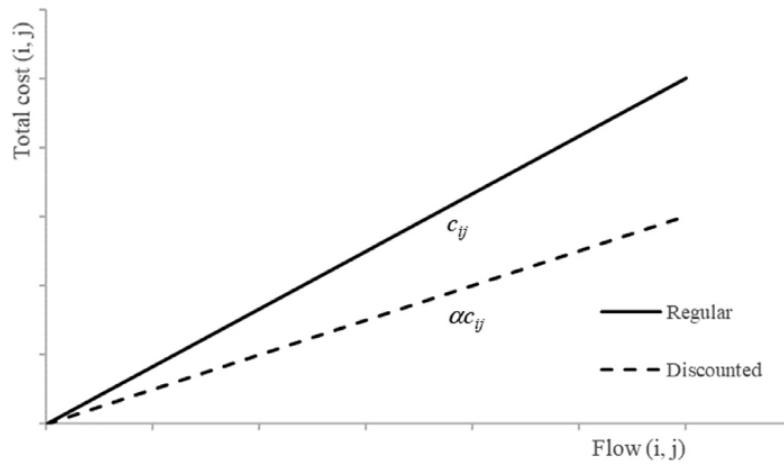


Figure 5.1: Cost function diagram based on the flow between cities i and j :
A regular cost-function and its discounted form by factor α [2].

5.1.2. Piece-Wise Arc Cost

Regarding the previous implementation, a more adequate representation of the effects of economies of scale would be to take into account the size of the flow over an arc. O’Kelly and Bryan (1998) propose a non-linear cost function, which represents the decrease in the marginal unit cost with an increase in the load factor of a vehicle [59]. A visual representation of the total operational cost against the total flow is shown as the curve in Figure 5.2 [2]. This formulation prevents incorrect effects from the discounted-arc method, such as incorrect pricing on spoke-hub connections with large flows.

O’Kelly and Bryan (1998) do remark that the use of non-linear formulations make the model impractical to solve and therefore propose a piece-wise linear approximation. For better modelling, this function can be adapted to a piece-wise function. Each of these pieces has their own slope, the discount factor, and a fixed starting cost [59]. Such a piece-wise function is shown as well in Figure 5.2, with discount-factors β_1 and β_2 for the two pieces.

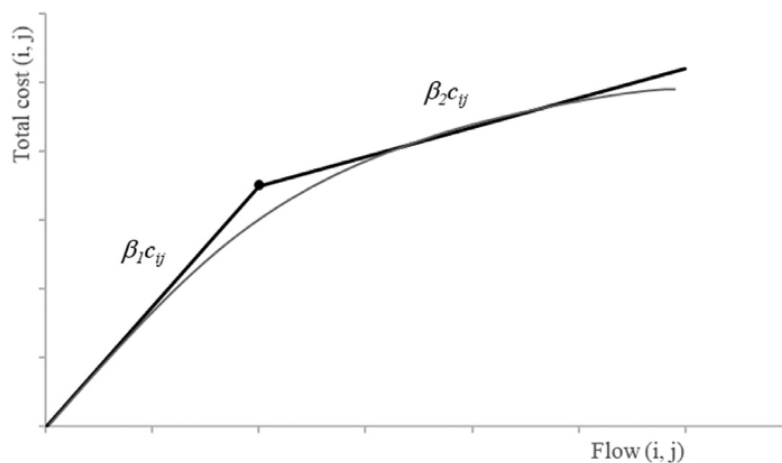


Figure 5.2: Cost function diagram based on the flow between cities i and j :
A non-linear cost-function and a piece-wise approximation [2].

The formulation presented by O’Kelly and Bryan (1998) implements this piece-wise arc cost on the inter-hub connection using the following method. The total operational cost C_{ijkm} from Equation 5.1 is updated

to Equation 5.2 [59]. In this equation, the discount factor is determined for a corresponding segment, q . The slope of a segment is a_q and the fixed cost of a segment is FC_q . The total flow on the inter-hub link (k, m) to which the given a_q is applied to is R_{qkm} . At last, Y_{qkm} is 1 if the flow on the inter-hub link (k, m) is charged the fixed cost FC_q , otherwise it is 0.

$$C_{ijkm} = c_{ik} + c_{mj} + c_{km} \frac{\sum_q (a_q R_{qkm} + FC_q Y_{qkm})}{\sum_q R_{qkm}} \quad (5.2)$$

In a computational study, this method was compared to the discounted-arc method and it was shown that the new method retains the properties of the original method while improving the properties of the cost function. However, a possible problem might be the property of user equilibrium, which can not be guaranteed in a system with flow-dependent costs. This could result in paths emerging in the network that are not the least-cost paths of a OD sub-market [59].

5.1.3. Multi-Aircraft Arcs

An interesting interpretation of the piece-wise approximation is to consider the segments to belong to different vehicle types. For example, a two-piece approximation might represent a small and large vehicle. A downside of using the piece-wise approximation, is that the fixed costs originate from the non-linear curve, instead of being adapted to the actual fixed costs of upsizing to a new vehicle. [2]

A variation of the piece-wise approximation is the use of step-wise functions, which rely on linear discount factors, but to take into account the fixed costs per vehicle. After a certain flow is reached, a new vehicle is needed and the fixed cost of a vehicle is charged. Kimms (2006) provides a method that also includes multiple types of aircraft in the cost function [41]. By overlapping the fixed cost and the variable cost functions of multiple aircraft, the cheapest option for each size of passenger flow can be determined. A visual representation is given in Figure 5.3 [2]. This figure shows the total operation cost functions for a small vehicle and a large vehicle. The minimum cost option per size of flow is highlighted.

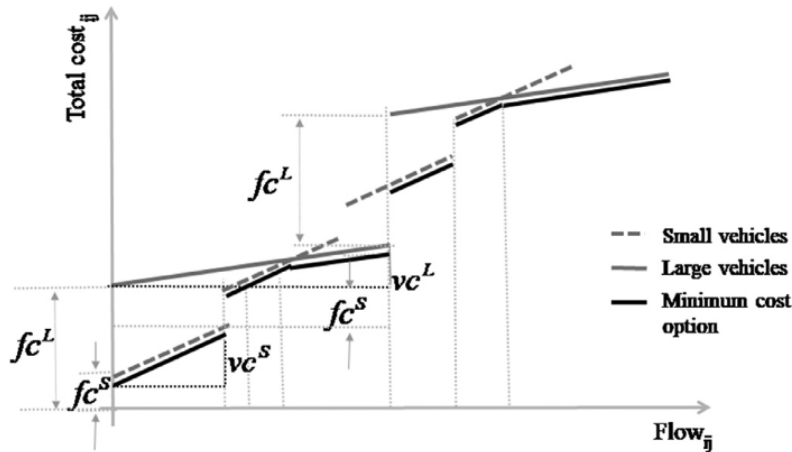


Figure 5.3: Cost function diagram based on the flow between cities i and j :
A piece-wise cost-function representing the minimum cost between a small and a large vehicle [2].

This approach of Kimms (2016) allows for the incorporation of economies of scale on non-hub connections and is implemented by adding indexes to the cost variable: c_{ij} is divided into fixed costs f and variable costs v , and a distinction is made between modes of transport m . This results in the variables $c_{ij}^{f,m}$ for fixed costs and $c_{ij}^{v,m}$ for variable costs. This does also come with a change in decision variables: the flow on a flight between i and j using mode m is f_{ij}^m , and the number of vehicles between i and j of mode m is z_{ij}^m . [41]

Another study presented by Serper and Alumur (2016) builds on this method by implementing different capacities for the various modes of transport. A computational study was performed by using a heuristic algorithm on a network of 25 nodes. The results showed that a network could be optimised in 30 minutes with solution gaps around 1% [64]. An additional complexity of the problem can be expected compared to the previous methods due to the added decision variables, but the result is a more realistic modelling of the economies of scale. In this case, an extra benefit is the determination of the types of vehicles on each route.

5.2. Price Sensitivity

In the previously described problems in chapter 2, it is assumed that the demands in the network are inelastic. This implies that the demand between a OD pair is not influenced by the type of service offered on the route. However, the use of a Hub-and-Spoke (HS) network in the hub location models, instead of a Point-to-Point (P2P) network, introduces changes to the transportation costs, routes and travel times. These changes can be expected to alter the demand for certain routes [32].

In this case, the demand in a OD sub-market is expected to be elastic, which means the demand is dependent on the price of the service offered. In a HS network, it is possible for multiple services to occur in a OD sub-market. For example, a direct flight, a one-stop flight or a two-stop flight, where each of these services has their own price. O'Kelly et al. (2015) presents an invertible demand function, $\rho = \phi(\mathbf{w})$, in order to show the connection between the prices and the demands of these services, where the vectors ρ and \mathbf{w} indicate the prices and the demand of the services respectively [60]. This function can be used to determine the willingness to pay for a service by taking the integral of the demand function for the given demand. This integral is shown in Equation 5.3 [60].

$$\int_0^{\mathbf{w}} \phi(\xi) d\xi = \sum_i \sum_j \int_0^{\mathbf{w}_{ij}} \phi(\xi_{ij}) d\xi_{ij} \quad (5.3)$$

In order to optimise for a network with elastic demand, the method of minimising the total operational costs does not suffice. Instead, to maximise the covered demand, strategic hub location decisions should be implemented with a focus on maximising the profit [42]. Such a shift in objective can lead to a fundamentally different hub network that is able to cover more demand, when assuming price elasticity [42].

An example of a profit maximisation model is presented by O'Kelly et al. (2015), where the conventional p-HMP is adapted to include the different types of service that are available in each OD sub-market [60]. The formulation of the model is given in Equation 5.4 - 5.16. The objective of the model is based on customer utilities for all the OD sub-markets, and subtracting the operational costs of the different services and the set-up costs of hub locations.

In this model, the decision variables are: x_{ijkm} , the flow between OD pair i and j using hubs k and m , y_{ijkm} , the flow between OD pair i and j using hub k , z_{ij} , the flow between OD pair i and j directly, and γ_k , an integer indicating if node k is a hub. The total demand of a sub-market is given by b_{ij} and the equilibrium demands of the different services are \dot{w}_{ij} , \bar{w}_{ij} and \tilde{w}_{ij} for the two-stop, one-stop and direct service respectively. The cost of each service \check{c}_{ij} , \bar{c}_{ij} and \tilde{c}_{ij} , uses the same notation. The cost of establishing a hub at node k is f_k .

$$\max \sum_i \sum_j \int_0^{\mathbf{w}_{ij}} \phi(\xi_{ij}) d\xi_{ij} - \sum_i \sum_j \sum_k \sum_m \check{c}_{ijkm} x_{ijkm} - \sum_i \sum_j \sum_k \bar{c}_{ijk} y_{ijk} - \sum_i \sum_j \tilde{c}_{ij} z_{ij} - \sum_k f_k \gamma_k \quad (5.4)$$

s.t.

$$Y_{ijk} + \sum_{m \neq k} x_{ijkm} + \sum_{m \neq k} x_{ijmk} \leq b_{ij} \gamma_k \quad \forall i, j, k \quad (5.5)$$

$$\sum_k \sum_m x_{ijkm} \geq \ddot{w}_{ij} \quad \forall i, j \quad (5.6)$$

$$\sum_k y_{ijk} \geq \bar{w}_{ij} \quad \forall i, j \quad (5.7)$$

$$z_{ij} \geq \tilde{w}_{ij} \quad \forall i, j \quad (5.8)$$

$$\sum_k \gamma_k = P \quad (5.9)$$

$$x_{ijkm} \geq 0 \quad \forall i, j, k, m \quad (5.10)$$

$$y_{ijk} \geq 0 \quad \forall i, j, k \quad (5.11)$$

$$z_{ij} \geq 0 \quad \forall i, j \quad (5.12)$$

$$\ddot{w}_{ij} \in \mathbb{R} \quad \forall i, j \quad (5.13)$$

$$\bar{w}_{ij} \in \mathbb{R} \quad \forall i, j \quad (5.14)$$

$$\tilde{w}_{ij} \in \mathbb{R} \quad \forall i, j \quad (5.15)$$

$$\gamma_k \in \{0, 1\} \quad \forall k \quad (5.16)$$

This model is presented by O’Kelly et al. (2015) as the first hub location model to integrate three different service types in the model. A computational study with test data showed that the location of the hubs are centrally clustered as the hubs provide multiple services, in this case the one-stop and two-stop itineraries. Lin and Lee (2018) present another hub location problem with elastic demands for less-than-truckload freight, but with capacities on the hub locations. With a different model formulation, the same behaviour in hub location is visible; the hub network is denser when the objective is profit maximisation, compared to when the objective is cost minimisation.

The incorporation of price elasticity improves the realism of the problem, however, not much research has been dedicated to this subject. Alumur et al. (2021) suggests the incorporation of a more realistic demand as a key topic in future research in hub location problems [2]. For example, a remaining question of the study of O’Kelly et al. (2015) is to connect the model to real cases by calibrating the demand functions with real data [60].

5.3. Demand Modelling

An obvious approach to obtaining the demand flows in a network is to directly use demand data from real-life. However, such data is only applicable to the current real-life airport network. The nature of demand is highly variable and the elasticity of demand regarding air fares, flight frequency and hub location all have an influence on the current demand [2]. Using such data could be less reliable in a hub location model where the network is different from the real-life network. An alternative to this could be to estimate the demand. A cross-sectional analysis looks into the different factors that influence the demand for an OD pair. Factors may include the population size and income figures, but could also be the type of city; a touristic city, such as Las Vegas, generates different traffic than a commercial city, such as New York City [54].

Various approaches to travel demand modelling are available, but Hsiao and Hansen (2011) note that the models can be categorised by two types. A distinction is made between demand generation models and demand assignment models. The first type concerns the determination of the size of the flows. The second type is able to generate the distribution of the traffic in a network, for example the choice of different routes between an OD pair [35]. The second type of model will be omitted from the research as distribution of traffic should be a result of the hub location model and not be an input.

Several approaches for demand generation models will be explained in the remainder of the chapter. The demand generation models can be divided into supply-side and demand-side formulations. This distinction is made by Hsiao and Hansen (2011), where the supply-side formulations are focused on factors such as flight frequency and air fares and the demand-side formulations are based on factors such as population and income figures. [35]

5.3.1. Supply-Side

This section will look at various models based on the first category of demand generation models based on supply-side factors. Examples of these factors are the flight frequencies and air fares of the flights between an OD pair. One of the earliest models is presented by Swan (1979). The quality of service is presented as an important decision factor of consumers, in addition to cost, when choosing a flight between an OD pair. The quality of service can be influenced by, for example, the inconvenience involved with low frequency flights. A flight scheduled with low frequency is likely to be at the desired time of the consumer, resulting in a displacement time subjected onto the consumer. Other qualities of service might be the duration and the comfort of the trip. [69]

These qualities of service, in combination with the air fare, can be represented as a the perceived price of the service. The formulation of the perceived price, PP , is shown in Equation 5.17. In this equation, F is the airfare, T is the total travel time, v is the value of time of the consumer, q is the variable representing the quantised quality dimensions, and h are the implied prices of the quality dimensions.

$$PP = F + v \cdot T + g \cdot q \quad (5.17)$$

The demand between an OD pair is then found using Equation 5.18. In this equation, k_1 is a market density constant and α represents the price elasticity. The price elasticity normally varies across different income groups, however, as the perceived price takes into account the actual price and time this factor is relatively constant. This assumption can be made as low income groups value time less compared to higher income groups, and the opposite is true for the actual airfare. [69].

$$D = k_1 \cdot PP^\alpha \quad (5.18)$$

Another supply-side based model is presented by Abrahams (1983). In the formulated model, demand is again based on the cost imposed on the traveler. The cost is defined as the airfare, as well as the value of time spent utilising the airline service. The time spent utilising the airline service is comparable to one of the qualities of service from the model of Swan (1979). The time lost due to infrequent flights is in this model called the schedule delay. A difference of this model is the addition of more factors, such as automobile costs, which is chosen as an alternative mode of travel. [1]

The demand equation formulated by Abrahams (1983) is given in Equation 5.19 [1]. In this equation, $X(i, j)$ is the demand between cities i and j , P is the lowest airfare, SD is the expected schedule delay, AC is the automobile costs, POP is the population of city i times the population of city j , Y is the income per capita, and $GGNP$ is the rate of growth of the Gross National Product. Each factor is multiplied with a factor α_x , which are determined by fitting the model to real-life data.

$$X(i, j) = \alpha_0 + \alpha_1 P(i, j) + \alpha_2 SD(i, j) + \alpha_3 AC(i, j) + \alpha_4 POP(i, j) + \alpha_5 Y(i, j) + \alpha_6 GGNP \quad (5.19)$$

Other supply-side based models are similar in formulation; a set of factors are assumed to be influential in the demand between an OD pair and the model is fitted against real-life data. The set of factors can be made more specific to the region that is to be modelled. An example is the model formulated by Bhadra (2002) [6]. This model considers the size of the presence of Southwest Airlines, a low-cost carrier, in a given OD

pair as a factor for the demand. This is in addition to other factors, such as the market power of dominant and non-dominant airlines. Another model presented by Wei and Hansen (2006) considers more detailed supply-side factors, such as the number of spokes of an airline serving the chosen hub, the capacity of the hub, and the average number of seats on the aircraft used on the given OD pair. [72]

A critique of the supply-side based models is that not all possible routes for a OD pair are considered [35]. This could lead to misleading results when for example the lowest travel time in a OD pair are considered, even though this flight is scheduled with a low frequency, or the flight has a high fare.

5.3.2. Demand-Side

The second category of demand generation models are based on demand-side factors. These factors are for example the population size, the income figures and the distances between the cities, which are not related to the characteristics of the airport network.

In early research, Verleger (1972) presents three different simple models that can be used to estimate the demand of a transportation network. The three types are gravity models, point-to-point models, and aggregate models, which use supply-side based factors. This section will focus on the first two types of models. [71]

The first type of model is the gravity model. These models follow the assumption that the demand between two cities will decrease with an increase in distance. However, the demand will grow if the two cities have larger populations. A basic formulation of the gravity model is shown in Equation 5.20. In this equation, T_{ij} is the travel demand between cities i and j , M_i is the population of city i , d_{ij} is the distance between cities i and j , and a is a variable for fitting the model. A variation of the model is shown in Equation 5.21, which incorporates different travel inducing effects by using variables α_i for city i . [71]

$$T_{ij} = a \frac{M_i M_j}{d_{ij}^2} \quad (5.20)$$

$$T_{ij} = a \frac{M_i^{\alpha_i} M_j^{\alpha_j}}{d_{ij}^2} \quad (5.21)$$

The presented models require much less data compared to the supply-side based models presented in subsection 5.3.1. However, Verleger (1972) outlines that heterogeneous markets are difficult to fit to such models. Satisfactory results have only been achieved with homogeneous markets, for example, the Northeast Corridor in the United States. [71]

Simple gravity models have been used however in hub location problems as a basis in the simulation of the models. For example, Jaillet et al (1996) uses the gravity model shown in Equation 5.22, where f_{ij} is the demand between cities i and j [37]. This model only uses the following variables: p_i being the population size of city i and α a constant.

$$f_{ij} = \alpha (p_i p_j)^{0.5} \quad (5.22)$$

Another more recent hub location model, formulated by Bernardes Real et al. (2018), is analysed using the gravity model shown in Equation 5.23. In this equation, w_{ij} is the demand between cities i and j , p_i is the population of city i divided by 100.000, g_i the factor representing the Gross Domestic Product (GDP) of city i , and d_{ij} is the distance between cities i and j . [5]

$$w_{ij} = p_i p_j g_i g_j \exp(-0.01 d_{ij}) \quad (5.23)$$

The apparent use case of the gravity models is not to accurately represent the demand flows of a network, rather the generated instances are used to obtain some meaningful results when analysing the formulated

models. In the case of the model formulated by Jaillet et al. (1996), different data sets are obtained by varying the constant factor α in the analysis [37].

Next to the gravity models, Verleger (1972) also presented point-to-point models. Such models are based on data specific to an OD city pair. These models do not regard the travel on other city pairs. Additional assumption followed in the given model are that general economic conditions and the distribution of business and leisure are omitted. [71]

The point-to-point model presented in the paper is shown in Equation 5.24. In this equation, $T_{ij}(t)$ is the travel demand between cities i and j at time t , P_{ij} is the price between cities i and j , M_i is the mass of city i , and a , α and β are constants.

$$T_{ij}(t) = aP_{ij}(t)^\alpha M_i(t)^{\beta_1} M_j(t)^{\beta_2} \epsilon \quad (5.24)$$

A downside of using such models is that every OD city pair needs to be fitted separately, which could lead to problems where much less data is available for certain city pairs than others. Verleger (1972) also states that aggregate models could also be able to provide better estimates compares to point-to-point models, as such models are able to distinguish between the different purposes that travelers may have, instead of grouping all travelers for an OD pair. However, the point-to-point models are much easier to construct as data is better accessible. [71]

The main purpose, however, of the formulated point-to-point model by Verleger (1972) was to perform an analysis between OD city pairs and the demand flows and find out if there are regularities to be found in these demand flows and if this could lead to feasible gravity models. [71]

5.4. Discussion

This chapter has presented a review on the methods of incorporating the dynamics of cost and demand in airport network models. The aim is to present the interaction of these two components of the airport network and to show methods of determining the demand in an airport network. This chapter has been divided into three components that encompass the dynamics of cost and demand: the incorporation of economies of scale into a hub location problem, the effect of price sensitivity on demand and the possible implementations, and the determination of demand itself in the airport network. This section will briefly discuss the results of the literature review.

First, the effect of economies of scale is reviewed. This effect describes the cost benefits that can be obtained by consolidating flows, for example in a HS network. Alumur et al. (2021) states that a key theme in the future of hub location problems is to improve the implementation of economies of scale [2]. Most implementations consider a discount-factor inter-hub arcs, to represent the use of larger and more cost efficient vehicles. This does result that no cost-benefits can be obtained on non-hub arcs, even though there could be large flows of passengers present. Kimms (2016) presents a better method that models a cost function that allows for a better adaptation to the size of the passenger flows [41], while also allowing for multiple aircraft types to be considered. A downside of the more accurate methods, such as the piece-wise cost functions, is the increase in computational effort.

Another key point presented by Alumur et al. (2021) is to improve the nature of the demand in hub location problems [2]. This chapter has focused on the incorporation of price sensitivity and demand modelling itself. A simple approach to determine the demand in a model is to use the demand data of the current network, for example, obtained from ticket sales. However, a change in the network can cause a response in the demand. The flow through a sub-market can downgrade due to higher prices or even stop to exist [60]. The realism of the model can be increased if such effects are taken into account, however, estimating

demand remains a complex task as it is related to various components of the network, such as price, level of service and network design [60]. An implementation of this effect is presented by O’Kelly et al. (2015), who includes different levels of service for different groups of consumers to maximise the profit of the network. An interesting extension to this problem could be the implementation of different classes on the same flight in order to maximise profits, compared to a passenger-mix problem. Further research should be performed in order to understand the correct implementation of real-life data into such models.

6

Conclusion

The aim of this report was to review the modelling approach of world-wide networks. The research question that was answered in this question is: How can a large scale world-wide airport network be modelled in order to analyse the traffic flows and emergence of hubs due to changes in cost? This question was divided up into four subjects regarding the formulation of the model, the method of optimising the problem, the airport and aircraft characteristic, and the dynamics of cost and demand in the network.

The first of these sub-questions is: How can an airport network with hubs be modelled to show the effects of cost? The review showed several possible models that are capable of projecting the traffic flows through a network, where the differences were mainly based on the structure of the network. In this case, there are models that inherently assume a Hub-and-Spoke network or models that show the emergence of hubs based on cost benefits on the consolidation of flows. Different formulations were presented that can improve the computational efficiency. For example, path-based and flow-based formulations were reviewed, where the latter is capable of reducing the size of the problem, but also introduces weaker LP bounds to the problem.

The next sub-question is: What are possible optimisation methods which allow for solving large scale problems? The review focused on exact and meta-heuristic methods that have been applied to hub location problems. Several implementations of the meta-heuristic methods display their ability to solve large-scale problems. Specialised exact methods are however also able to solve large-scale problems, given that several optimisation techniques are combined. Some of the largest networks of hub location problems that have been reviewed vary between 100 and 500 nodes.

The third sub-question regarded is: What methods are available to model the airport and aircraft characteristics in the model? The review first considered the determination of the characteristics of airports and aircraft in the network. For airports, the important part is the implementation of capacity. For aircraft, it is the range, fuel burn, and capacity. Current literature of hub location problems does not mainly focus on implementing the characteristics of aircraft, besides fuel cost into the models. Only some literature is available on implementing multiple aircraft in the modelling of world-wide airport networks.

The last sub-question is: How can the dynamics of cost and demand be incorporated into the model? The review focuses on methods to implement effects of flow consolidation, also known as economies of scale, and the effects of price sensitivity into the model. In addition, estimating demand remains a complex task due to the many influences, such as price, level of service, and network design. Further research should be performed in order to understand better implementations of real-life data into such models.

This literature review presents a good basis for the next phases of the research. Some decisions will need to be made based on the desired level of detail of the model. If more complex methods are desired, such as a better implementation of aircraft characteristics, it is important to analyse the effects it may have on the computational efficiency of the model.

Bibliography

- [1] Abrahams, M. (1983). A service quality model of air travel demand: An empirical study. *Transportation Research Part A: General*, 17(5):385–393.
- [2] Alumur, S. A., Campbell, J. F., Contreras, I., Kara, B. Y., Marianov, V., and O’Kelly, M. E. (2021). Perspectives on modeling hub location problems. *European Journal of Operational Research*, 291(1):1–17.
- [3] Araque G, J. R., Kudva, G., Morin, T. L., and Pekny, J. F. (1994). A branch-and-cut algorithm for vehicle routing problems. *Annals of Operations Research*, 50(1):37–59.
- [4] Berkelaar, M. (2010). Ip_solve reference guide. <http://lpsolve.sourceforge.net/>.
- [5] Bernardes Real, L., O’Kelly, M., de Miranda, G., and Saraiva de Camargo, R. (2018). The gateway hub location problem. *Journal of Air Transport Management*, 73:95–112.
- [6] Bhadra, D. (2002). Demand for Air Travel in the United States: Bottom-Up Econometric Estimation and Implications for Forecasts by Origin-Destination Pairs. *Journal of Air Transportation*, 8.
- [7] Blum, C. (2005). Ant colony optimization: Introduction and recent trends. *Physics of Life Reviews*, 2(4):353–373.
- [8] Boland, N., Krishnamoorthy, M., Ernst, A. T., and Ebery, J. (2004). Preprocessing and cutting for multiple allocation hub location problems. *European Journal of Operational Research*, 155(3):638–653.
- [9] Boyd, S. and Mattingley, J. (2007). Branch and bound methods. *Notes for EE364b, Stanford University*, 2006:07.
- [10] Campbell, J. F. (1994). Integer programming formulations of discrete hub location problems. *European Journal of Operational Research*, 72(2):387–405.
- [11] Carello, G., Della Croce, F., Ghirardi, M., and Tadei, R. (2004). Solving the Hub location problem in telecommunication network design: A local search approach. *Networks*, 44(2):94–105. _eprint: <https://onlinelibrary.wiley.com/doi/pdf/10.1002/net.20020>.
- [12] Chen, J.-F. (2007). A hybrid heuristic for the uncapacitated single allocation hub location problem. *Omega*, 35(2):211–220.
- [13] Choi, S. and Kim, Y. J. (2021). Artificial neural network models for airport capacity prediction. *Journal of Air Transport Management*, 97:102146.
- [14] Contreras, I. (2015). Hub Location Problems. In Laporte, G., Nickel, S., and Saldanha da Gama, F., editors, *Location Science*, pages 311–344. Springer International Publishing, Cham.
- [15] Contreras, I., Cordeau, J.-F., and Laporte, G. (2011a). Benders Decomposition for Large-Scale Uncapacitated Hub Location. *Operations Research*, 59(6):1477–1490. Publisher: INFORMS.
- [16] Contreras, I., Diaz, J., and Fernandez, E. (2011b). Branch and Price for Large-Scale Capacitated Hub Location Problems with Single Assignment. *INFORMS Journal on Computing*, 23:41–55.
- [17] Cánovas, L., García, S., and Marín, A. (2007). Solving the uncapacitated multiple allocation hub location problem by means of a dual-ascent technique. *European Journal of Operational Research*, 179(3):990–1007.
- [18] de Camargo, R. S., de Miranda, G., and Ferreira, R. P. M. (2011). A hybrid Outer-Approximation/Benders Decomposition algorithm for the single allocation hub location problem under congestion. *Operations Research Letters*, 39(5):329–337.

- [19] de Camargo, R. S. and Miranda, G. (2012). Single allocation hub location problem under congestion: Network owner and user perspectives. *Expert Systems with Applications*, 39(3):3385–3391.
- [20] de Camargo, R. S., Miranda, G., and Luna, H. P. (2008). Benders decomposition for the uncapacitated multiple allocation hub location problem. *Computers & Operations Research*, 35(4):1047–1064.
- [21] De Jong, B. (2006). Schiphol Airport Amsterdam: to Understand the Past Is to Secure Future Economic Growth. In *46th Congress of the European Regional Science Association: "Enlargement, Southern Europe and the Mediterranean"*. Louvain-la-Neuve: European Regional Science Association (ERSA).
- [22] Delft University of Technology (2021). AE4423 Lecture 6.3: Crew Scheduling Algorithms. https://www.youtube.com/watch?v=YDqegcUu5Y4&ab_channel=AirlineModelling. Accessed: 2023-04-18.
- [23] Dorigo, M. and Stützle, T. (2004). *Ant Colony Optimization*. The MIT Press.
- [24] Ernst, A. T. and Krishnamoorthy, M. (1998). Exact and heuristic algorithms for the uncapacitated multiple allocation p-hub median problem. *European Journal of Operational Research*, 104(1):100–112.
- [25] FAA (1983). *Advisory Circular (AC) 150/5060-5: Airport Capacity and Delay*. Federal Aviation Administration, United States of America.
- [26] Farahani, R. Z., Hekmatfar, M., Arabani, A. B., and Nikbakhsh, E. (2013). Hub location problems: A review of models, classification, solution techniques, and applications. *Computers & Industrial Engineering*, 64(4):1096–1109.
- [27] García, S., Landete, M., and Marín, A. (2012). New formulation and a branch-and-cut algorithm for the multiple allocation p-hub median problem. *European Journal of Operational Research*, 220(1):48–57.
- [28] Gelareh, S., Neamatian Monemi, R., and Nickel, S. (2015). Multi-period hub location problems in transportation. *Transportation Research Part E: Logistics and Transportation Review*, 75:67–94.
- [29] Gilbo, E. (1993). Airport capacity: representation, estimation, optimization. *IEEE Transactions on Control Systems Technology*, 1(3):144–154. Conference Name: IEEE Transactions on Control Systems Technology.
- [30] Guang Andy, L. J., Alam, S., Piplani, R., Lilith, N., and Dhief, I. (2021). A Decision-Tree Based Continuous Learning Framework for Real-Time Prediction of Runway Capacities. In *2021 Integrated Communications Navigation and Surveillance Conference (ICNS)*, pages 1–14. ISSN: 2155-4951.
- [31] Hamacher, H. W., Labbé, M., Nickel, S., and Sonneborn, T. (2004). Adapting polyhedral properties from facility to hub location problems. *Discrete Applied Mathematics*, 145(1):104–116.
- [32] Han, L. and Zhang, N. (2013). P-Hub Airline Network Design Incorporating Interaction Between Elastic Demand and Network Structure. In Wong, W. E. and Ma, T., editors, *Emerging Technologies for Information Systems, Computing, and Management*, Lecture Notes in Electrical Engineering, pages 89–96, New York, NY: Springer.
- [33] Hillier, F. S. and Lieberman, G. J. (2015). Introduction to operations research.
- [34] Hockaday, S. L. M. and Kanafani, A. K. (1974). Developments in airport capacity analysis. *Transportation Research*, 8(3):171–180.
- [35] Hsiao, C.-Y. and Hansen, M. (2011). A passenger demand model for air transportation in a hub-and-spoke network. *Transportation Research Part E: Logistics and Transportation Review*, 47(6):1112–1125.
- [36] Ishfaq, R. and Sox, C. R. (2011). Hub location–allocation in intermodal logistic networks. *European Journal of Operational Research*, 210(2):213–230.
- [37] Jaillet, P., Song, G., and Yu, G. (1996). Airline network design and hub location problems. *Location Science*, 4(3):195–212.
- [38] Karimi, H. and Bashiri, M. (2011). Hub covering location problems with different coverage types. *Scientia Iranica*, 18(6):1571–1578.
- [39] Kicinger, R., Chen, J.-T., Steiner, M., and Pinto, J. (2016). Airport Capacity Prediction with Explicit

- Consideration of Weather Forecast Uncertainty. *Journal of Air Transportation*, 24(1):18–28.
- [40] Kicinger, R., Cross, C., Myers, T., Krozel, J., Mauro, C., and Kierstead, D. (2011). Probabilistic Airport Capacity Prediction Incorporating the Impact of Terminal Weather. In *AIAA Guidance, Navigation, and Control Conference*, number 6691 in AIAA 2011. American Institute of Aeronautics and Astronautics, Portland, OR. _eprint: <https://arc.aiaa.org/doi/pdf/10.2514/6.2011-6691>.
- [41] Kimms, A. (2006). Economies of Scale in Hub & Spoke Network Design Models: We Have It All Wrong. In Morlock, M., Schwindt, C., Trautmann, N., and Zimmermann, J., editors, *Perspectives on Operations Research: Essays in Honor of Klaus Neumann*, pages 293–317. DUV, Wiesbaden.
- [42] Lin, C.-C. and Lee, S.-C. (2018). Hub network design problem with profit optimization for time-definite LTL freight transportation. *Transportation Research Part E: Logistics and Transportation Review*, 114:104–120.
- [43] Lin, C.-C., Lin, J.-Y., and Chen, Y.-C. (2012). The capacitated p-hub median problem with integral constraints: An application to a Chinese air cargo network. *Applied Mathematical Modelling*, 36(6):2777–2787.
- [44] Lowe, T. J. and Sim, T. (2013). The hub covering flow problem. *Journal of the Operational Research Society*, 64(7):973–981.
- [45] Lübbecke, M. E. and Desrosiers, J. (2005). Selected Topics in Column Generation. *Operations Research*, 53(6):1007–1023. Publisher: INFORMS.
- [46] Mahmoodjanloo, M., Tavakkoli-Moghaddam, R., Baboli, A., and Jamiri, A. (2020). A multi-modal competitive hub location pricing problem with customer loyalty and elastic demand. *Computers & Operations Research*, 123:105048.
- [47] Marianov, V. and Serra, D. (2003). Location models for airline hubs behaving as M/D/c queues. *Computers & Operations Research*, 30(7):983–1003.
- [48] Marín, A. (2005). Uncapacitated Euclidean Hub Location: Strengthened Formulation, New Facets and a Relax-and-cut Algorithm. *Journal of Global Optimization*, 33(3):393–422.
- [49] Mascio, P. D., Rappoli, G., and Moretti, L. (2020). Analytical Method for Calculating Sustainable Airport Capacity. *Sustainability*, 12(21):9239. Number: 21 Publisher: Multidisciplinary Digital Publishing Institute.
- [50] Mokhtar, H., Krishnamoorthy, M., and Ernst, A. T. (2017). A new Benders decomposition acceleration procedure for large scale multiple allocation hub location problems. In *Proceedings - 22nd International Congress on Modelling and Simulation, MODSIM 2017*, pages 340–346. Modelling and Simulation Society of Australia and New Zealand (MSSANZ).
- [51] Murça, M. C. R. and Hansman, R. J. (2019). Identification, Characterization, and Prediction of Traffic Flow Patterns in Multi-Airport Systems. *IEEE Transactions on Intelligent Transportation Systems*, 20(5):1683–1696. Conference Name: IEEE Transactions on Intelligent Transportation Systems.
- [52] Najy, W. and Diabat, A. (2020). Benders decomposition for multiple-allocation hub-and-spoke network design with economies of scale and node congestion. *Transportation Research Part B: Methodological*, 133:62–84.
- [53] Nuic, A. (2010). User manual for the base of aircraft data (bada) revision 3.10. *Atmosphere*, 2010:001.
- [54] O’Connor, W. E. (2001). *Introduction to Airline Economics*. Greenwood Publishing Group, Westport, UNITED STATES.
- [55] O’Kelly, M. E. (1986). The Location of Interacting Hub Facilities. *Transportation Science*, 20(2):92–106. Publisher: INFORMS.
- [56] O’Kelly, M. E. (1987). A quadratic integer program for the location of interacting hub facilities. *European Journal of Operational Research*, 32(3):393–404.

- [57] O’Kelly, M. E. (1998). A geographer’s analysis of hub-and-spoke networks. *Journal of Transport Geography*, 6(3):171–186.
- [58] Oktal, H. and Ozger, A. (2013). Hub location in air cargo transportation: A case study. *Journal of Air Transport Management*, 27:1–4.
- [59] O’Kelly, M. E. and Bryan, D. L. (1998). Hub location with flow economies of scale. *Transportation Research Part B: Methodological*, 32(8):605–616.
- [60] O’Kelly, M. E., Luna, H. P. L., de Camargo, R. S., and de Miranda, G. (2015). Hub Location Problems with Price Sensitive Demands. *Networks and Spatial Economics*, 15(4):917–945.
- [61] Ponboon, S., Qureshi, A. G., and Taniguchi, E. (2016). Branch-and-price algorithm for the location-routing problem with time windows. *Transportation Research Part E: Logistics and Transportation Review*, 86:1–19.
- [62] Randall, M. (2008). Solution approaches for the capacitated single allocation hub location problem using ant colony optimisation. *Computational Optimization and Applications*, 39(2):239–261.
- [63] Ruijgrok, G. J. (2009). *Elements of airplane performance*. VSSD.
- [64] Serper, E. Z. and Alumur, S. A. (2016). The design of capacitated intermodal hub networks with different vehicle types. *Transportation Research Part B: Methodological*, 86:51–65.
- [65] Silva, M. R. and Cunha, C. B. (2009). New simple and efficient heuristics for the uncapacitated single allocation hub location problem. *Computers & Operations Research*, 36(12):3152–3165.
- [66] Skorin-Kapov, D., Skorin-Kapov, J., and O’Kelly, M. (1996). Tight linear programming relaxations of uncapacitated p-hub median problems. *European Journal of Operational Research*, 94(3):582–593.
- [67] Stanojević, P., Marić, M., and Stanimirović, Z. (2015). A hybridization of an evolutionary algorithm and a parallel branch and bound for solving the capacitated single allocation hub location problem. *Applied Soft Computing*, 33:24–36.
- [68] Subramanian, P. (2002). A Simulation Study to Investigate Runway Capacity Using TAAM. *Master’s Theses - Daytona Beach*.
- [69] Swan, W. M. (1979). A systems analysis of scheduled air transportation networks. Technical Report, Cambridge, Mass. : Massachusetts Institute of Technology, Flight Transportation Laboratory, [1979]. Accepted: 2012-01-06T06:45:54Z.
- [70] Swedish, W. J. (1981). Upgraded FAA Airfield Capacity Model. Volume 1. Supplemental User’s Guide. Technical Report MTR-81W16, The MITRE Corporation, McLean, VA. Section: Technical Reports.
- [71] Verleger, P. K. (1972). Models of the Demand for Air Transportation. *The Bell Journal of Economics and Management Science*, 3(2):437–457. Publisher: [Wiley, RAND Corporation].
- [72] Wei, W. and Hansen, M. (2006). An aggregate demand model for air passenger traffic in the hub-and-spoke network. *Transportation Research Part A: Policy and Practice*, 40(10):841–851.
- [73] Çetiner, S., Sepil, C., and Süral, H. (2010). Hubbing and routing in postal delivery systems. *Annals of Operations Research*, 181(1):109–124.

Bibliography

- [1] Airfinance Journal. Air investor 2023, 2023. URL <https://www.airfinancejournal.com/Magazine/Download/216>.
- [2] Airline Data Project MIT. Average daily block hour utilization, 2020. URL <https://web.mit.edu/airlinedata/www/Aircraft&Related.html>.
- [3] Amsterdam Airport Schiphol. Schiphol airport charges and conditions, 2023. URL <https://www.schiphol.nl/en/route-development/page/ams-airport-charges-levies-slots-and-conditions/>.
- [4] Amsterdam Airport Schiphol. Schiphol airport traffic figures, 2024. URL <https://www.schiphol.nl/nl/schiphol-group/pagina/verkeer-en-vervoer-cijfers/>.
- [5] Eurocontrol. Standard inputs for economic analyses, 2020. URL <https://www.eurocontrol.int/sites/default/files/2021-03/eurocontrol-standard-inputs-economic-analysis-ed-9.pdf>.
- [6] Stefan Grebe and Marco Kouwenhoven. Effects of an aviation tax on aviation in the netherlands. 2019. URL <https://aetransport.org/past-etc-papers/conference-papers-2019?abstractId=6374&state=b>.
- [7] J. Thorbeck and Z. Scholz. DOC - assesment method, 2019. URL https://www.fzt.haw-hamburg.de/pers/Scholz/Aero/TU-Berlin_DOC-Method_with_remarks_13-09-19.pdf.
- [8] Ministry of Infrastructure and Water Management. Kabinet beperkt aantal vluchten op schiphol, 2022. URL <https://www.rijksoverheid.nl/actueel/nieuws/2022/06/24/kabinet-beperkt-aantal-vluchten-op-schiphol>.